

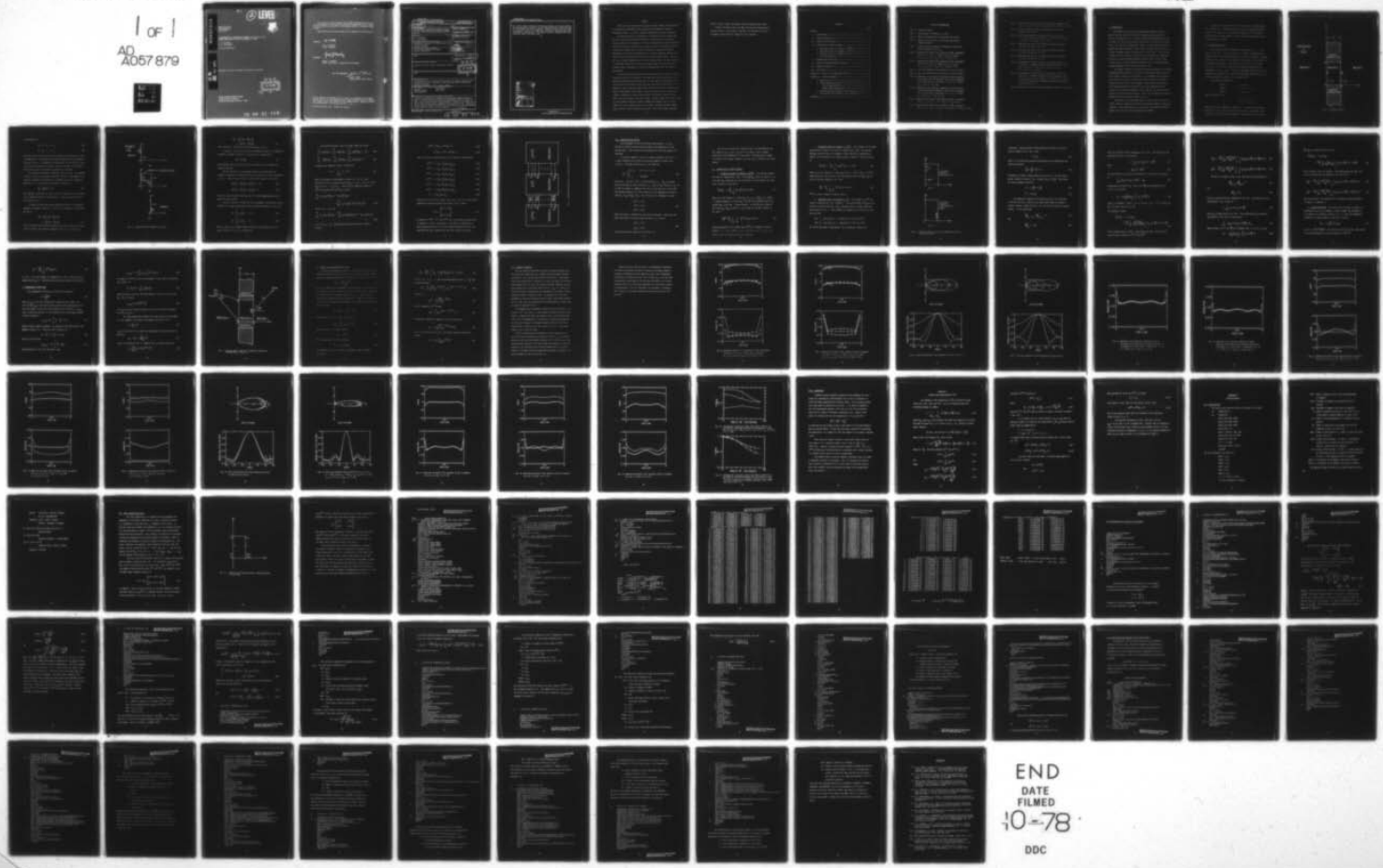
AD-A057 879 SYRACUSE UNIV NY DEPT OF ELECTRICAL AND COMPUTER EN--ETC F/G 20/14
ELECTROMAGNETIC TRANSMISSION THROUGH A FILLED SLIT IN A CONDUCT--ETC(U)
JUL 78 D T AUCKLAND, R F HARRINGTON F30602-75-C-0121

UNCLASSIFIED

RADC-TR-78-159

NL

| OF |
AD
A057 879



END
DATE FILMED
10-78
DDC



MICROCOPY RESOLUTION TEST CHART

ADA 057879

(2)

LEVEL II

RADC-TR-78-159
Interim Report
July 1978



ELECTROMAGNETIC TRANSMISSION THROUGH A FILLED SLIT IN A
CONDUCTING PLANE OF FINITE THICKNESS, TE CASE

D. T. Auckland
R. F. Harrington

Syracuse University

AU No. _____
DDC FILE COPY

Approved for public release; distribution unlimited.

DDC
REF ID: A
AUG 23 1978
REGULUS B

ROME AIR DEVELOPMENT CENTER
Air Force Systems Command
Griffiss Air Force Base, New York 13441

78 08 21 118

This report has been reviewed by the RADC Information Office (OI) and is releasable to the National Technical Information Service (NTIS). At NTIS it will be releasable to the general public, including foreign nations.

RADC-TR-78-159 has been reviewed and is approved for publication.

APPROVED:

Roy F. Stratton

ROY F. STRATTON
Project Engineer

APPROVED:

Joseph J. Naresky
JOSEPH J. NARESKY
Chief, Reliability & Compatibility Division

FOR THE COMMANDER:

John P. Huss
JOHN P. HUSS
Acting Chief, Plans Office

If your address has changed or if you wish to be removed from the RADC mailing list, or if the addressee is no longer employed by your organization, please notify RADC (RBCT) Griffiss AFB NY 13441. This will assist us in maintaining a current mailing list.

Do not return this copy. Retain or destroy.

UNCLASSIFIED

SECURITY CLASSIFICATION OF THIS PAGE (When Data Entered)

19 REPORT DOCUMENTATION PAGE		READ INSTRUCTIONS BEFORE COMPLETING FORM
1. REPORT NUMBER RADC TR-78-159	2. GOVT ACCESSION NO.	3. RECIPIENT'S CATALOG NUMBER
4. TITLE (and subtitle) ELECTROMAGNETIC TRANSMISSION THROUGH A FILLED SLIT IN A CONDUCTING PLANE OF FINITE THICKNESS, TE CASE.		5. TYPE OF REPORT / PERIOD COVERED Interim Report
6. AUTHOR(s) D. T. Auckland R. F. Harrington		7. PERFORMING ORG. REPORT NUMBER N/A
8. CONTRACT OR GRANT NUMBER(s) F30602-75-C-0121		9. PERFORMING ORGANIZATION NAME AND ADDRESS Department of Electrical & Computer Engineering Syracuse University Syracuse NY 13210
10. PROGRAM ELEMENT, PROJECT, TASK AREA & WORK UNIT NUMBERS 62702F 233803P		11. CONTROLLING OFFICE NAME AND ADDRESS Rome Air Development Center (RBCT) Griffiss AFB NY 13441
12. REPORT DATE July 1978		13. NUMBER OF PAGES 93
14. MONITORING AGENCY NAME & ADDRESS (if different from Controlling Office) Same		15. SECURITY CLASS. (of this report) UNCLASSIFIED
		15a. DECLASSIFICATION / DOWNgrading SCHEDULE N/A
16. DISTRIBUTION STATEMENT (of this Report) Approved for public release; distribution unlimited.		
17. DISTRIBUTION STATEMENT (of the abstract entered in Block 20, if different from Report) Same		
18. SUPPLEMENTARY NOTES A preliminary version of this report was printed as Technical Report TR-77-9, September 1977, by the Department of Electrical and Computer Engineering, Syracuse University. RADC Project Engineer: Roy F. Stratton (RBCT)		
19. KEY WORDS (Continue on reverse side if necessary and identify by block number) Apertures Filled slits Computer program Thick slits Electromagnetics		
20. ABSTRACT (Continue on reverse side if necessary and identify by block number) A solution is developed for computing the transmission characteristics of a slit in a conducting screen of finite thickness placed between two different media. The slit may be filled with lossy material while the two regions on either side of the screen are assumed lossless. A magnetic line source excitation is used (TE case) which is parallel to the axis of the slit. The equivalence principle is invoked to replace the two slit faces by equivalent magnetic current sheets on perfect electric conductors.		

406 737

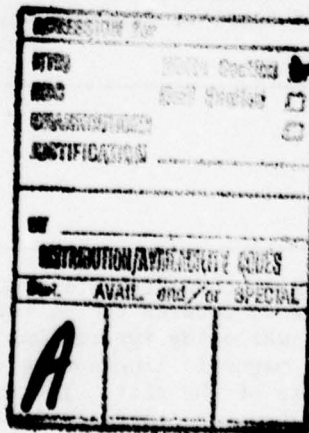
78 08 21 118

Liu

UNCLASSIFIED

SECURITY CLASSIFICATION OF THIS PAGE(When Data Entered)

Two coupled integral equations containing the magnetic currents as unknowns are then obtained and solved for by the method of moments. Pulses are used for the expansion and testing functions. Quantities computed are the equivalent magnetic currents, the transmission coefficient, the gain pattern, and normalized far field pattern. The computer program is described and listed along with sample input-output data.



UNCLASSIFIED

SECURITY CLASSIFICATION OF THIS PAGE(When Data Entered)

PREFACE

This effort was conducted by Syracuse University under the sponsorship of the Rome Air Development Center Post-Doctoral Program for Rome Air Development Center. Dr. Roy F. Stratton, RADC/RBCT, was project engineer.

The RADC Post-Doctoral Program is a cooperative venture between RADC and some sixty-five universities eligible to participate in the program.

Syracuse University (Department of Electrical Engineering), Purdue University (School of Electrical Engineering), Georgia Institute of Technology (School of Electrical Engineering), and State University of New York at Buffalo (Department of Electrical Engineering) act as prime contractor schools with other schools participating via sub-contracts with prime schools. The U.S. Air Force Academy (Department of Electrical Engineering), Air Force Institute of Technology (Department of Electrical Engineering), and the Naval Post Graduate School (Department of Electrical Engineering) also participate in the program.

The Post-Doctoral Program provides an opportunity for faculty at participating universities to spend up to one year full time on exploratory development and problem-solving efforts with the post-doctorals splitting their time between the customer location and their educational institutions. The program is totally customer-funded with current projects being undertaken for Rome Air Development Center (RADC), Space and Missile Systems Organization (SAMSO), Aeronautical System Division (ASD), Electronics Systems Division (ESD), Air Force Avionics Laboratory (AFAL), Foreign Technology Division (FTD), Air Force Weapons Laboratory (AFWL), Armament Development and Test Center (ADTC), Air Force Communications Service (AFCS), Aerospace Defense Command (ADC), Hq USAF, Defense Communications Agency (DCA), Navy, Army, Aerospace

Medical Division (AMD), and Federal Aviation Administration (FAA).

Further information about the RADC Post-Doctoral Program can be obtained from Mr. Jacob Scherer, RADC/RBC, Griffiss AFB, NY, 13441, telephone Autovon 587-2543, Commercial (315) 330-2543.

CONTENTS

	Page
ABSTRACT	
I. INTRODUCTION-----	1
II. PROBLEM FORMULATION-----	2
III. PROBLEM SPECIALIZATION-----	10
IV. COMPUTATION OF MATRIX ELEMENTS-----	11
1. Admittance Matrix for Region a, $[Y^{hsa}]$ -----	11
2. Admittance Matrix for Region c, $[Y^{hsc}]$ -----	12
3. Admittance Matrix for Region b, $[Y^b]$ -----	12
4. Excitation Matrix-----	17
V. TRANSMISSION COEFFICIENT-----	18
VI. POWER GAIN AND MEASUREMENT VECTORS-----	21
VII. NUMERICAL EXAMPLES-----	23
VIII. DISCUSSION-----	40
APPENDIX A - NOTES ON THE COMPUTATION OF $[Y^b]$ -----	41
APPENDIX B. COMPUTER PROGRAMS-----	44
1. Required Data-----	44
2. Main Program Description-----	47
Main Program Listing-----	50
Sample Input-Output Data-----	52
3. Descriptions and Listings of Subroutines-----	57
4. Descriptions and Listings of Plot Subroutines-----	71
REFERENCES-----	83

LIST OF ILLUSTRATIONS

- Fig. 1 Original problem.
- Fig. 2 Equivalences for regions a, b, and c.
- Fig. 3 Network representation for Equations (11a and b).
- Fig. 4 Region b broken up into two problems each with an equivalent source.
- Fig. 5 Geometry used in computing transmission coefficient and measurement of \bar{H}_m at r_m .
- Fig. 6 Magnitude and phase of \bar{M}_1 (squares) and \bar{M}_2 (triangles) for slit $w = .4\lambda_a$, $d = .001\lambda_a$, $k_b = k_a = k_o$ and
a) $\epsilon_c = \epsilon_o$; b) $\epsilon_c = 5\epsilon_o$; c) $\epsilon_c = 10\epsilon_o$. $N = 10$.
- Fig. 7 Magnitude and phase of \bar{M}_1 (squares) and \bar{M}_2 (triangles) for slit $w = .4\lambda_a$, $d = .001\lambda_a$, $k_b = k_a = k_o$ and
a) $\mu_c = \mu_o$; b) $\mu_c = 3\mu_o$; c) $\mu_c = 10\mu_o$. $N = 10$.
- Fig. 8 Gain and normalized field patterns for slits in Fig. 6.
- Fig. 9 Gain and normalized field patterns for slits in Fig. 7.
- Fig. 10 Magnitude of \bar{M}_2 (squares) compared to values obtained from results given by Neerhoff and Mur [4] (triangles) for a slit with $w = 1\mu$ (micron), $d = .1\mu$, $\lambda_o = .4353\mu$,
 $k_a = 1.5k_o$, $k_c = k_b = k_o$.
- Fig. 11 Magnitude of \bar{M}_2 (squares) compared to values obtained from results given by Neerhoff and Mur [4] (triangles) for a slit with $w = 1\mu$ (micron), $d = .1\mu$, $\lambda_o = .4353\mu$,
 $k_a = 1.5k_o$, $k_c = 1.6k_o$, $k_b = k_o$.
- Fig. 12 Magnitude and phase of \bar{M}_1 (squares) and \bar{M}_2 (triangles) for $\epsilon_a = \epsilon_c = \epsilon_b = \epsilon_o$, $d = .25\lambda_a$, $w = 1\lambda_a$. $N = 20$.
- Fig. 13 Magnitude and phase of \bar{M}_1 (squares) and \bar{M}_2 (triangles) for $\epsilon_a = \epsilon_c = \epsilon_o$, $d = .25\lambda_a$, $w = 1\lambda_a$, and $\epsilon_b = (1-j)\epsilon_o$. $N = 20$.

Fig. 14 Magnitude and phase of \bar{M}_1 (squares) and \bar{M}_2 (triangles) for $\epsilon_a = \epsilon_c = \epsilon_o$, $d = .25\lambda_a$, $w = 1\lambda_a$, and $\epsilon_b = (1-j10)\epsilon_o$. $N = 20$.

Fig. 15 Gain and normalized far field patterns for slits in Figures 12,13, and 14.

Fig. 16 Gain and normalized field patterns for $k_a = k_c = k_o$, $w = 2.148\lambda_a$ and a) $d = .0417\lambda_a$, $\epsilon_b = \epsilon_o$; b) $d = 1.331\lambda_a$, $\epsilon_b = \epsilon_o$; c) $d = 1.331\lambda_a$, $\epsilon_b = 2.59\epsilon_o$.

Fig. 17 Magnitude and phase of \bar{M}_1 (squares) and \bar{M}_2 (triangles) for slit a in Fig. 16. $N = 30$.

Fig. 18 Magnitude and phase of \bar{M}_1 (squares) and \bar{M}_2 (triangles) for slit b in Fig. 16. $N = 30$.

Fig. 19 Magnitude and phase of \bar{M}_1 (squares) and \bar{M}_2 (triangles) for slit c in Fig. 16. $N = 30$.

Fig. 20 Transmission coefficient times $\cos\phi$ versus ϕ where ϕ is the angle of incidence measured from the negative x axis for $w = .8\lambda_a$, $d = .25\lambda_a$, $k_a = k_c = k_o$; a) $\epsilon_b = \epsilon_o$, b) $\epsilon_b = 5\epsilon_o$, c) $\epsilon_b = 10\epsilon_o$.

Fig. 21 Transmission coefficient times $\cos\phi$ versus ϕ where ϕ is the angle of incidence measured from the negative x axis for $k_a = k_b = k_c$; a) $w = 1.02\lambda_a$, $d = 10^{-5}\lambda_a$, b) $w = .51\lambda_a$, $d = 10^{-4}\lambda_a$. Squares and triangles represent values taken from [13] for $d = 0$.

Fig. B-1 Expansion and testing function numbering system on slit faces.

I. INTRODUCTION

The problem of diffraction of plane waves through a slit in a perfect electric conductor of finite thickness has been studied by several investigators [1-4]. The most extensive investigation was that of Lehman [1], who used the analytic properties of finite Fourier transforms. The solution of Kashyap and Hamid [2] used a Wiener-Hopf and generalized matrix technique. Both of these solutions were done for the TM case (incident electric field parallel to slit axis). The solutions of Hongo [3] and of Neerhoff and Mur [4], were obtained by a numerical solution of coupled integral equations and were done for the TE case. In this report, we use the method of moments to solve coupled integral equations similar in form to those derived in [4].

This report utilizes the generalized network formulation of coupling through apertures developed in [5] and [6] and extends these results to three regions coupled by two apertures. To accomplish this the equivalence principle is used to replace both faces of the slit by perfect conductors, each of which carry magnetic current sheets on both sides. The original problem is now broken up into three regions which are coupled by the postulated magnetic current sheets. The two half space regions are loss-free with arbitrary μ and ϵ and the medium in the slit is assumed lossy with arbitrary complex μ and ϵ .

Continuity of the tangential magnetic field is used to derive two coupled operator equations involving the equivalent magnetic currents as unknowns. These equations are put into matrix form using the method of moments, and solved by using standard matrix methods.

The aperture coupling between the three regions is characterized by a combination of "admittance matrices" computed separately for each region. This gives rise to a network interpretation of the problem which treats the unknown magnetic currents as port voltages and the excitation as port currents.

II. PROBLEM FORMULATION

The original problem configuration is shown in Fig. 1. It consists of a perfect electric conductor of thickness d separating two regions a and c which may have different electrical properties. Coupling between the two regions occurs through a slit of width w filled with an arbitrarily lossy medium. The conductor is infinite in the z and y directions. The problem consists of three regions separated by two boundaries (the slit faces). Using the equivalence principle, the three regions can be separated by covering the slits with perfect electric conductors and magnetic current sheets, as described in [5].

The regions are defined by

$$\text{region } a \quad x < 0, \text{ all } y$$

$$\text{region } b \quad 0 < x < d, \quad 0 < y < w$$

$$\text{region } c \quad x > d, \text{ all } y$$

and the boundaries as:

$$\Gamma_1 \quad x = 0, \quad 0 < y < w$$

$$\Gamma_2 \quad x = d, \quad 0 < y < w$$

which are the two boundaries of separation. To utilize the equivalence principle, Γ_1 and Γ_2 are covered by perfect electric conductors, and on each side of these conductors a magnetic current sheet is placed which

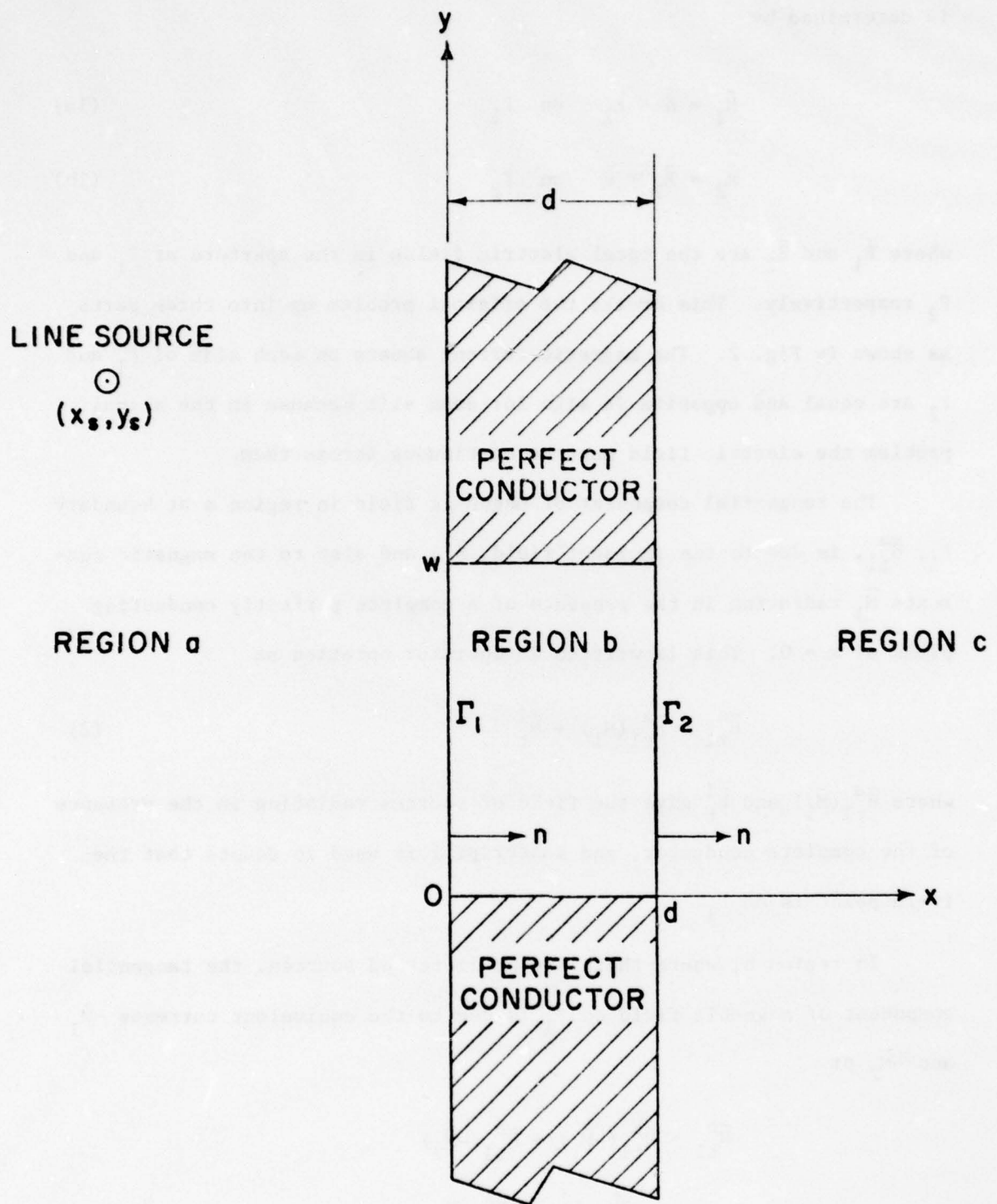


Fig. 1. Original problem.

is determined by

$$\bar{M}_1 = \hat{n} \times \bar{E}_1 \quad \text{on } \Gamma_1 \quad (1a)$$

$$\bar{M}_2 = \bar{E}_2 \times \hat{n} \quad \text{on } \Gamma_2 \quad (1b)$$

where \bar{E}_1 and \bar{E}_2 are the total electric fields in the aperture at Γ_1 and Γ_2 respectively. This breaks the original problem up into three parts as shown in Fig. 2. The magnetic current sheets on each side of Γ_1 and Γ_2 are equal and opposite in sign for each slit because in the actual problem the electric field must be continuous across them.

The tangential component of magnetic field in region a at boundary Γ_1 , \bar{H}_{t1}^a , is due to the incident field, \bar{H}_t^i , and also to the magnetic currents \bar{M}_1 radiating in the presence of a complete perfectly conducting plane at $x = 0$. This is written in operator notation as

$$\bar{H}_{t1}^a = \bar{H}_{t1}^a(\bar{M}_1) + \bar{H}_t^i \quad (2)$$

where $\bar{H}_{t1}^a(\bar{M}_1)$ and \bar{H}_t^i give the field of sources radiating in the presence of the complete conductor, and subscript 1 is used to denote that the field point is on Γ_1 .

In region b, where there are no impressed sources, the tangential component of magnetic field on Γ_1 is due to the equivalent currents $-\bar{M}_1$ and $-\bar{M}_2$ or

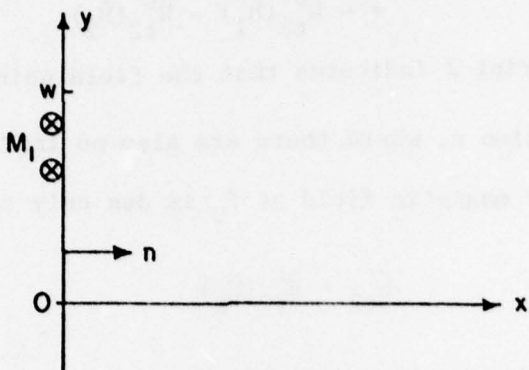
$$\begin{aligned} \bar{H}_{t1}^b &= \bar{H}_{t1}^b(-\bar{M}_1) + \bar{H}_{t1}^b(-\bar{M}_2) \\ &= -\bar{H}_{t1}^b(\bar{M}_1) - \bar{H}_{t1}^b(\bar{M}_2) \end{aligned} \quad (3)$$

where the minus signs factor out because the field operators are linear.

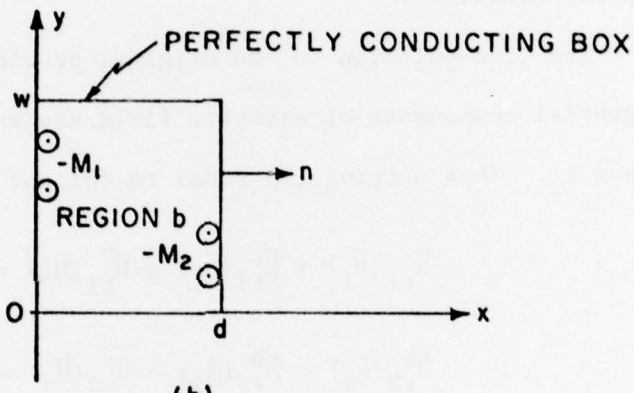
Also in region b the tangential magnetic field at Γ_2 is written as

LINE SOURCE
 (x_s, y_s)

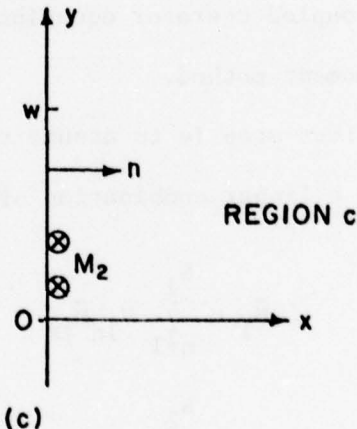
REGION a



(a)



(b)



(c)

Fig. 2. Equivalences for regions a, b, and c.

$$\begin{aligned}\bar{H}_{t2}^b &= \bar{H}_{t2}^b(-\bar{M}_1) + \bar{H}_{t2}^b(-\bar{M}_2) \\ &= -\bar{H}_{t2}^b(\bar{M}_1) - \bar{H}_{t2}^b(\bar{M}_2)\end{aligned}\quad (4)$$

where subscript 2 indicates that the field point is on Γ_2 .

In region c, where there are also no impressed sources, the tangential component of magnetic field at Γ_2 is due only to currents \bar{M}_2 or

$$\bar{H}_{t2}^c = \bar{H}_{t2}^c(\bar{M}_2) \quad (5)$$

where $\bar{H}_{t2}^c(\bar{M}_2)$ gives the field of sources radiating in the presence of a complete conductor.

The true solution to the original problem is obtained when the tangential components of magnetic field are continuous on the two boundaries Γ_1 and Γ_2 . Thus setting (2) equal to (3) and (4) equal to (5) we have

$$\bar{H}_{t1}^a(\bar{M}_1) + \bar{H}_{t1}^b(\bar{M}_1) + \bar{H}_{t1}^b(\bar{M}_2) = -\bar{H}_t^i \quad (6a)$$

$$\bar{H}_{t2}^b(\bar{M}_1) + \bar{H}_{t2}^b(\bar{M}_2) + \bar{H}_{t2}^c(\bar{M}_2) = 0 \quad (6b)$$

These two coupled operator equations must be solved simultaneously and we apply the moment method.

The first step is to assume that the two magnetic current sheets may be expanded by a linear combination of basis functions defined on Γ_1 and Γ_2 as

$$\bar{M}_1 = \sum_{n=1}^{N_1} v_{1n} \bar{M}_{1n} \quad \text{on } \Gamma_1 \quad (7a)$$

$$\bar{M}_2 = \sum_{n=1}^{N_2} v_{2n} \bar{M}_{2n} \quad \text{on } \Gamma_2 \quad (7b)$$

Here v_{1n} and v_{2n} are unknown complex scalars and \bar{M}_{1n} and \bar{M}_{2n} are vector basis functions on Γ_1 and Γ_2 respectively.

Now substituting Eqs. (7a,b) into Eqs. (6a,b) we obtain

$$\sum_{n=1}^{N_1} v_{1n} \bar{H}_{t1}^a (\bar{M}_{1n}) + \sum_{n=1}^{N_1} v_{1n} \bar{H}_{t1}^b (\bar{M}_{1n}) + \sum_{n=1}^{N_2} v_{2n} \bar{H}_{t1}^b (\bar{M}_{2n}) = - \bar{H}_t^1 \quad (8a)$$

$$\sum_{n=1}^{N_1} v_{1n} \bar{H}_{t2}^b (\bar{M}_{1n}) + \sum_{n=1}^{N_2} v_{2n} \bar{H}_{t2}^b (\bar{M}_{2n}) + \sum_{n=1}^{N_2} v_{2n} \bar{H}_{t2}^c (\bar{M}_{2n}) = 0 \quad (8b)$$

An appropriate symmetric product is defined as

$$\langle X, Y \rangle = \int_{\Gamma_1 \cup \Gamma_2} \bar{X} \cdot \bar{Y} dy \quad (9)$$

where the variable of integration is either on Γ_1 or Γ_2 . Also needed are a set of testing functions $\{\bar{W}_{1m}, m = 1, 2, \dots, N_1\}$ on Γ_1 and $\{\bar{W}_{2m}, m = 1, 2, \dots, N_2\}$ on Γ_2 . Next take the symmetric product of (8a) with \bar{W}_{1m} and (8b) with \bar{W}_{2m} to obtain

$$\begin{aligned} & \sum_{n=1}^{N_1} v_{1n} [\langle W_{1m}, H_{t1}^a (M_{1n}) \rangle + \langle W_{1m}, H_{t1}^b (M_{1n}) \rangle] \\ & + \sum_{n=1}^{N_2} v_{2n} \langle W_{1m}, H_{t1}^b (M_{2n}) \rangle = - \langle W_{1m}, H_t^1 \rangle \end{aligned} \quad (10a)$$

for $m = 1, 2, \dots, N_1$, and

$$\begin{aligned} & \sum_{n=1}^{N_1} v_{1n} \langle W_{2m}, H_{t2}^b (M_{1n}) \rangle + \sum_{n=1}^{N_2} v_{2n} [\langle W_{2m}, H_{t2}^b (M_{2n}) \rangle + \langle W_{2m}, H_{t2}^c (M_{2n}) \rangle] \\ & = 0 \end{aligned} \quad (10b)$$

for $m = 1, 2, \dots, N_2$. These equations may be rewritten in matrix form as

$$[Y^{hsa} + Y^{11}] \bar{v}_1 + [Y^{12}] \bar{v}_2 = \bar{I}^1 \quad (11a)$$

$$[Y^{21}] \bar{v}_1 + [Y^{22} + Y^{hsc}] \bar{v}_2 = 0 \quad (11b)$$

where the various component matrices are explicitly identified by

$$[Y^{hsa}] = - [\langle W_{1m}, H_{t1}^a(M_{1n}) \rangle]_{N_1 \times N_1} \quad (12a)$$

$$[Y^{hsc}] = - [\langle W_{2m}, H_{t2}^c(M_{2n}) \rangle]_{N_2 \times N_2} \quad (12b)$$

$$[Y^{11}] = - [\langle W_{1m}, H_{t1}^b(M_{1n}) \rangle]_{N_1 \times N_1} \quad (12c)$$

$$[Y^{12}] = - [\langle W_{1m}, H_{t1}^b(M_{2n}) \rangle]_{N_1 \times N_2} \quad (12d)$$

$$[Y^{21}] = - [\langle W_{2m}, H_{t2}^b(M_{1n}) \rangle]_{N_2 \times N_1} \quad (12e)$$

$$[Y^{22}] = - [\langle W_{2m}, H_{t2}^b(M_{2n}) \rangle]_{N_2 \times N_2} \quad (12f)$$

$$\bar{I}^1 = [\langle W_{1m}, H_t^1 \rangle]_{N_1 \times 1} \quad (12g)$$

Equations (11a) and (11b) compose a $(N_1 + N_2) \times (N_1 + N_2)$ system which suggests the network representation shown in Fig. 3 where

$$[Y^b] = \begin{bmatrix} [Y^{11}] & [Y^{12}] \\ [Y^{21}] & [Y^{22}] \end{bmatrix} \quad (13)$$

The matrices $[Y^{hsa}]$, $[Y^b]$, and $[Y^{hsc}]$ are the network representations of regions a, b, and c respectively. The explicit computation of these quantities which, to carry the network analogy further we call admittance matrices, depends only upon their respective regions.

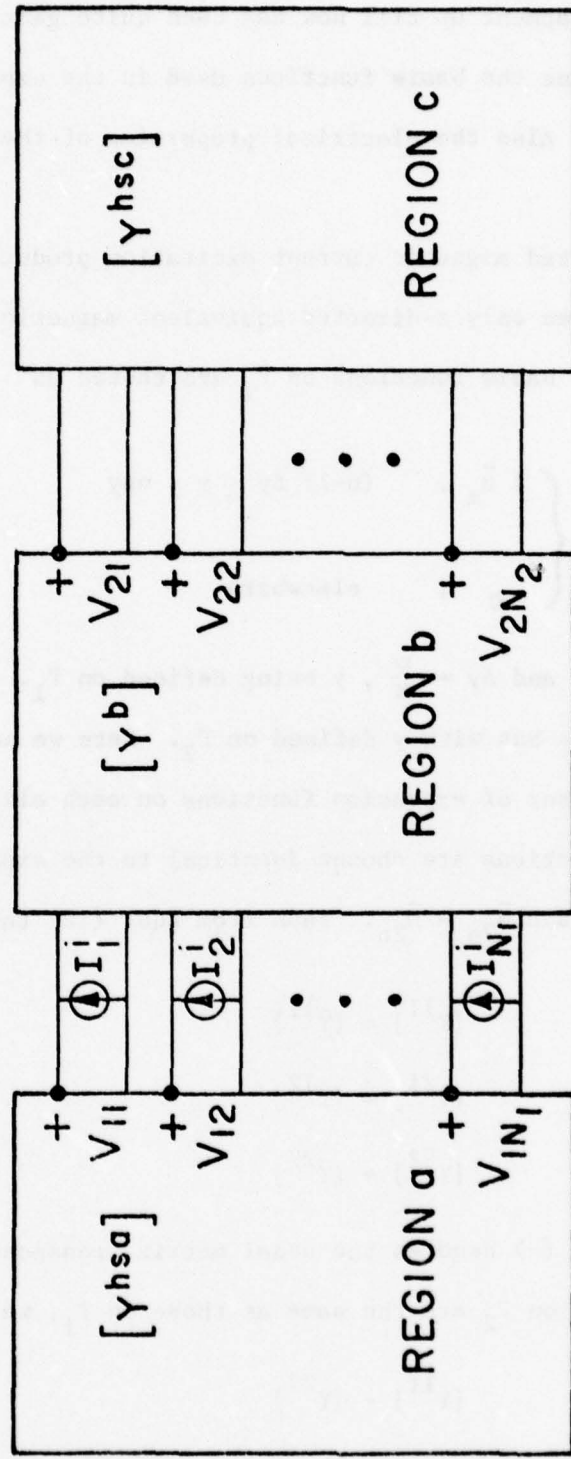


Fig. 3. Network representation for Equations (11a and b).

III. PROBLEM SPECIALIZATION

The development up till now has been quite general. In this section we define the basis functions used in the expansion and testing procedure. Also the electrical properties of the three regions are described.

A z-directed magnetic current excitation produces a field TE to z , which requires only z-directed equivalent magnetic currents over Γ_1 and Γ_2 . The basis functions on Γ_1 are chosen as

$$\bar{M}_{1n} = \begin{cases} 1 \bar{u}_z, & (n-1) \Delta y \leq y \leq n\Delta y \\ 0, & \text{elsewhere} \end{cases} \quad (14)$$

for $n=1,2,\dots,N$ and $\Delta y = \frac{w}{N}$, y being defined on Γ_1 . \bar{M}_{2n} is defined exactly the same but with y defined on Γ_2 . Here we have taken $N_1 = N_2 = N$ so that the number of expansion functions on each slit face is the same. The testing functions are chosen identical to the expansion functions so that $\bar{W}_{1n} = \bar{M}_{1n}$ and $\bar{W}_{2n} = \bar{M}_{2n}$. Thus from Eqs. (12c through f) we have

$$\begin{aligned} [Y^{11}] &= [\tilde{Y}^{11}] \\ [Y^{21}] &= [\tilde{Y}^{12}] \\ [Y^{22}] &= [\tilde{Y}^{22}] \end{aligned} \quad (15)$$

where the tilda (~) denotes the usual matrix transpose. Also since the basic functions on Γ_2 are the same as those on Γ_1 , we have

$$\begin{aligned} [Y^{11}] &= [Y^{22}] \\ [Y^{21}] &= [Y^{12}] \end{aligned} \quad (16)$$

as will be seen more explicitly in Section IV-3.

The electrical properties of regions a and c are specified by the real numbers ϵ_a/ϵ_0 , μ_a/μ_0 , ϵ_c/ϵ_0 and μ_c/μ_0 where ϵ_0 and μ_0 denote permittivity and permeability of free space. The properties of region b are given by the complex numbers ϵ_b/ϵ_0 and μ_b/μ_0 to describe the losses present.

IV. COMPUTATION OF MATRIX ELEMENTS

1. Admittance matrix for Region a, $[Y^{hsa}]$. These matrix elements are found by computing Eq. (12a). Since $\bar{H}_{tl}^a(\bar{M}_{ln})$ gives the field of current sheet \bar{M}_{ln} radiating into the half space a in the presence of a complete conductor, we may write

$$\bar{H}_{tl}^a(\bar{M}_{ln}) = -\frac{k_a}{2n_a} \int_{\Delta y_n} \bar{M}_{ln} H_o^{(2)}(k_a |y-y'|) dy' \quad (17)$$

Here Δy_n is the region on Γ_1 where $\bar{M}_{ln} \neq 0$, $k_a = \omega \sqrt{\mu_a \epsilon_a}$, $n_a = \sqrt{\mu_a / \epsilon_a}$, ω = radian frequency of line source, and $H_o^{(2)}$ is the Hankel function of second kind, order zero. Substituting Eq. (14) for \bar{M}_{ln} and using the fact that $\bar{W}_{lm} = \bar{M}_{lm}$ for $m=1,2,\dots,N$, we have for the mnth element of Eq. (12a):

$$Y_{mn}^{hsa} = \frac{k_a}{2n_a} \int_{\Delta y_m} \int_{\Delta y_n} H_o^{(2)}(k_a |y-y'|) dy dy' \quad (18)$$

From this equation it is evident that $[Y^{hsa}]$ is a symmetric Toeplitz matrix, i.e., the elements are functions only of $|m-n|$ and hence only one column need be computed.

2. Admittance matrix for Region c, $[Y^{hsc}]$. The elements for the admittance matrix of region c are found by computing Eq. (12b). The operator $\bar{H}_{t2}^c(\bar{M}_{2n})$ gives the field of a magnetic current sheet \bar{M}_{2n} radiating into region c in the presence of a complete perfect conductor. This is written as

$$\bar{H}_{t2}^c(\bar{M}_{2n}) = -\frac{k_c}{2n_c} \int_{\Delta y_n} \bar{M}_{2n} H_o^{(2)}(k_c |y - y'|) dy' \quad (19)$$

where Δy_n is the region on Γ_2 where $\bar{M}_{2n} \neq 0$, $k_c = \omega\sqrt{\mu_c \epsilon_c}$, and $n_c = \sqrt{\mu_c/\epsilon_c}$. Substituting Eq. (19) into Eq. (12b) and using the fact that $\bar{M}_{2n} = \bar{W}_{2n}$ we have for the mnth element of Eq. (12b):

$$Y_{mn}^{hsc} = \frac{k_c}{2n_c} \int_{\Delta y_m} \int_{\Delta y_n} H_o^{(2)}(k_c |y - y'|) dy dy' \quad (20)$$

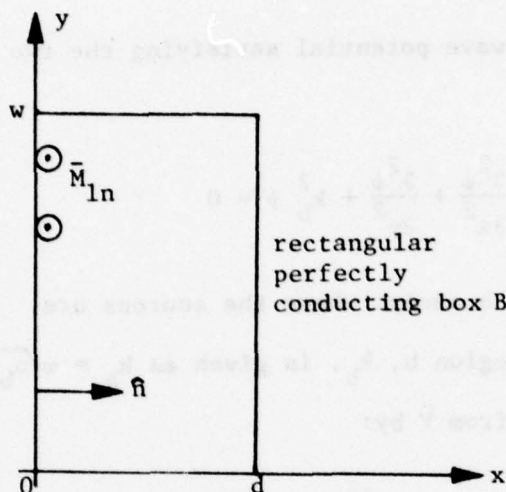
$[Y^{hsc}]$ is also a symmetric Toeplitz matrix.

3. Admittance matrix for Region b, $[Y^b]$. The elements of $[Y^b]$ are found by computing Eqs. (12c through f). The operators \bar{H}_{t1}^b or \bar{H}_{t2}^b give the fields of current sheets \bar{M}_{1n} or \bar{M}_{2n} radiating inside a closed conducting box as shown in Fig. 4. Thus breaking the computation of $[Y^b]$ up into two parts we have

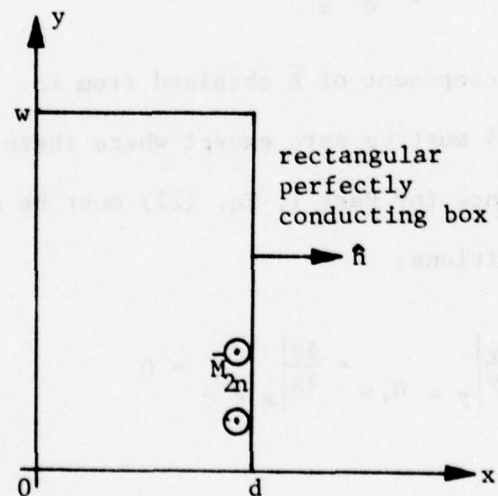
Part I: Source \bar{M}_{1n} on Γ_1 , computation of $[Y^{11}]$ and $[Y^{21}]$.

Part II: Source \bar{M}_{2n} on Γ_2 , computation of $[Y^{12}]$ and $[Y^{22}]$.

For the TE case under consideration, all the magnetic currents are



Part I



Part II

Fig. 4. Region b broken up into two problems each with an equivalent source.

z -directed. Thus an electric vector potential function \bar{F} can be defined in region b as [7, sec. 3-12]:

$$\bar{F} = \psi \bar{u}_z \quad (21)$$

where ψ is a scalar wave potential satisfying the two dimensional differential equation

$$\frac{\partial^2 \psi}{\partial x^2} + \frac{\partial^2 \psi}{\partial y^2} + k_b^2 \psi = 0 \quad (22)$$

everywhere in region b except where the sources are. The wave propagation constant in region b, k_b , is given as $k_b = \omega \sqrt{\mu_b \epsilon_b}$. The fields are then determined from \bar{F} by:

$$\bar{E} = - \bar{u}_x \frac{\partial \psi}{\partial y} + \bar{u}_y \frac{\partial \psi}{\partial x} \quad (23)$$

$$\bar{H} = - j \omega \epsilon_b \psi \bar{u}_z \quad (24)$$

The tangential component of \bar{E} obtained from Eq. (23) evaluated on the box B in Fig. 4 must be zero except where there are magnetic surface currents. Hence for Part I, Eq. (22) must be solved in region b subject to the conditions:

$$\left. \frac{\partial \psi}{\partial y} \right|_{y=0, w} = \left. \frac{\partial \psi}{\partial x} \right|_{x=d} = 0 \quad (25)$$

and

$$\left. \frac{\partial \psi}{\partial x} \right|_{\Gamma_1} = - M_{ln} \quad (26)$$

which are obtained from the components of Eq. (23). The solution to (22) satisfying Eq. (25) is of the form

$$\psi = \sum_{p=0}^{\infty} A_p \cos k_{xp} (x-d) \cos \frac{p\pi y}{w} \quad (27)$$

where

$$k_{xp}^2 = k_b^2 - \left(\frac{p\pi}{w}\right)^2 \quad (28)$$

The coefficients A_p are found by satisfying Eq. (26) which is rewritten as

$$\sum_{p=0}^{\infty} A_p k_{xp} \sin k_{xp} d \cos \frac{p\pi y}{w} = - M_{ln} \quad (29)$$

Multiplying both sides of Eq. (29) by $\cos \frac{p\pi y}{w}$ and integrating from 0 to w on Γ_1 , we obtain

$$A_p = \frac{-\epsilon_p}{w k_{xp} \sin k_{xp} d} \int_0^w M_{ln} \cos \frac{p\pi y}{w} dy \quad (30)$$

where ϵ_p is Neumann's number ($\epsilon_p = 1$ for $p=0$ and $\epsilon_p = 2$, $p > 0$). Now \bar{H}_{t1}^b and \bar{H}_{t2}^b are simply given by Eq. (24).

Thus $H_{t1}^b(M_{ln})$ becomes

$$\begin{aligned} H_{t1}^b(M_{ln}) &= - j\omega \epsilon_b \psi(M_{ln}) \\ &= \frac{j\omega \epsilon_b}{w} \sum_{p=0}^{\infty} \frac{\epsilon_p \cos k_{xp} d}{k_{xp} \sin k_{xp} d} \int_{\Gamma_1} M_{ln} \cos \frac{p\pi y'}{w} dy' \cos \frac{p\pi y}{w} \end{aligned} \quad (31)$$

with a similar result for H_{t2}^b . Substituting into Eqs. (12c and e) we obtain the mth elements of $[Y^{11}]$ and $[Y^{21}]$:

$$Y_{mn}^{11} = - \frac{j\omega\epsilon_b}{w} \sum_{p=0}^{\infty} \frac{\epsilon_p \cot k_{xp} d}{k_{xp}} \int_{\Gamma_1} \int_{\Gamma_1} M_{1n} W_{1m} \cos \frac{p\pi y'}{w} \cos \frac{p\pi y}{w} dy dy' \quad (32)$$

$$Y_{mn}^{21} = - \frac{j\omega\epsilon_b}{w} \sum_{p=0}^{\infty} \frac{\epsilon_p \csc k_{xp} d}{k_{xp}} \int_{\Gamma_2} \int_{\Gamma_1} M_{1n} W_{2m} \cos \frac{p\pi y'}{w} \cos \frac{p\pi y}{w} dy dy' \quad (33)$$

For Part II as shown in Fig. 4, Eq. (22) must be solved subject to

$$\left. \frac{\partial \psi}{\partial y} \right|_{y=0, w} = \left. \frac{\partial \psi}{\partial x} \right|_{x=0} = 0 \quad (34)$$

and

$$\left. \frac{\partial \psi}{\partial x} \right|_{\Gamma_2} = M_{2n} \quad (35)$$

which are obtained from the components of Eq. (23). The solution to (22) satisfying Eq. (34) is given by

$$\psi = \sum_{p=0}^{\infty} B_p \cos k_{xp} x \cos \frac{p\pi y}{w} \quad (36)$$

where k_{xp} is again given by Eq. (28). The coefficients B_p are found by satisfying Eq. (35) which is rewritten as

$$\sum_{p=0}^{\infty} - B_p k_{xp} \sin k_{xp} d \cos \frac{p\pi y}{w} = M_{2n} \quad (37)$$

Again multiply (37) by $\cos \frac{p\pi y}{w}$ and integrate from 0 to w on Γ_2 to get

$$B_p = - \frac{\epsilon_p}{w k_{xp} \sin k_{xp} d} \int_0^w M_{2n} \cos \frac{p\pi y}{w} dy \quad (38)$$

$H_{t1}^b(M_{2n})$ is again given by Eq. (24):

$$H_{t1}^b(M_{2n}) = -j\omega\epsilon_b \psi(M_{2n}) \\ = \frac{j\omega\epsilon_b}{w} \sum_{p=0}^{\infty} \frac{\epsilon_p}{k_{xp} \sin k_{xp} d} \int_{\Gamma_2} M_{2n} \cos \frac{p\pi y'}{w} dy' \cos \frac{p\pi y}{w} \quad (39)$$

with a similar result for $H_{t2}^b(M_{2n})$. Thus substituting into Eqs. (12d) and f) we obtain the mnth element of $[Y^{12}]$ and $[Y^{22}]$:

$$Y_{mn}^{12} = -\frac{j\omega\epsilon_b}{w} \sum_{p=0}^{\infty} \frac{\epsilon_p \csc k_{xp} d}{k_{xp}} \int_{\Gamma_1} \int_{\Gamma_2} W_{1m} M_{2n} \cos \frac{p\pi y'}{w} \cos \frac{p\pi y}{w} dy dy' \quad (40)$$

$$Y_{mn}^{22} = -\frac{j\omega\epsilon_b}{w} \sum_{p=0}^{\infty} \frac{\epsilon_p \cot k_{xp} d}{k_{xp}} \int_{\Gamma_2} \int_{\Gamma_1} W_{2m} M_{2n} \cos \frac{p\pi y'}{w} \cos \frac{p\pi y}{w} dy dy' \quad (41)$$

More is said about the computation of the admittance matrix elements of region b in Appendix A.

4. Excitation Matrix. The source which is placed in region a at coordinates (x_s, y_s) is a magnetic current filament Ku_z radiating in the presence of a complete conductor at $x = 0$. Hence the tangential component of incident magnetic field, \bar{H}_t^i , is given by

$$\bar{H}_t^i = -\bar{u}_z \frac{k_a K}{2\eta_a} H_o^{(2)}(k_a R_s) \quad (42)$$

where $R_s = \sqrt{x_s^2 + (y-y_s)^2}$. Substitution of this \bar{H}_t^i into Eq. (12g) yields the following formula for the mth element of vector \bar{I}^i :

$$I_m^i = - \frac{k_a K}{2n_a} \int_{\Delta y_m} H_o^{(2)}(k_a R_s) dy \quad (43)$$

$m = 1, 2, \dots, N$. The variable of integration, y , is on Γ_1 and Δy_m is the region where $\bar{W}_{lm} \neq 0$. Equations (11a,b) may now be solved for \bar{V}_1 and \bar{V}_2 .

V. TRANSMISSION COEFFICIENT

The transmission coefficient of the slit is defined as

$$T = \frac{P_{trans}}{P_{inc}} \quad (44)$$

where P_{trans} is the time average power transmitted into region c by the slit and P_{inc} is the time average incident power intercepted by the slit from region a, both for a unit length in the z direction. P_{trans} then, is just the real part of the Poynting vector flux through boundary Γ_2 which is given by

$$P_{trans} = \operatorname{Re} \int_0^w \bar{E}_2 \times \bar{H}_2^* \cdot \hat{n} dy \quad (45)$$

where * denotes complex conjugate. \bar{E}_2 and \bar{H}_2 are the total electric and magnetic fields at Γ_2 . Using the vector identity [7]:

$$\bar{E}_2 \times \bar{H}_2^* \cdot \hat{n} = \bar{H}_2^* \cdot (\hat{n} \times \bar{E}_2) \quad (46)$$

and Eq. (1b) we obtain

$$P_{trans} = - \operatorname{Re} \int_0^w \bar{H}_2^* \cdot \bar{M}_2 dy \quad (47)$$

Now substitute Eq. (7b) into the above to get

$$P_{trans} = - \operatorname{Re} \sum_{n=1}^N v_{2n} \left\{ \int_0^w \bar{H}_2^* \cdot \bar{M}_{2n} dy \right\} \quad (48)$$

The magnetic field \bar{H}_2 is due to the magnetic current sheet \bar{M}_2 radiating into region c or

$$\bar{H}_2 = \bar{H}_{t2}^c(\bar{M}_2) = \sum_{n=1}^N v_{2n} \bar{H}_{t2}^c(\bar{M}_{2n}) \quad (49)$$

Substituting Eq. (49) into (48) and using Eq. (12b) and the fact that $\bar{M}_{2n} = \bar{W}_{2n}$, we obtain

$$P_{trans} = \operatorname{Re} \tilde{V}_2 [Y^{hsc}]^* \tilde{V}_2^* \quad (50)$$

This is the usual formula for power flow into the network represented by $[Y^{hsc}]$ of Fig. 3.

The time average power radiated into whole space per unit length in z by a magnetic line source of strength K is given by [7]:

$$P_f = \frac{k_a}{4\pi a} |K|^2 \quad (51)$$

P_{inc} is that portion of P_f which is intercepted by the aperture and is given by

$$P_{inc} = \frac{\theta}{2\pi} P_f = \frac{\theta k_a}{8\pi n_a} |K|^2 \quad (52)$$

where θ is defined in Fig. 5. Equation (44) is finally written as

$$T = \frac{8\pi n_a}{\theta k_a |K|^2} \operatorname{Re} \{ \tilde{V}_2 [Y^{hsc}]^* \tilde{V}_2^* \} \quad (53)$$

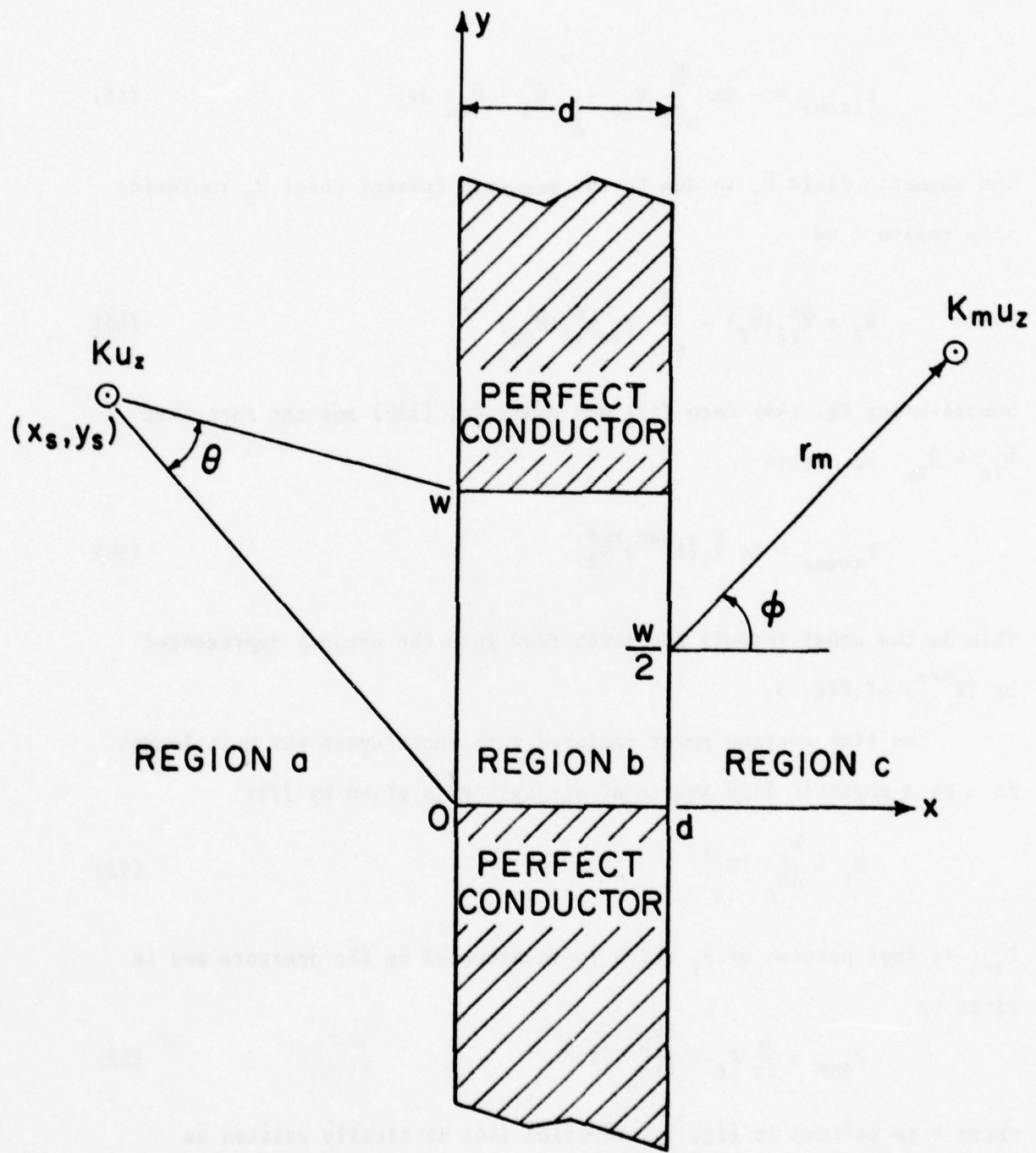


Fig. 5. Geometry used in computing transmission coefficient and measurement of R_m at r_m .

VI. POWER GAIN AND MEASUREMENT VECTOR

The power gain pattern in region c is defined as the ratio of the radiation intensity which would exist if the transmitted time average power were radiated uniformly over half space to P_{trans} in Eq. (44), or

$$G(\phi) = \frac{\pi r_m n_c |\bar{H}_m|^2}{P_{trans}} \quad (54)$$

\bar{H}_m is the component of the magnetic field in region c in the direction of a magnetic test line current $K_m \bar{u}_z$ due to current sheet \bar{M}_2 radiating in the presence of a complete conductor at $x = d$. $K_m \bar{u}_z$ is used to measure \bar{H}_m at position (r_m, ϕ) by reciprocity. If \bar{H}_K^I is the field at r_2 due to $K_m \bar{u}_z$ radiating in the presence of a complete conductor, then from reciprocity

$$\bar{H}_m \cdot K_m \bar{u}_z = \int_{r_2} \bar{H}_K^I \cdot \bar{M}_2 dy \quad (55)$$

Substitution of Eq. (7b) into (55) results in

$$H_m K_m = \sum_{n=1}^N V_{2n} \langle M_{2n}, H_K^I \rangle \quad (56)$$

which is rewritten in matrix form as

$$H_m K_m = \bar{I}^m \bar{V}_2 \quad (57)$$

\bar{I}^m is a measurement vector defined as

$$\bar{I}^m = [\langle M_{2n}, H_K^I \rangle]_{N \times 1} \quad (58)$$

The elements of \bar{I}^m are essentially the same as those of \bar{I}^I and are given by

$$I_n^m = -\frac{k_c K_m}{2n_c} \int_0^w \bar{M}_{2n} \cdot \bar{u}_z H_o^{(2)}(k_c |\bar{r}_m + (\frac{w}{2} - y)\bar{u}_y|) dy \quad (59)$$

$n=1, 2, \dots, N$. If $r_m \gg \lambda_c$ (far field measurements) where $\lambda_c = \frac{2\pi}{k_c}$ then the above becomes

$$I_n^m = -\frac{K_m}{n_c} \sqrt{\frac{j k_c}{2\pi r_m}} e^{-j k_c r_m} \int_0^w M_{2n} e^{j k_c (y - \frac{w}{2}) \sin \phi} dy \quad (60)$$

Adjust K_m to

$$\frac{1}{K_m} = -\frac{1}{n_c} \sqrt{\frac{j k_c}{2\pi r_m}} e^{-j k_c r_m} \quad (61)$$

and the components of \bar{I}^m become

$$I_n^m = \int_0^w \bar{M}_{2n} e^{j k_c (y - \frac{w}{2}) \sin \phi} dy \quad (62)$$

The measured component of magnetic field is now given by

$$H_m = -\frac{1}{n_c} \sqrt{\frac{j k_c}{2\pi r_m}} e^{-j k_c r_m} \{ \bar{I}^m \bar{v}_2 \} \quad (63)$$

and is in the direction of $K_m \bar{u}_z$. The final formula for power gain becomes

$$G(\phi) = \frac{k_c}{2n_c P_{trans}} | \bar{I}^m \bar{v}_2 |^2 \quad (64)$$

VII. NUMERICAL EXAMPLES

All the examples given here are done for normal incidence with the source far enough away ($x_s = -100\lambda_a$) and the strength adjusted to simulate a unit incident plane wave at slit face Γ_1 . The permeability and permittivity of regions a, b, and c are that of free space except where noted. To check the computer program, magnetic currents were computed for a relatively thin slit ($w = .4\lambda_a$, $d = .001\lambda_a$) for different values of permittivity and permeability in region c. These results are given in Figures 6 and 7. As expected, $\bar{M}_1 = -\bar{M}_2$, and agreement is quite good between results in Fig. 6 and those obtained for $d = 0$ [8]. Gain and normalized far field patterns for these cases are given in Figures 8 and 9.

Two examples done by Neerhoff and Mur [4] for a slit with $w = 1\mu$ (micron), $d = .1\mu$, and $\lambda_o = .4353\mu$ appear in Figures 10 and 11 when region b contains free space and regions a and c have different permittivities. The magnitude of currents \bar{M}_2 is compared and agreement is quite good. Figures 12 through 15 show the effects of having a lossy medium in region b for a slit with $w = 1\lambda_a$, $d = .25\lambda_a$, when regions a and c are free space.

Figure 16 shows gain and normalized far field patterns for a slit with varying thickness and different values of ϵ_b . Our results agree well with the same example computed in [4]. This case was also experimentally measured in [9] with slight discrepancies in the magnitudes of the sidelobes and nulls when compared with our results. Figures 17 through 19 show the magnitudes and phases of magnetic currents computed for the slits in Fig. 16.

Figures 20 and 21 show the effect on transmission coefficient for various slits when the source is placed at different angles of incidence as measured from the negative x-axis. This transmission coefficient is different from Eq. (44) in that P_{inc} is now the time average power intercepted by the slit when the source is at normal incidence which, for plane wave simulation as we have done, amounts to multiplying Eq. (44) by $\cos\phi$ where ϕ is the angle of incidence. This is done to facilitate comparisons with results given in [12] and [13].

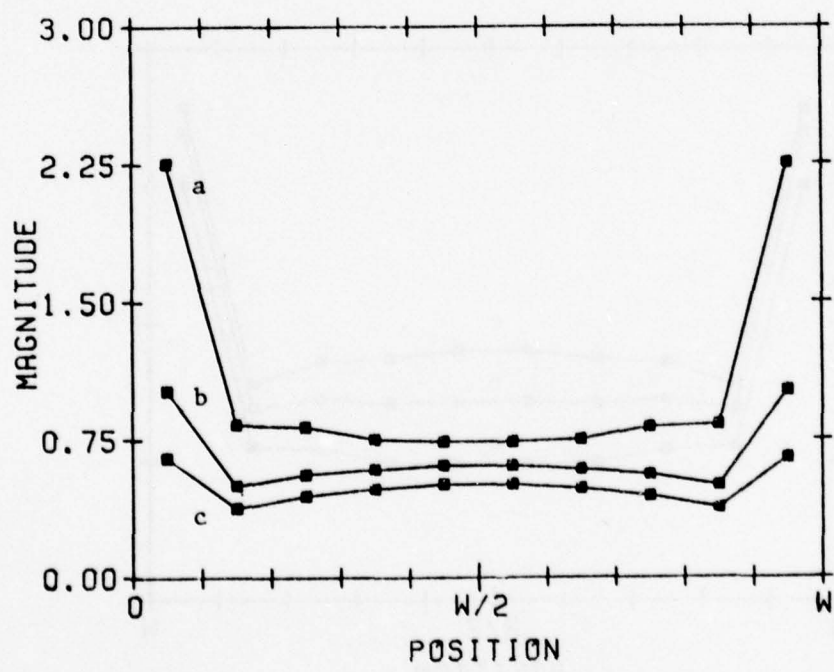
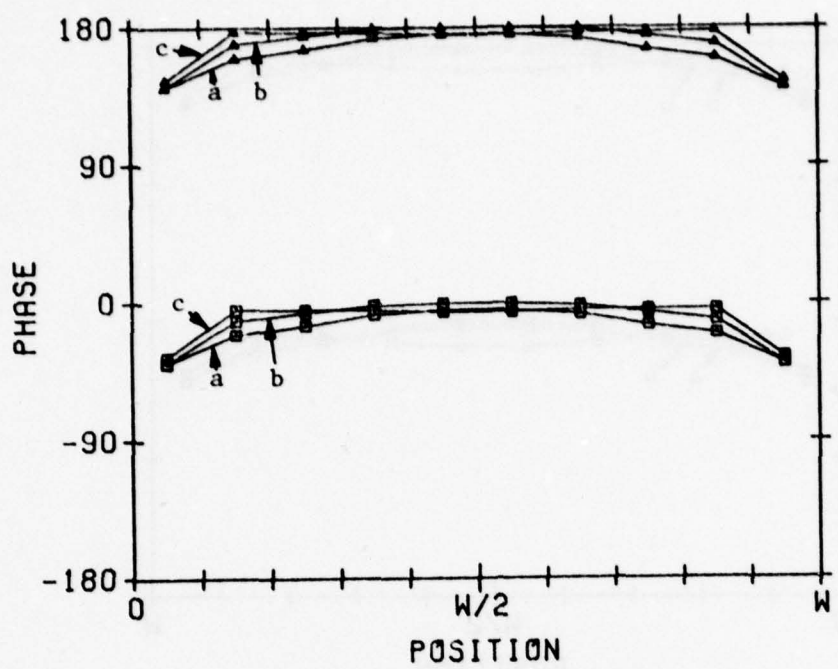


Fig. 6. Magnitude and phase of \bar{M}_1 (squares) and \bar{M}_2 (triangles) for slit $w = .4\lambda_a$, $d = .001\lambda_a$, $k_b = k_a = k_o$ and
a) $\epsilon_c = \epsilon_o$; b) $\epsilon_c = 5\epsilon_o$; c) $\epsilon_c = 10\epsilon_o$. $N = 10$.

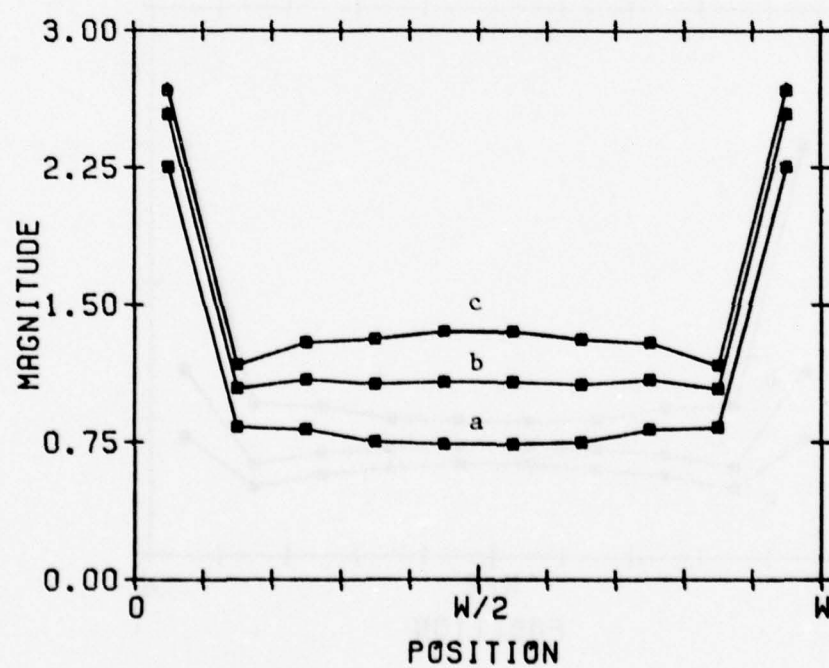
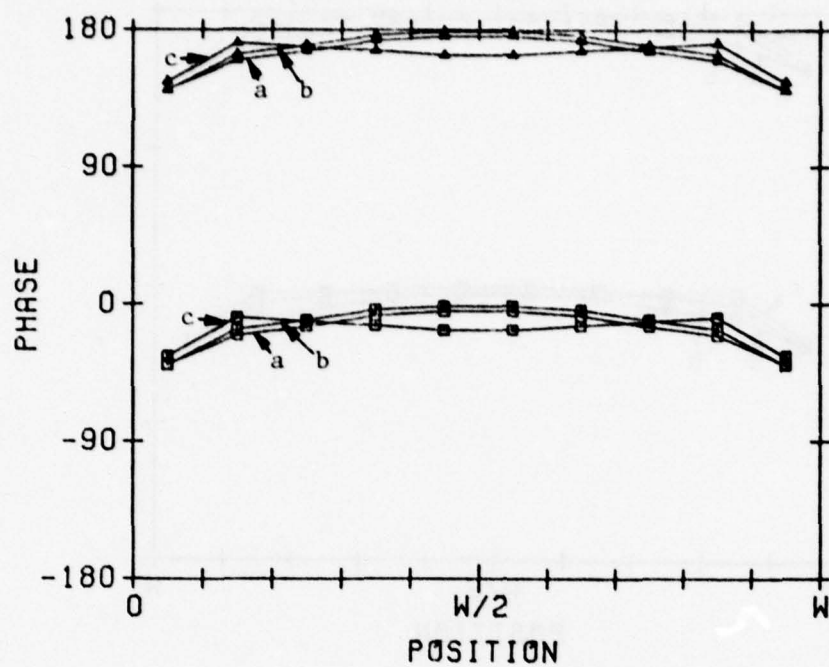


Fig. 7. Magnitude and phase of \bar{M}_1 (squares) and \bar{M}_2 (triangles)
for slit $w = .4\lambda_a$, $d = .001\lambda_a$, $k_b = k_a = k_o$ and
a) $\mu_c = \mu_o$; b) $\mu_c = 3\mu_o$; c) $\mu_c = 10\mu_o$. $N = 10$.

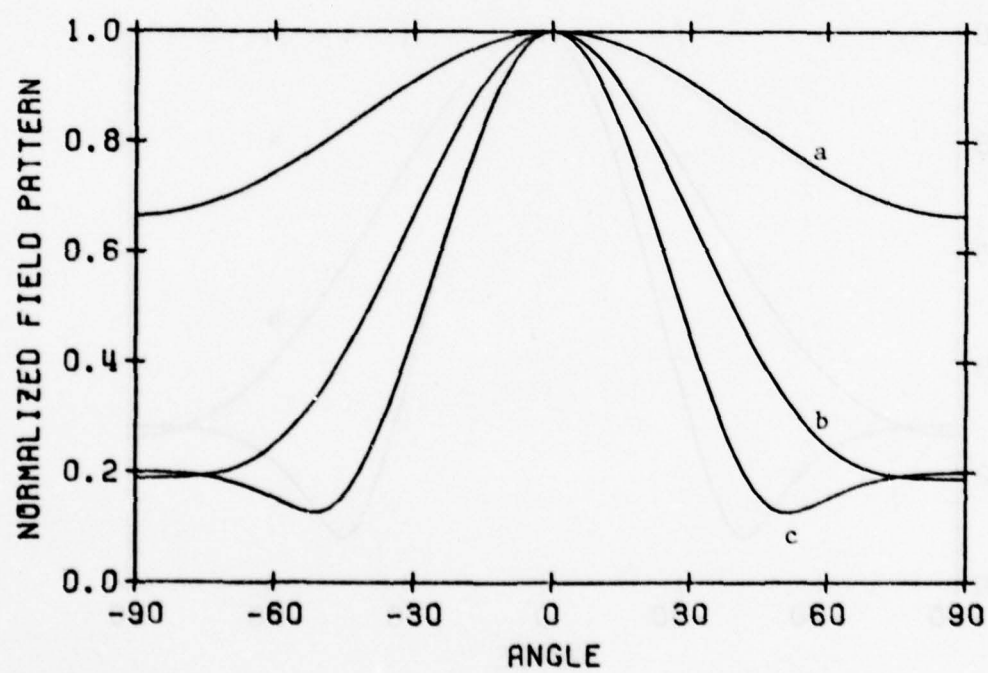
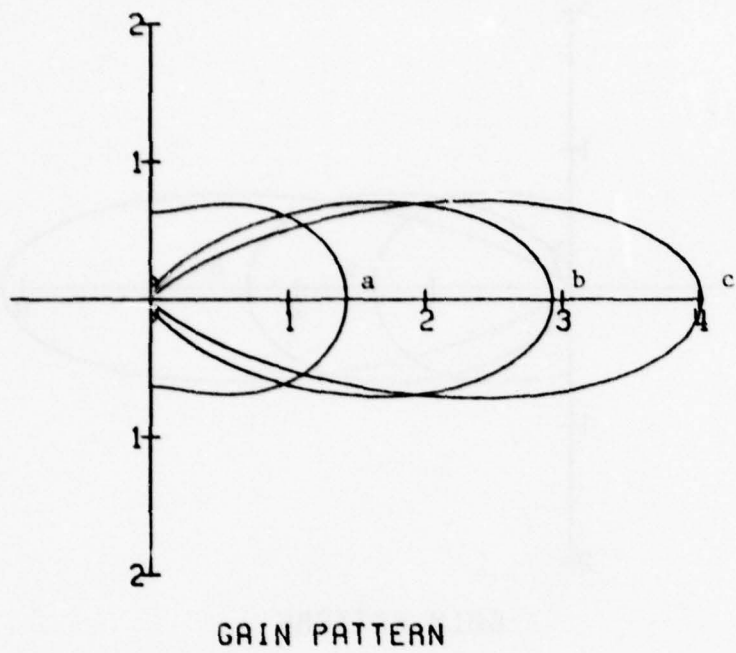
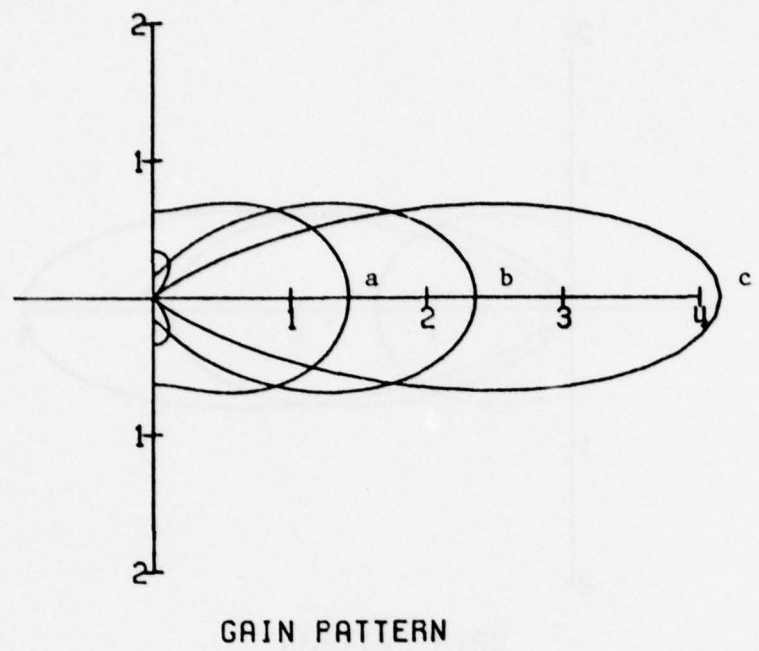


Fig. 8. Gain and normalized field patterns for slits in Fig. 6.



GAIN PATTERN

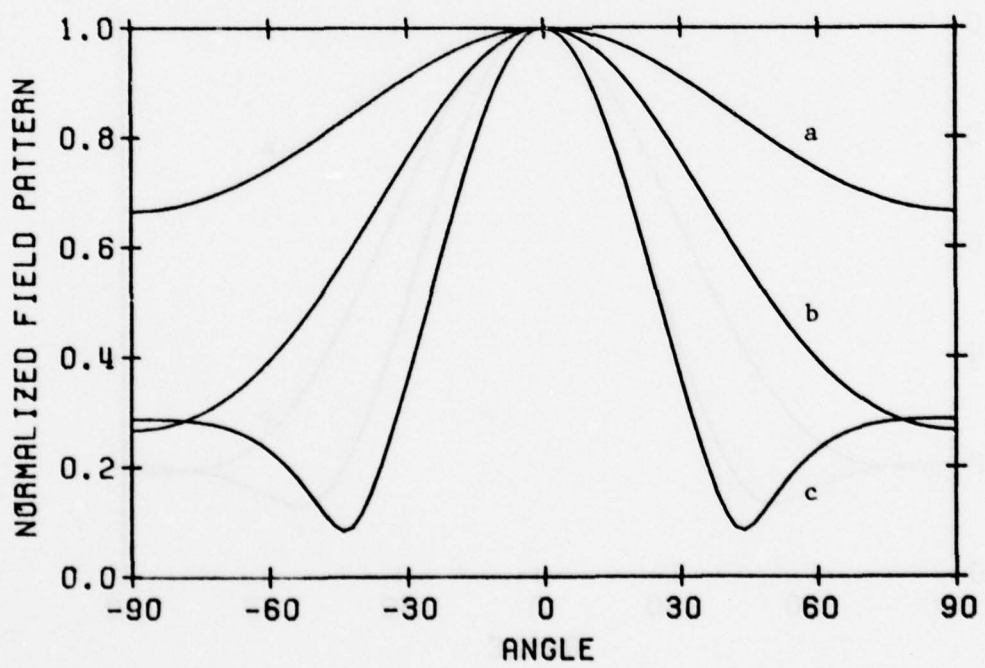


Fig. 9. Gain and normalized field patterns for slits in Fig. 7.

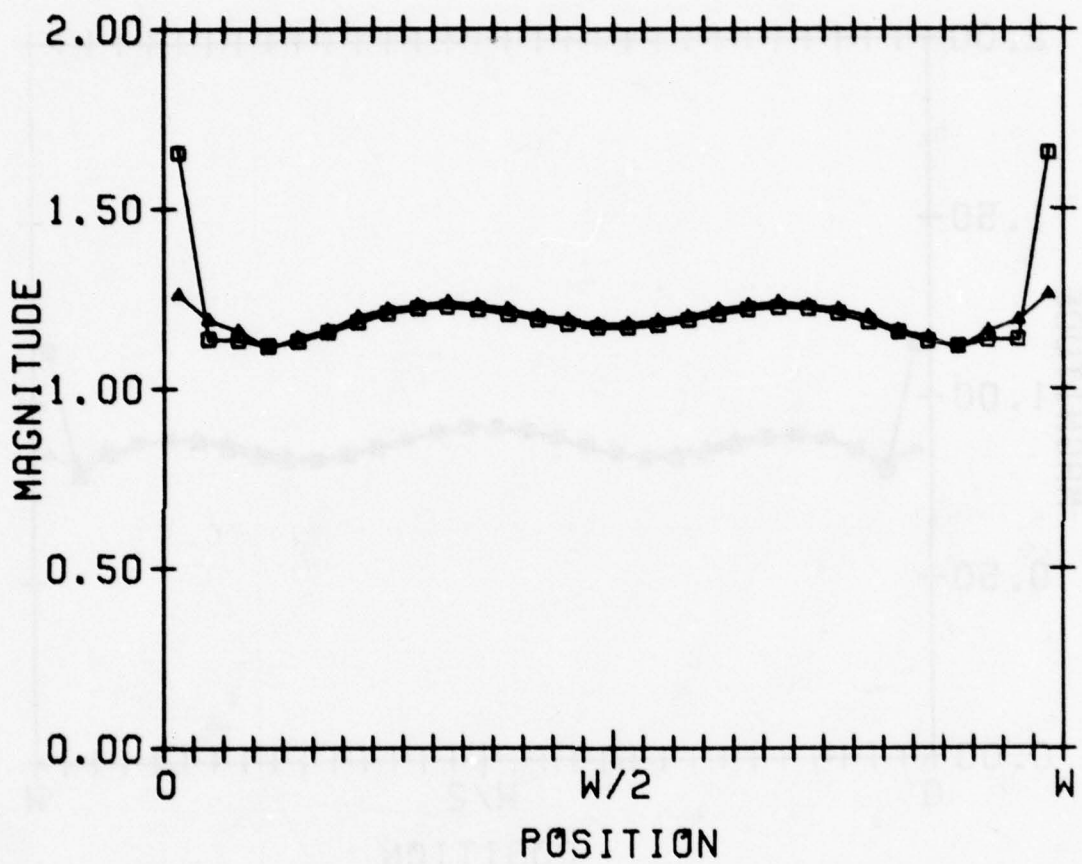


Fig. 10. Magnitude of \bar{M}_2 (squares) compared to values obtained from results given by Neerhoff and Mur [4] (triangles) for a slit with $w = 1\mu$ (micron), $d = .1\mu$, $\lambda_o = .4353\mu$, $k_a = 1.5k_o$, $k_c = k_b = k_o$.

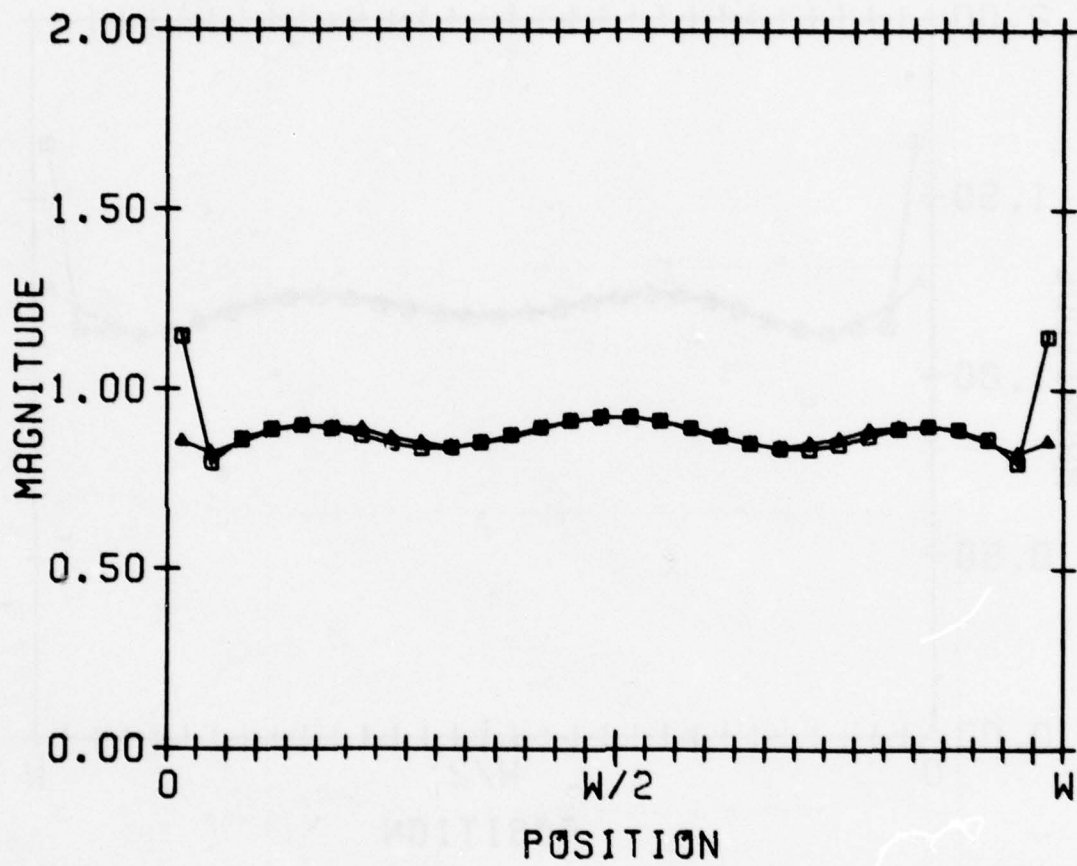


Fig. 11. Magnitude of \bar{M}_2 (squares) compared to values obtained from results given by Neerhoff and Mur [4] (triangles) for a slit with $w = 1\mu$ (micron), $d = .1\mu$, $\lambda_o = .4353\mu$, $k_a = 1.5k_o$, $k_c = 1.6k_o$, $k_b = k_o$.

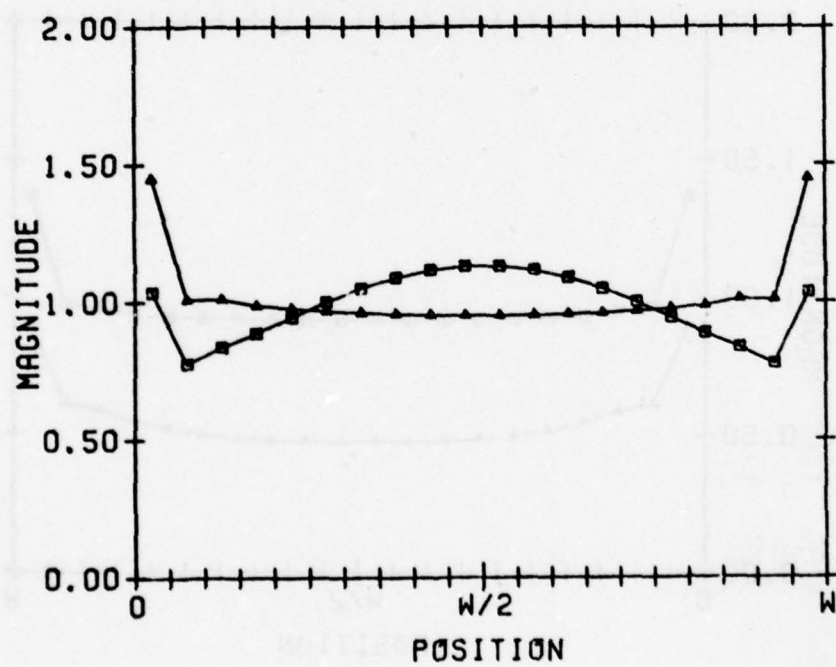
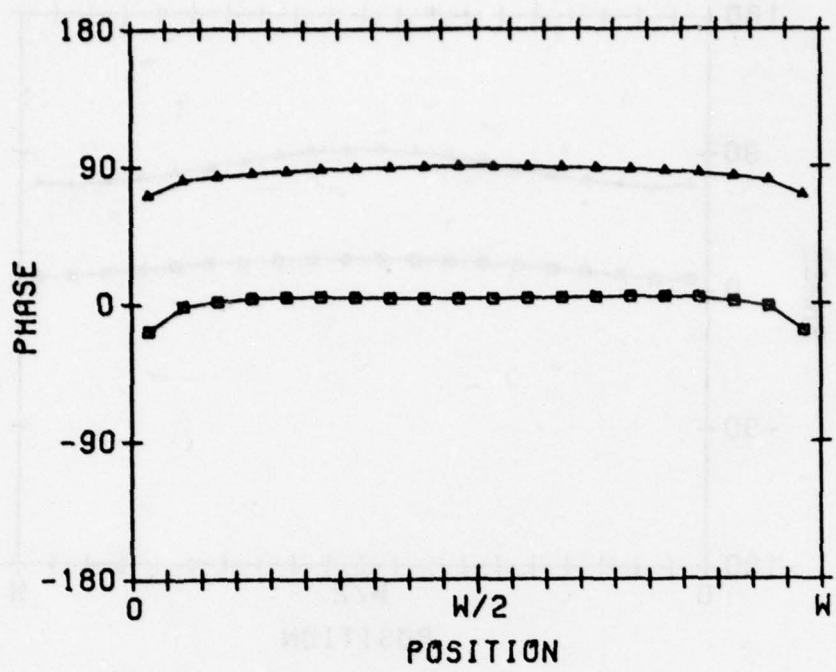


Fig. 12. Magnitude and phase of \bar{M}_1 (squares) and \bar{M}_2 (triangles)
 for $\epsilon_a = \epsilon_c = \epsilon_b = \epsilon_o$, $d = .25\lambda_a$, $w = 1\lambda_a$. $N = 20$.

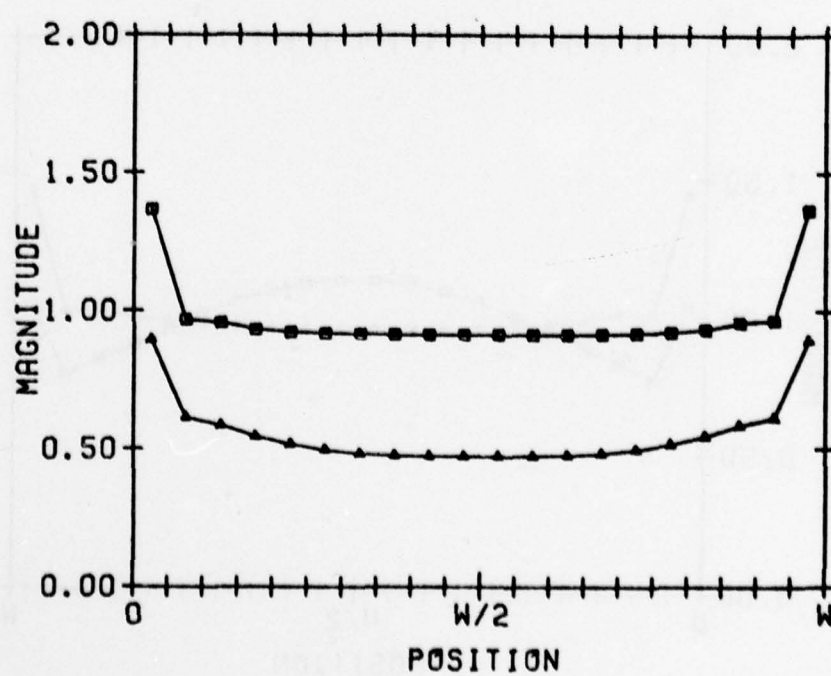
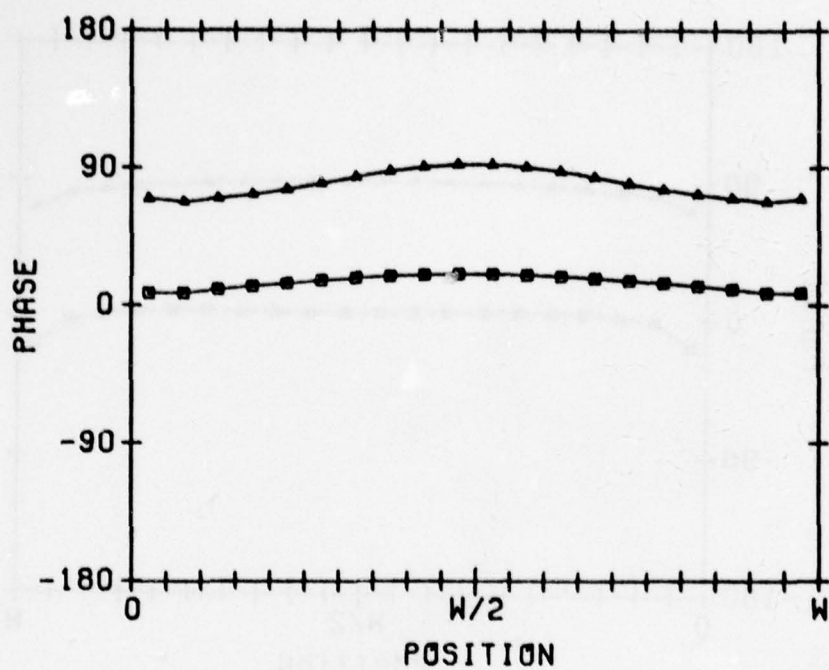


Fig. 13. Magnitude and phase of \bar{M}_1 (squares) and \bar{M}_2 (triangles)
 for $\epsilon_a = \epsilon_c = \epsilon_o$, $d = .25\lambda_a$, $w = 1\lambda_a$, and
 $\epsilon_b = (1-j)\epsilon_o$. $N = 20$.

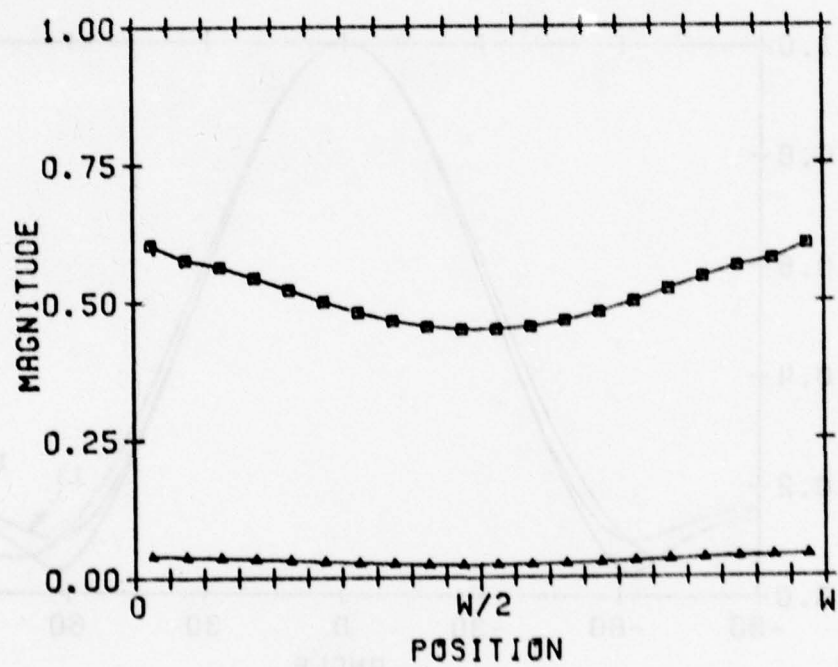
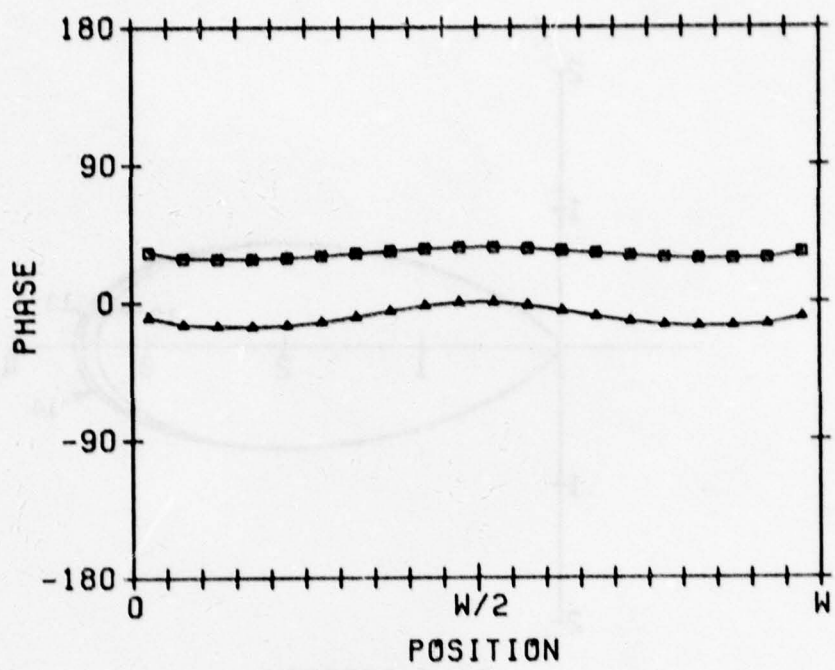


Fig. 14. Magnitude and phase of \bar{M}_1 (squares) and \bar{M}_2 (triangles)
 for $\epsilon_a = \epsilon_c = \epsilon_0$, $d = .25\lambda_a$, $w = 1\lambda_a$, and
 $\epsilon_b = (1-j10)\epsilon_0$. $N = 20$.

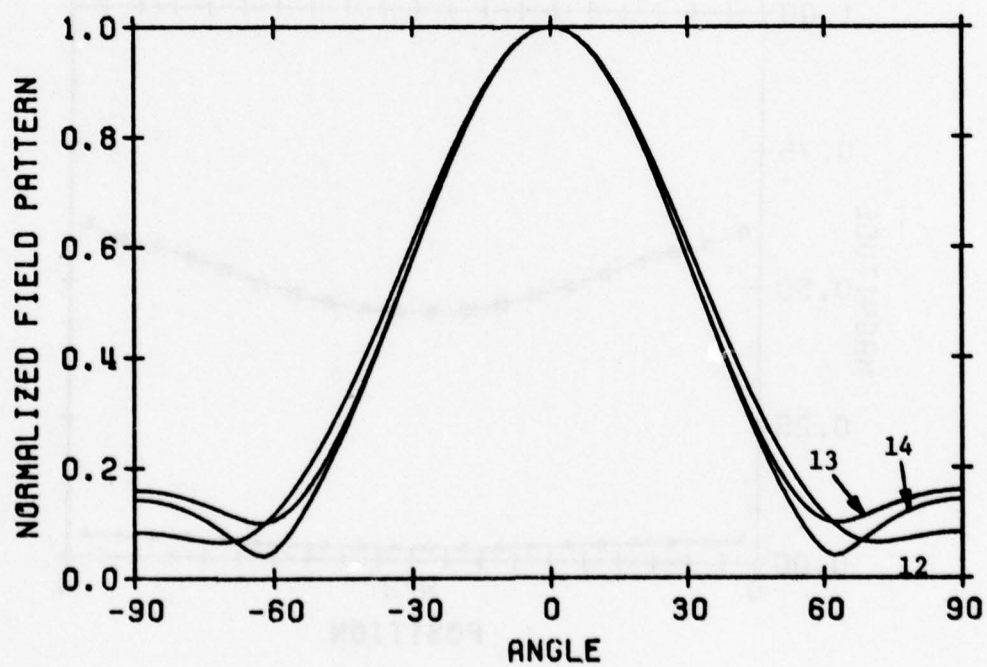
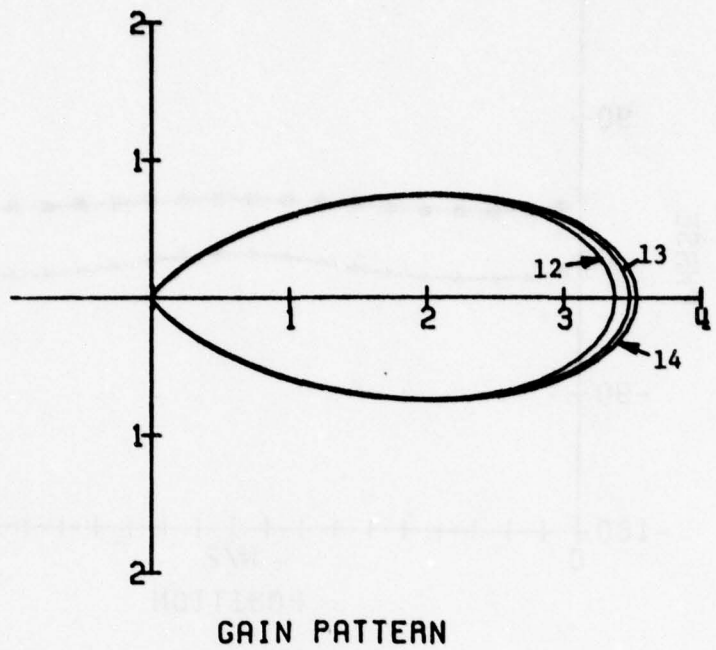
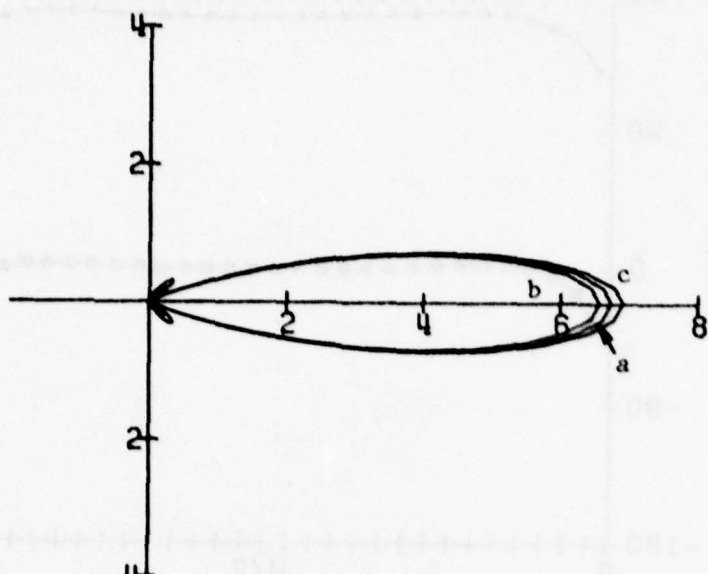


Fig. 15. Gain and normalized far field patterns for slits
in Figures 12, 13, and 14.



GAIN PATTERN

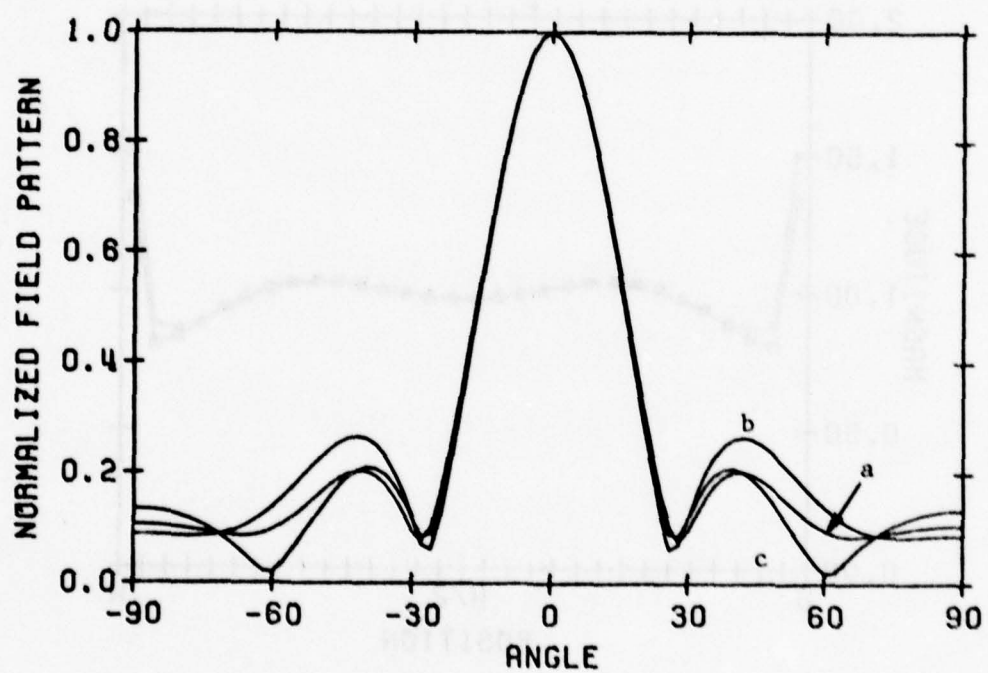


Fig. 16. Gain and normalized field patterns for $k_a = k_c = k_o$,
 $w = 2.148\lambda_a$ and a) $d = .0417\lambda_a$, $\epsilon_b = \epsilon_o$; b) $d = 1.331\lambda_a$,
 $\epsilon_b = \epsilon_o$; c) $d = 1.331\lambda_a$, $\epsilon_b = 2.59\epsilon_o$.

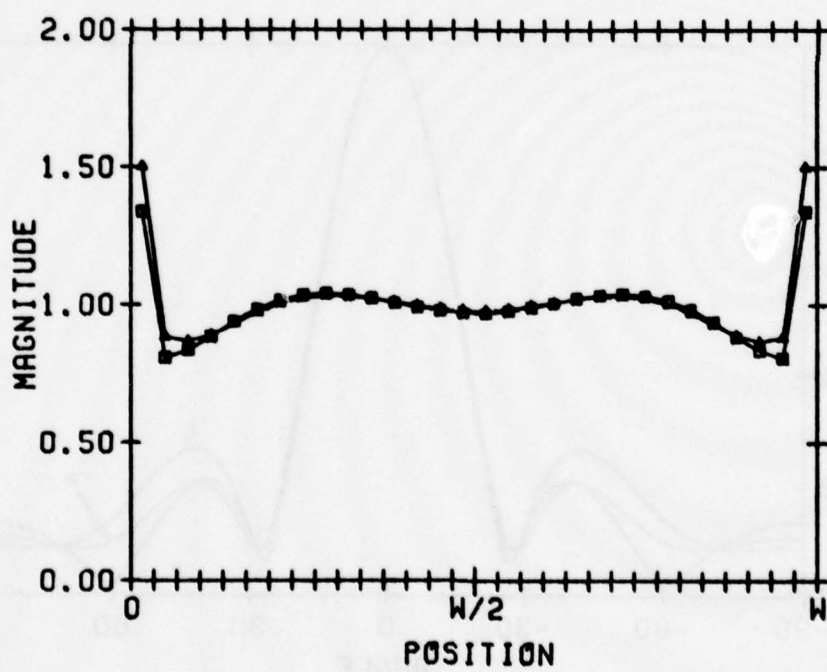
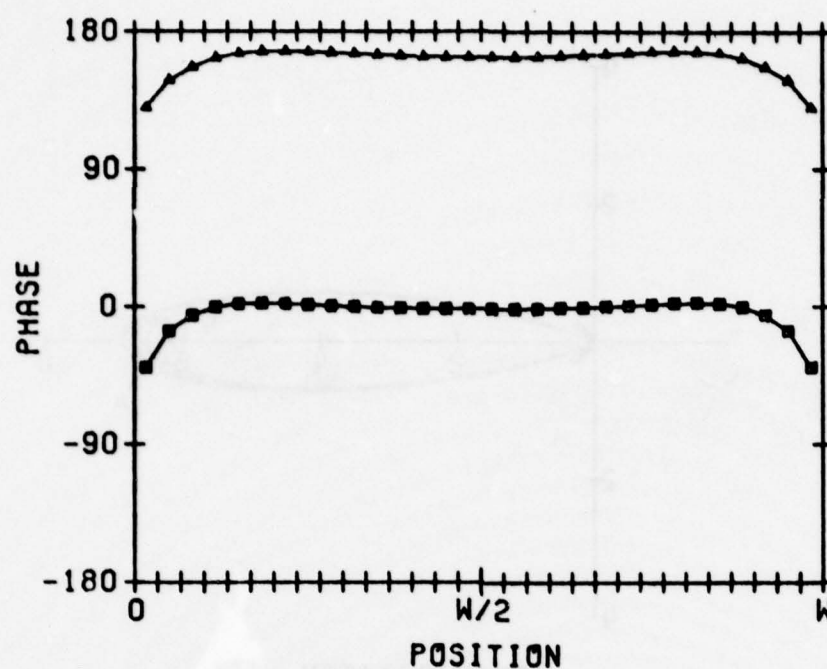


Fig. 17. Magnitude and phase of \bar{M}_1 (squares) and \bar{M}_2 (triangles)
for slit a in Fig. 16. $N = 30$.

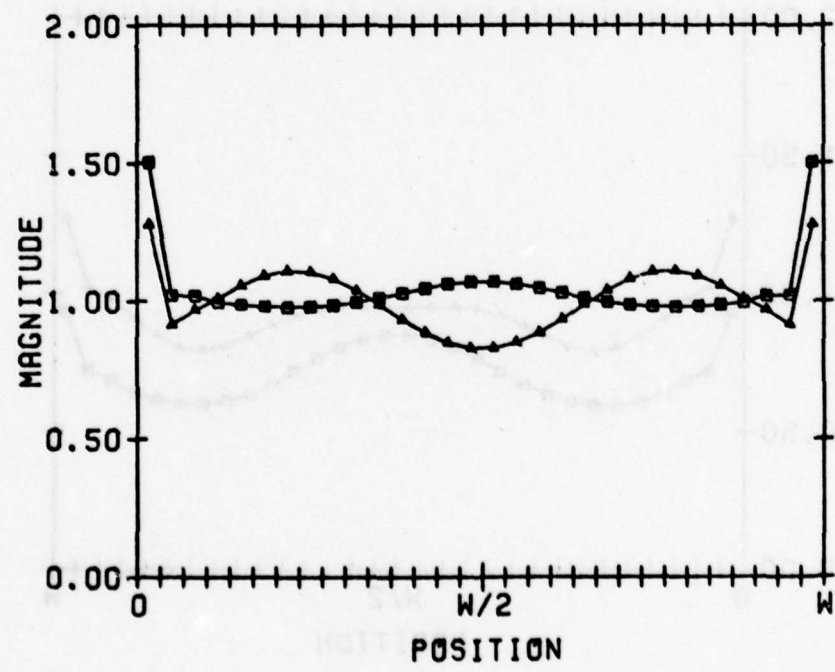
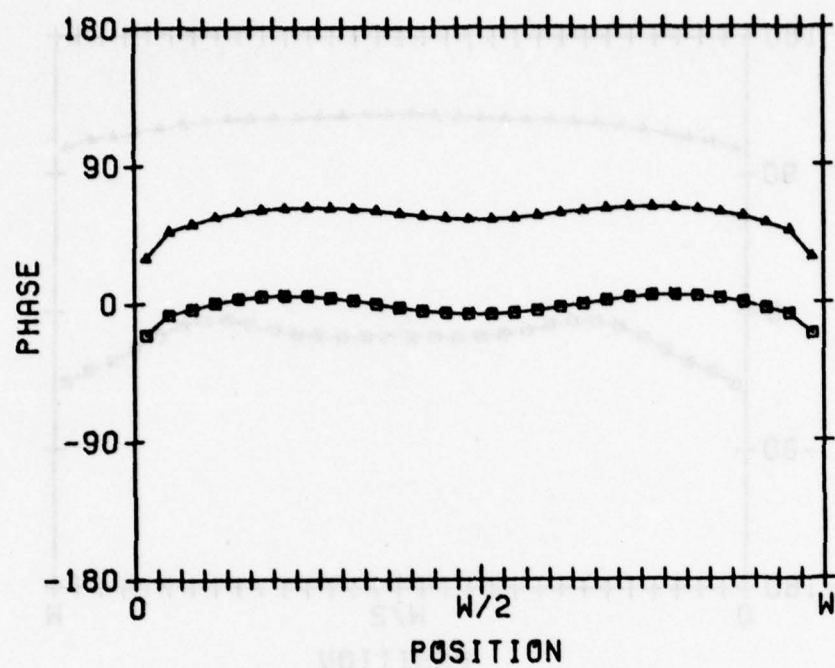


Fig. 18. Magnitude and phase of \bar{M}_1 (squares) and \bar{M}_2 (triangles)
for slit b in Fig. 16. $N = 30$.

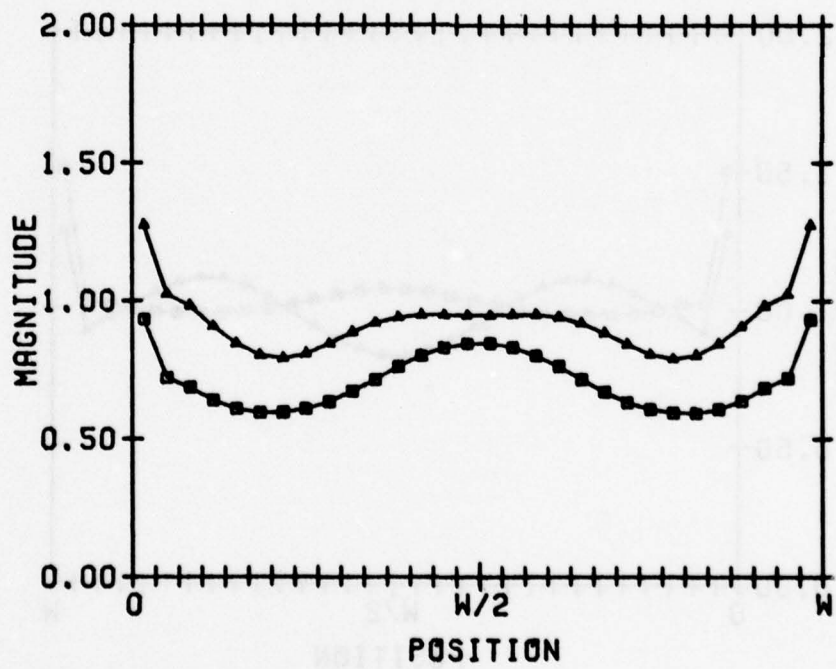
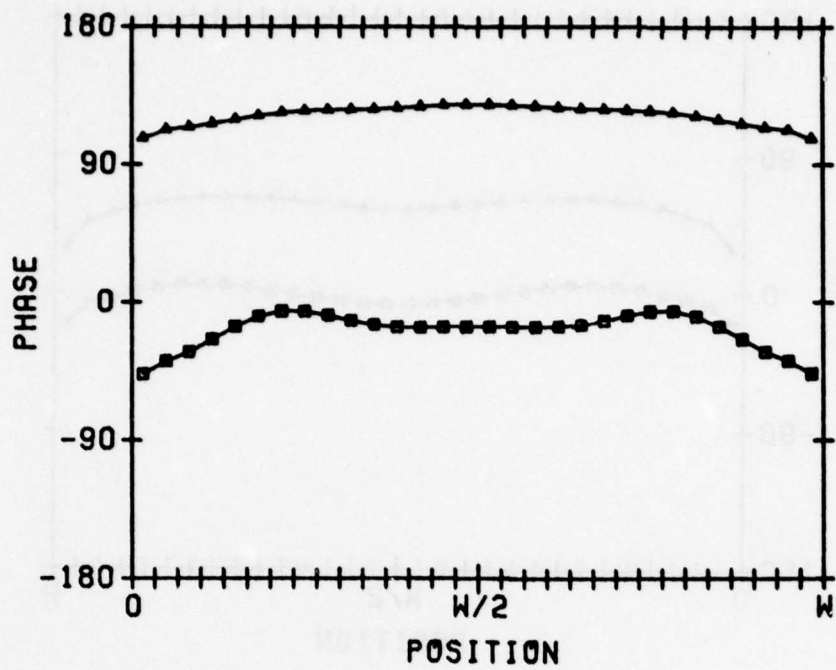


Fig. 19. Magnitude and phase of \bar{M}_1 (squares) and \bar{M}_2 (triangles)
for slit c in Fig. 16. $N = 30$.

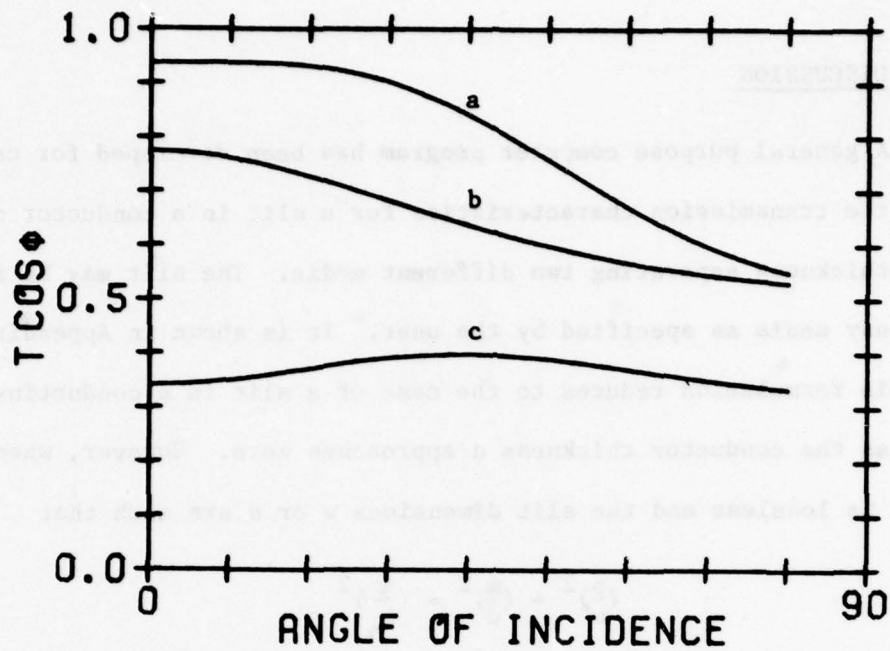


Fig. 20. Transmission coefficient times $\cos \phi$ versus ϕ where ϕ is the angle of incidence measured from the negative x axis for $w = .8\lambda_a$, $d = .25\lambda_a$, $k_a = k_c = k_o$; a) $\epsilon_b = \epsilon_o$, b) $\epsilon_b = 5\epsilon_o$, c) $\epsilon_b = 10\epsilon_o$.

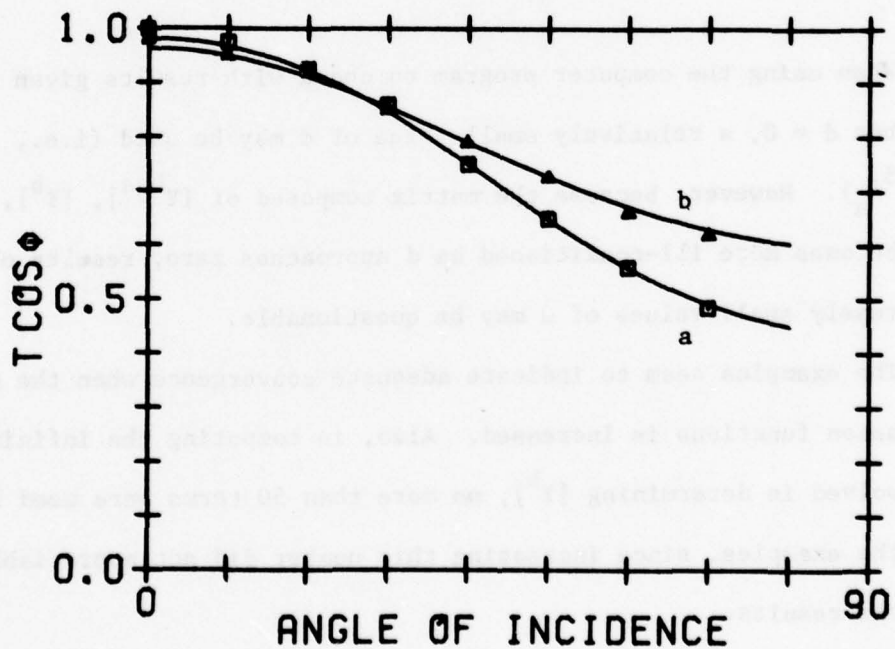


Fig. 21. Transmission coefficient times $\cos \phi$ versus ϕ where ϕ is the angle of incidence measured from the negative x axis for $k_a = k_c = k_o$; a) $w = 1.02\lambda_a$, $d = 10^{-5}\lambda_a$, b) $w = .51\lambda_a$, $d = 10^{-4}\lambda_a$. Squares and triangles represent values taken from [13] for $d = 0$.

VIII. DISCUSSION

A general purpose computer program has been developed for calculating the transmission characteristics for a slit in a conductor of finite thickness separating two different media. The slit may be filled with lossy media as specified by the user. It is shown in Appendix A that this formulation reduces to the case of a slit in a conducting screen as the conductor thickness d approaches zero. However, when media b is lossless and the slit dimensions w or d are such that

$$\left(\frac{p}{w}\right)^2 + \left(\frac{m}{d}\right)^2 = \left(\frac{2}{\lambda_b}\right)^2$$

is satisfied for any integer p and m , some terms of $[Y^b]$ become infinite and our solution fails. In this case we obtain a solution by perturbing the dimensions w or d slightly so that the region b is no longer a resonant cavity.

When using the computer program to check with results given for slits when $d = 0$, a relatively small value of d may be used (i.e., $d \approx 10^{-5} \lambda_a$). However, because the matrix composed of $[Y^{hsa}]$, $[Y^b]$, and $[Y^{hsc}]$ becomes more ill-conditioned as d approaches zero, results obtained for extremely small values of d may be questionable.

The examples seem to indicate adequate convergence when the number of expansion functions is increased. Also, in computing the infinite sums involved in determining $[Y^b]$, no more than 50 terms were used for any of the examples, since increasing this number did not appreciably affect the results.

Appendix A
NOTES ON THE COMPUTATION OF $[Y^b]$

The elements of the submatrices of $[Y^b]$ are given by equations (32), (33), (40), and (41). All of the equations have the following integral in common:

$$I = \int_{\Delta m_{1,2}} \int_{\Delta n_{1,2}} \cos \frac{p\pi y}{w} \cos \frac{p\pi y'}{w} dy dy' \quad (A-1)$$

where $\Delta m_{1,2}$ and $\Delta n_{1,2}$ are intervals over which the expansion or testing function is nonzero on Γ_1 or Γ_2 for $m, n=1,2,\dots,N$. Using the trigonometric identity

$$\sin px - \sin p(n-1)x = 2 \sin \frac{px}{2} \cos \left[p \left(n - \frac{1}{2} \right) x \right]$$

where p and n are integers, Eq. (A-1) becomes

$$I = (\Delta y)^2 \frac{\sin^2 \frac{p\pi}{2N}}{\left(\frac{p\pi}{2N}\right)^2} \cos \left[\frac{p\pi}{N} \left(m - \frac{1}{2} \right) \right] \cos \left[\frac{p\pi}{N} \left(n - \frac{1}{2} \right) \right] \quad (A-2)$$

where $\Delta y = \frac{w}{N}$. Now write matrices $[Y^{11}]$ and $[Y^{12}]$ as

$$[Y^{11}] = \sum_{p=0}^{\infty} a_p [F^{(p)}] \quad (A-3)$$

and

$$[Y^{12}] = \sum_{p=0}^{\infty} b_p [F^{(p)}] \quad (A-4)$$

where

$$a_p = - \frac{j\omega \epsilon_b \epsilon_p (\Delta y)^2}{w} \frac{\cot k_{xp} d}{k_{xp}} \frac{\sin^2 \frac{p\pi}{2N}}{\left(\frac{p\pi}{2N}\right)^2} \quad (A-5)$$

$$b_p = - \frac{j\omega \epsilon_b \epsilon_p (\Delta y)^2}{w} \frac{\csc k_{xp} d}{k_{xp}} \frac{\sin^2 \frac{p\pi}{2N}}{\left(\frac{p\pi}{2N}\right)^2} \quad (A-6)$$

The matrix $[F^{(p)}]$ is given by

$$[F^{(p)}] = \bar{f}_p \tilde{f}_p \quad (A-7)$$

where

$$\tilde{f}_p = [\cos \frac{p\pi}{2N}, \cos 3\frac{p\pi}{2N}, \dots, \cos 2 \frac{p\pi(N - \frac{1}{2})}{2N}] \quad (A-8)$$

Matrices $[Y^{12}]$ and $[Y^{22}]$ may be written in terms of the above according to Eq. (16).

It is evident that for various values of k_{xp} or $k_{xp}d$ when the medium in region b is lossless, the coefficients a_p and b_p become infinite. These cases are summarized as

- 1) $d = 0, k_{xp} \neq 0.$
- 2) $k_{xp}d = m\pi \quad \text{for } m = 0, 1, 2, \dots$

To examine these cases in further detail we rewrite Eqs. (11a,b) using Eq. (16):

$$[Y^{11} + Y^{hsa}] \bar{v}_1 + [Y^{12}] \bar{v}_2 = \bar{i}^1 \quad (A-9)$$

$$[Y^{12}] \bar{v}_1 + [Y^{11} + Y^{hsc}] \bar{v}_2 = \bar{0} \quad (A-10)$$

For case 1 when d is very small, a suitable approximation to $\cot x$ and $\csc x$ yields

$$[Y^{11}] \approx [Y^{12}]$$

and

$$[Y^{11}]^{-1} \rightarrow [0]$$

Next multiply Eq. (A-10) by $[Y^{11}]^{-1}$ to obtain

$$\bar{v}_1 = - \bar{v}_2 \quad (A-11)$$

then subtract (A-10) from (A-9) and use Eq. (A-11) to get

$$[Y^{\text{hsa}} + Y^{\text{hsc}}] \bar{v}_1 = \bar{I}^1 \quad (A-12)$$

This is the expected result when the thickness of the conducting screen is zero [5, p. 7].

An analytical expression for Eqs. (A-9) and (A-10) as $k_{xp} d + mw$ in case 2 is not attempted here. Instead, when the dimensions w and d are such that case 2 arises for some integers m and p , the computations are done for dimensions $w + \Delta\lambda_b$ or $d + \Delta\lambda_b$ wherever appropriate where $\Delta\lambda_b$ is a small fraction of the wavelength in region b.

Appendix B
COMPUTER PROGRAM

B-1. Required Data

The required data cards are read in according to the format:

```
100      FORMAT(6E11.4)  
  
101      FORMAT(6I5)  
  
        READ(1,100) NMUA, NEPSA  
        READ(1,100) NMUB, NEPSB  
        READ(1,100) NMUC, NEPSC  
        READ(1,100) W, D  
        READ(1, 100)PHIO, DPHI, FMC  
        READ(1,101)N, NI, NT, NEXC  
        READ(1,101) ICUR, IGA  
        DO 1 I = 1, NEXC  
        READ(1,100) XSC(I), YSC(I)  
  
1       CONTINUE
```

The input parameters are defined as

$$\begin{aligned} \text{NMUA} &= \mu_a / \mu_0 \\ \text{NEPSA} &= \epsilon_a / \epsilon_0 \\ \text{NEPSB} &= \epsilon_b / \epsilon_0 \\ \text{NMUB} &= \mu_b / \mu_0 \\ \text{NMUC} &= \mu_c / \mu_0 \\ \text{NEPSC} &= \epsilon_c / \epsilon_0 \\ \text{W} &= \text{slit width in meters.} \\ \text{D} &= \text{slit thickness d, in meters} \end{aligned}$$

PHIO = angle in degrees at which first gain measurement
is computed.

DPHI = increment in degrees at which gain pattern is
computed.

FMC = frequency of magnetic line source in megahertz.

N = number of expansion functions on slit face Γ_1 or Γ_2
(total number of unknown magnetic currents = 2N).

NI = number of gain measurements to be computed for each
pattern.

NT = number of terms used to approximate the infinite
summations in Eqs. (A-3) and (A-4).

NEXC = number of excitations (i.e., number of right hand sides
to Eqs. (11a, b)).

ICUR = integer option variable. If ICUR = 1, the magnetic
currents will be printed for each excitation. If
ICUR \neq 1, printout will be bypassed.

IGA = integer option variable. If IGA = 1, a gain pattern and
far field patterns will be computed for each excitation.
If IGA \neq 1, this computation will be bypassed.

XSC(J) = x coordinate of jth magnetic line source in meters.

YSC(J) = y coordinate of jth magnetic line source in meters.

The minimum storage allocations in the main program are given
by:

```
COMPLEX Y(N*(2*N+1)), VM(2*N), YHSA(N),  
YHS (N), VM2(NEXC*2*N)  
DIMENSION GA(NI), FP(NI), PHI(NI),  
PHIR(NI), XSC(NEXC), YSC(NEXC)
```

For subroutine TRANS the minimum allocation is

```
COMPLEX YAUX(N)
```

for subroutine GELS,

```
COMPLEX R(N*2*NEXC) , AUX(N*2*NEXC)
```

and for subroutine YB,

```
COMPLEX ST1(NT), ST2(NT), CXP(NT)
```

```
DIMENSION SINC2(NT)
```

B-2. Main Program Description

The first quantities to be computed are the wavenumbers and impedances in each region normalized by k_o and η_o respectively where k_o = wavenumber of free space and η_o = impedance of free space. It has been noted that whenever the dimensions w or d are integral multiples of a half wavelength in region b (for the lossless case) computational difficulties are encountered. This condition is checked for in statement 50 where the dimensions are perturbed slightly if necessary. Next the dimensions are changed to electrical lengths by multiplying by k_o . The actual ordering of the magnetic current expansion functions along slit faces Γ_1 and Γ_2 is shown in Fig. B-1. Here, $\{\Delta y_1, \Delta y_2, \dots, \Delta y_N\}$ are the regions on which $\bar{M}_{1n} \neq 0$ for $n=1, 2, \dots, N$ and $\{\Delta y_{N+1}, \Delta y_{N+2}, \dots, \Delta y_{2N}\}$ are the regions on which $\bar{M}_{2m} \neq 0$, for $m = 1, 2, \dots, N$.

The first step in solving Eqs. (11a,b) is to compute the necessary matrix elements as given by Eqs. (12). For convenience, each side of Eqs. (11a,b) are multiplied by the factor $\eta_o k_o$. Since $[Y^{hsa}]$ and $[Y^{hsc}]$ are symmetric Toeplitz matrices and $[Y^{11}]$ and $[Y^{12}]$ are symmetric, only the upper right triangular portion of

$$[Y] = \eta_o k_o \begin{bmatrix} [Y^{11} + Y^{hsa}] & [Y^{12}] \\ [Y^{12}] & [Y^{11} + Y^{hsc}] \end{bmatrix} \quad (B-1)$$

is computed. This is stored in array Y in the main program by columns. The first column of $\eta_o k_o [Y^{hsa}]$ is computed from Eq. (18) with statement 51 and the result is stored in array YHSA. The first column of

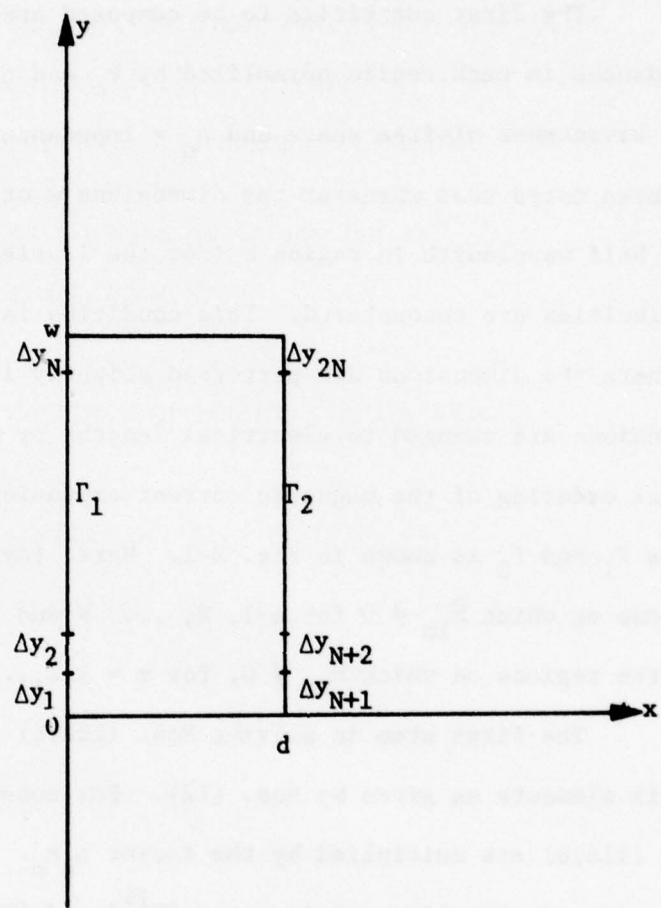


Fig. B-1. Expansion and testing function numbering system on slit faces.

$\eta_o k_o [Y^{hsc}]$ is next computed and stored in array YHSC in statement 52.

Statement 53 computes the upper right triangle of the matrix

$$\eta_o k_o \begin{bmatrix} [H^{11}] & [Y^{12}] \\ [Y^{12}] & [Y^{11}] \end{bmatrix}$$

and stores the result temporarily in array Y. DO loop 2 then adds $\eta_o k_o [Y^{hsa}]$ and $\eta_o k_o [Y^{hsc}]$ to the proper elements of the above temporary matrix and stores the final result in array Y which is the upper right triangular portion of Eq. (B-1).

Each excitation vector $\eta_o k_o \tilde{I}^1$ corresponding to a magnetic line source at (XSC(I), YSC(I)) is computed in statement 54 and stored temporarily in array VM. This operation is done NEXC times in DO loop 3 where each VM is stored consecutively in array VM2. The solution to Eqs. (11a and b) is then found by statement 55 where the input array VM2 now contains the solution for each excitation. The coefficients of magnetic currents are printed out in DO loop 4 of ICUR = 1. DO loop 17 computes a transmission coefficient for each excitation and a gain and normalized field pattern if IGA = 1.

MAIN PROGRAM LISTING

THIS PAGE IS BEST QUALITY PRACTICABLE
FROM COPY FURNISHED TO DDC

```

$JOB      AUCK,TIME=2,RAGES=40
C-----CORRECTED TRANSVERSE ELECTRIC THICK SLIT PROGRAM
C      EASED ON REPORT TR-77-9
COMPLEX VM2(1820),Y(528),YHSA(16),YHSC(16),VM(32)
COMPLEX CSQRT,CSIN,ECOS,HANK02,HANK12,CONJG
COMPLEX ETANB,U,NMUB,NEPSB,WAVNB,STK
DIMENSION XSC(91),YSC(91),PHI(91),PHIR(91),GA(91),FP(91)
COMMON WAVNO,PI,U
REAL NMUA,NMUC,NEPSA,NEPSC
DATA ETA/376.730/,EPS0/8.85E-12/
PI=3.141593
U=(0.,1.)
100 FORMAT(6E11.4)
101 FORMAT(6I5)
READ(1,100) NMUA,NERSA
READ(1,100) NMUB,NEPSB
READ(1,100) NMUC,NERSC
READ(1,100) W,D
READ(1,100) PHI0,CPHI,FMC
READ(1,101) N,NI,NT,NEXC
READ(1,101) ICUR,IGA
DO 1 I=1,NEXC
READ(1,100) XSC(I),YSC(I)
PRINT,I,XSC(I),YSC(I)
1 CONTINUE
PRINT,"NEPSB=",NEPSB,"NMUB=",NMUB
PRINT,"NMUA=",NMUA,"NEPSA=",NEPSA
PRINT,"NMUC=",NMUC,"NEPSC=",NEPSC
PRINT,"W=",W,"D=",D
PRINT,"PHI0=",PHI0,"DPHI=",DPHI,"FMC=",FMC
PRINT,"N=",N,"NI=",NI,"NT=",NT,"NEXC=",NEXC
PRINT,"ICUR= ",ICUR,"IGA= ",IGA
C-----CCMPUTE WAVENUMBER OF FREE SPACE.
WAVNO=PI*FMC/150.
C-----COMPUTE WAVE NCES OF REGIONS A,B, AND C NORMALIZED
C      BY WAVNO.
WAVNA=SQRT(NMUA*NEPSA)
WAVNE=CSQRT(NMUB*NEPSB)
WAVNC=SQRT(NMUC*NEPSC)
C-----COMPUTE INTRINSIC IMPEDANCES OF REGIONS A, B, AND C
C      NORMALIZED BY ETA.
ETANA=SQRT(NMUA/NEPSA)
ETANE=CSQRT(NMUB/NEPSB)
ETANC=SQRT(NMUC/NEPSC)
PRINT,WAVNB,ETANB,WAVNO
M=N*(N+1)/2
N2=2*N
M2=N2*(N2+1)/2
50    CALL PTB(W,D,WAVNB)

```

THIS PAGE IS BEST QUALITY PRACTICABLE
FROM COPY FURNISHED TO DDC

C-----CHANGE DIMENSIONS TO FREE SPACE ELECTRICAL LENGTHS.
W=WAVNO
D=D*WAVNO
DY=W/N
C-----CCMP. FIRST ROW OF ADMITTANCE MATRICES FOR REGIONS
C A AND B... STORE IN ARRAYS YHSA AND YHSC RESP.
51 CALL YHS(WAVNA*DY,N,YHSA,WAVNA,ETANA)
52 CALL YHS(WAVNC*DY,N,YHSC,WAVNC,ETANC)
53 CALL YB(Y,M2,WAVNB,ETANB,W,DY,NT,D,N)
DO 20 I=1,N
PRINT,YHSA(I),YHSC(I)
20 CONTINUE
C-----ADD HALF SPACE ADMITTANCE MATRICES TO Y11 AND Y22
C OF TOTAL ADMITTANCE MATRIX Y...
K=1
DO 2 J=1,N
DO 2 I=1,J
Y(K)=Y(K)+YHSA(J-I+1)
Y(M+J+N+K)=Y(M+J+N+K)+YHSC(J-I+1)
K=K+1
2 CONTINUE
DO 21 I=1,M2
PRINT,I,Y(I)
21 CONTINUE
C-----CCMP. EXCITATION MATRIX.
DO 3 I=1,NEXC
XS=XSC(I)*WAVNO
YS=YSC(I)*WAVNO
54 CALL TEEXC(WAVNA,WAVNA*XS,WAVNA*YS,N,WAVNA*DY,VM,N2,ETANA,STK,W
1AVNA*W)
DO 3 J=1,N2
VM2(J+(I-1)*N2)=VM(J)
3 CONTINUE
C-----SOLUTION OF MAGNETIC CURRENTS.
55 CALL GELS(VM2,Y,N2,NEXC,M2)
IF(ICUR.NE.1) GO TO 5
102 FORMAT(I5,4E17.7)
103 FORMAT('1',15X,'MAGNETIC CURRENTS FOR XS =',F8.3,3X,
*'AND YS =',F8.3)
DO 4 J=1,NEXC
WRITE(3,103) XSC(J),YSC(J)
DO 4 I=1,N2
K=I+(J-1)*N2
AI=AIMAG(VM2(K))
AR=REAL(VM2(K))
PHASE=180.*ATAN2(AI,AR)/PI
VA=CABS(VM2(K))
WRITE(3,102) I,VM2(K),VA,PHASE
4 CONTINUE
5 CONTINUE
DO 6 I=1,NI
PHI(I)=PHI0+(I-1)*DPHI
PHIF(I)=PI*PHI(I)/180.
5 CONTINUE

THIS PAGE IS BEST QUALITY PRACTICABLE
FROM COPY FURNISHED TO DDC

C-----COMP. OF TRANSMISSION COEFFICIENT.

```
105  FORMAT('1',18X,'XS',18X,'YS',1X,'TRANSMISSION COEFF.')
      WRITE(3,105)
      DO 7 J=1,NEXC
      DO 8 I=1,N2
        VM(I)=VM2(I+(J-1)*N2)
    8  CONTINUE
      XS=XSC(J)*WAVNO
      YS=YSC(J)*WAVNO
  56   CALL TRANS(N,N2,YHSA,PT,T,VM,STK,W,XS,YS,ETANA,WAVNA,TN)
  108  FORMAT(' ',4E20.7)
      WRITE(3,108) XSC(J),YSC(J),T,TN
      WRITE(2,109) XSC(J),YSC(J),T,TN
      IF(IGA.NE.1) GO TO 9
C-----COMP. GAIN PATTERN.
  57   CALL GAIN(PHIR,NI,N,N2,VM,DY,W,GA,WAVNC,ETANC,PT,FP)
  106  FORMAT(F20.1,2E20.7)
  107  FORMAT('1','POWER GAIN PATTERN IN REGION C AND ANGLE IN DEGREES')
      WRITE(3,107)
      DO 10 I=1,NI
        WRITE(3,106) PHI(I),GA(I),FP(I)
  10  CONTINUE
  9   CONTINUE
  7   CONTINUE
  STOF
  END
```

SAMPLE INPUT-OUTPUT

```
$DATA
      1 -0.1000000E 03  0.4000000E 00
NEPSB= ( 0.1000000E 01 , 0.0000000E 00)
NMUB= ( 0.1000000E 01 , 0.0000000E 00)
NMUA= 0.1000000E 01 NEPSA= 0.1000000E 01
NMUC= 0.1000000E 01 NEpsc= 0.1000000E 01
W= 0.8000000E 00 D= 0.2500000E 00
PHI0= -0.5000000E 02 Cphi= 0.8000000E 02
N= 10 NI= 19 NT= 50
ICUR= 1 IGA= 1
FMC= 0.3000000E 03
NEXC= 1
( 0.1000000E 01 , 0.0000000E 00)
( 0.1000000E 01 , 0.0000000E 00) 0.6283185E 01
```

THIS PAGE IS BEST QUALITY PRACTICABLE
FROM COPY FURNISHED TO DDC

PRINTOUT OF FIRST COLUMN OF YM_A AND YM_C...

```
( 0.1250820E 00 , 0.1858855E 00) ( 0.1250820E 00 , 0.1858855E 00)
( 0.1172774E 00 , 0.6457388E-01) ( 0.1172774E 00 , 0.6457388E-01)
( 0.9551698E-01 , -0.9290889E-02) ( 0.9551698E-01 , -0.9290889E-02)
( 0.6373584E-01 , -0.4697579E-01) ( 0.6373584E-01 , -0.4697579E-01)
( 0.2769190E-01 , -0.612484F-01) ( 0.2769190E-01 , -0.612484F-01)
( -0.6279565E-02 , -0.6151736E-01) ( -0.6279565E-02 , -0.6151736E-01)
( -0.3253630E-01 , -0.4625398E-01) ( -0.3253630E-01 , -0.4625398E-01)
( -0.4722714E-01 , -0.2274257E-01) ( -0.4722714E-01 , -0.2274257E-01)
( -0.4898727E-01 , 0.2879364E-02) ( -0.4898727E-01 , 0.2879364E-02)
( -0.3909317E-01 , 0.2479246E-01) ( -0.3909317E-01 , 0.2479246E-01)
```

PRINTOUT OF UPPER RT. TRIANGLE OF Y...

1 (0.1250820E 00 , 0.3844130E 00)	58 (0.0000000E 00 , -0.1531681E 00)
2 (0.1172774E 00 , 0.7049739E-01)	59 (0.0000000E 00 , -0.1692446E 00)
3 (0.1250820E 00 , 0.2748093E 00)	60 (0.0000000E 00 , -0.1534147E 00)
4 (0.9551698E-01 , -0.1129717E 00)	61 (0.0000000F 00 , -0.1040408E 00)
5 (0.1172774E 00 , 0.2554401E-01)	62 (0.0000000E 00 , -0.3081196E-01)
5 (0.1250820E 00 , 0.2786530E 00)	63 (0.0000000E 00 , 0.4924359E-01)
7 (0.6373584E-01 , -0.1956093E 00)	64 (0.0000000E 00 , 0.1167789E 00)
9 (0.9551698E-01 , -0.1091290E 00)	65 (0.0000000E 00 , 0.1552752E 00)
9 (0.1172774E 00 , 0.6990689E-01)	65 (0.1250820E 00 , 0.3844130E 00)
10 (0.1250820E 00 , 0.3497829E 00)	67 (0.0000000E 00 , -0.1198969E 00)
11 (0.2769190E-01 , -0.2079151E 00)	68 (0.0000000E 00 , -0.1266469E 00)
12 (0.6373584E-01 , -0.1512464E 00)	69 (0.0000000F 00 , -0.1359733E 00)
13 (0.9551698E-01 , -0.3799730E-01)	70 (0.0000000E 00 , -0.1373387E 00)
14 (0.1172774E 00 , 0.1490885E 00)	71 (0.0000000E 00 , -0.1198705E 00)
15 (0.1250820E 00 , 0.4169617E 00)	72 (0.0000000F 00 , -0.8018625E-01)
15 (-0.6279565E-02 , -0.1619459E 00)	73 (0.0000000E 00 , -0.2398527E-01)
17 (0.2769190E-01 , -0.1367847E 00)	74 (0.0000000E 00 , 0.3672381E-01)
18 (0.6373584E-01 , -0.7206637E-01)	75 (0.0000000E 00 , 0.8773917E-01)
19 (0.9551698E-01 , 0.2918159E-01)	75 (0.0000000E 00 , 0.1167789E 00)
20 (0.1172774E 00 , 0.1874563E 00)	77 (0.1172774E 00 , 0.7049739E-01)
21 (0.1250820E 00 , 0.4169624E 00)	78 (0.1250820E 00 , 0.2748093E 00)
22 (-0.3253630E-01 , -0.7555091E-01)	79 (0.0000000E 00 , -0.1531681E 00)
23 (-0.6279565E-02 , -0.8276433E-01)	80 (0.0000000E 00 , -0.1359733E 00)
24 (0.2769190E-01 , -0.6960593E-01)	81 (0.0000000E 00 , -0.1108171E 00)
25 (0.6373584E-01 , -0.3360741E-01)	82 (0.0000000F 00 , -0.8659899E-01)
26 (0.9551698E-01 , 0.2918159E-01)	83 (0.0000000E 00 , -0.6410986E-01)
27 (0.1172774E 00 , 0.1490886E 00)	84 (0.0000000E 00 , -0.3981519E-01)
28 (0.1250820E 00 , 0.3497834E 00)	85 (0.0000000E 00 , -0.1265056E-01)
29 (-0.4722714E-01 , 0.2714213E-01)	85 (0.0000000E 00 , 0.1451089E-01)
30 (-0.3253630E-01 , -0.6372154E-02)	87 (0.0000000F 00 , 0.3672393E-01)
31 (-0.6279565E-02 , -0.4439541E-01)	88 (0.0000000E 00 , 0.4924377E-01)
32 (0.2769190E-01 , -0.6960541E-01)	89 (0.9551698E-01 , -0.1129717E 00)
33 (0.6373584E-01 , -0.7206637E-01)	90 (0.1172774E 00 , 0.2554401E-01)
34 (0.9551698E-01 , -0.3799713E-01)	91 (0.1250820E 00 , 0.2786530E 00)
35 (0.1172774E 00 , 0.6990725E-01)	92 (0.0000000E 00 , -0.1692446E 00)
36 (0.1250820E 00 , 0.2786530E 00)	93 (0.0000000E 00 , -0.1373387E 00)
37 (-0.4898727E-01 , 0.1199413E 00)	94 (0.0000000E 00 , -0.8659899E-01)
38 (-0.4722714E-01 , 0.6551129E-01)	95 (0.0000000E 00 , -0.3758830E-01)
39 (-0.3253630E-01 , -0.8371789E-02)	95 (0.0000000E 00 , -0.6543554E-02)
40 (-0.6279565E-02 , -0.8276445E-01)	97 (0.0000000F 00 , 0.3425784E-02)
41 (0.2769190E-01 , -0.1367845E 00)	98 (0.0000000E 00 , -0.1318946E-02)
42 (0.6373584E-01 , -0.1512459E 00)	99 (0.0000000E 00 , -0.1265041E-01)
43 (0.9551698E-01 , -0.1091290E 00)	100 (0.0000000E 00 , -0.2398506E-01)
44 (0.1172774E 00 , 0.2554396E-01)	101 (0.0000000E 00 , -0.3081169E-01)
45 (0.1250820E 00 , 0.2748093E 00)	102 (0.6373584E-01 , -0.1956093E 00)
46 (-0.3909317E-01 , 0.1802235E 00)	103 (0.9551698E-01 , -0.1091290E 00)
47 (-0.4898727E-01 , 0.1199415E 00)	104 (0.1172774E 00 , 0.6990689E-01)
48 (-0.4722714E-01 , 0.2714225E-01)	105 (0.1250820E 00 , 0.3497829E 00)
49 (-0.3253630E-01 , -0.7555103E-01)	106 (0.0000000E 00 , -0.1534147E 00)
50 (-0.6279565E-02 , -0.1619456E 00)	107 (0.0000000E 00 , -0.1198705E 00)
51 (0.2769190E-01 , -0.2079150E 00)	108 (0.0000000E 00 , -0.6410986E-01)
52 (0.6373584E-01 , -0.1956096E 00)	109 (0.0000000E 00 , -0.6543554E-02)
53 (0.9551698E-01 , -0.1129715E 00)	110 (0.0000000E 00 , 0.294736F-01)
54 (0.1172774E 00 , 0.7049751E-01)	111 (0.0000000E 00 , 0.3195258E-01)
55 (0.1250820E 00 , 0.3844125E 00)	112 (0.0000000E 00 , 0.3425881E-02)
56 (0.0000000E 00 , -0.9337544E-01)	113 (0.0000000E 00 , -0.3981496E-01)
57 (0.0000000E 00 , -0.1198969E 00)	114 (0.0000000E 00 , -0.8018595E-01)

THIS PAGE IS BEST QUALITY PRACTICABLE
 KNOM COPY FURNISHED TO DDG

115 (0.0000000E 00	, -0.1040404E 00)
116 (0.2769190E-01	, -0.2079151E 00)
117 (0.6373584E-01	, -0.1572464E 00)
118 (0.9551698E-01	, -0.3799730E-01)
119 (0.1172774E 00	, 0.1490885E 00)
120 (0.1250820E 00	, 0.4169617E 00)
121 (0.0000000E 00	, -0.1040408E 00)
122 (0.0000000E 00	, -0.8018625E-01)
123 (0.0000000E 00	, -0.3981519E-01)
124 (0.0000000E 00	, 0.3425784E-02)
125 (0.0000000E 00	, 0.3195258E-01)
126 (0.0000000E 00	, 0.2994754E-01)
127 (0.0000000E 00	, -0.6543308E-02)
128 (0.0000000E 00	, -0.6641095E-01)
129 (0.0000000E 00	, -0.1198702E 00)
130 (0.0000000E 00	, -0.1534145E 00)
131 (-0.6279565E-02	, -0.1619459E 00)
132 (0.2769190E-01	, -0.1367847E 00)
133 (0.6373584E-01	, -0.7206637E-01)
134 (0.9551698E-01	, 0.2918159E-01)
135 (0.1172774E 00	, 0.1874563E 00)
136 (0.1250820E 00	, 0.4159624E 00)
137 (0.0000000E 00	, -0.3081196E-01)
138 (0.0000000E 00	, -0.2396527E-01)
139 (0.0000000E 00	, -0.1265056E-01)
140 (0.0000000E 00	, -0.1318946E-02)
141 (0.0000000E 00	, 0.3425881E-02)
142 (0.0000000E 00	, -0.6543308E-02)
143 (0.0000000E 00	, -0.3758802E-01)
144 (0.0000000E 00	, -0.8659875E-01)
145 (0.0000000E 00	, -0.1373385E 00)
145 (0.0000000E 00	, -0.1592445E 00)
147 (-0.3253630E-01	, -0.7555091E-01)
149 (-0.6279565E-02	, -0.8276433E-01)
149 (0.2769190E-01	, -0.6960583E-01)
150 (0.6373584E-01	, -0.3369741E-01)
151 (0.9551698E-01	, 0.2918183E-01)
152 (0.1172774E 00	, 0.1490886E 00)
153 (0.1250820E 00	, 0.3497834E 00)
154 (0.0000000F 00	, 0.4924359E-01)
155 (0.0000000E 00	, 0.3672381E-01)
156 (0.0000000E 00	, 0.1451089E-01)
157 (0.0000000E 00	, -0.1265041E-01)
158 (0.0000000F 00	, -0.3981496E-01)
159 (0.0000000F 00	, -0.6410956E-01)
160 (0.0000000E 00	, -0.8659875E-01)
161 (0.0000000E 00	, -0.1108170E 00)
162 (0.0000000E 00	, -0.1359733E 00)
163 (0.0000000E 00	, -0.1531681E 00)
164 (-0.4722714E-01	, 0.2714213E-01)
165 (-0.3253630E-01	, -0.8372154E-02)
166 (-0.6279565E-02	, -0.4439541E-01)
167 (0.2769190E-01	, -0.6960541E-01)
168 (0.6373584E-01	, -0.7206637E-01)
169 (0.9551698E-01	, -0.3799713E-01)
170 (0.1172774E 00	, 0.6990725E-01)
171 (0.1250820E 00	, 0.2786530E 00)
172 (0.0000000E 00	, 0.1167789E 00)
173 (0.0000000E 00	, 0.8773917E-01)
174 (0.0000000E 00	, 0.3672393E-01)
175 (0.0000000E 00	, -0.2398506E-01)
176 (0.0000000E 00	, -0.8018595E-01)
177 (0.0000000F 00	, -0.1198702E 00)
178 (0.0000000E 00	, -0.1373385E 00)
179 (0.0000000E 00	, -0.1359733E 00)
180 (0.0000000E 00	, -0.1266469E 00)
181 (0.0000000E 00	, -0.1198970E 00)
182 (-0.4898727E-01	, 0.1199413E 00)
183 (-0.4722714E-01	, 0.6551129E-01)
184 (-0.3253630E-01	, -0.8371789E-02)
185 (-0.6279565E-02	, -0.8276445E-01)
186 (0.2769190E-01	, -0.1367845E 00)
187 (0.6373584E-01	, -0.1512459E 00)
188 (0.9551698E-01	, -0.1091290E 00)
189 (0.1172774E 00	, 0.2554396E-01)
190 (0.1250820E 00	, 0.2748093E 00)
191 (0.0000000E 00	, 0.1552752E 00)
192 (0.0000000E 00	, 0.1167789E 00)
193 (0.0000000E 00	, 0.4924377E-01)
194 (0.0000000E 00	, -0.3081169E-01)
195 (0.0000000E 00	, -0.1040404E 00)
196 (0.0000000E 00	, -0.1534145E 00)
197 (0.0000000E 00	, -0.1692445E 00)
198 (0.0000000E 00	, -0.1531681E 00)
199 (0.0000000E 00	, -0.1198970E 00)
200 (0.0000000F 00	, -0.9337544E-01)
201 (-0.3909317E-01	, 0.1802235E 00)
202 (-0.4898727E-01	, 0.1199415E 00)
203 (-0.4722714E-01	, 0.2714225E-01)
204 (-0.3253630E-01	, -0.7555103E-01)
205 (-0.6279565E-02	, -0.1619456E 00)
206 (0.2769190E-01	, -0.2079150E 00)
207 (0.6373584E-01	, -0.1956096E 00)
208 (0.9551698E-01	, -0.1129715E 00)
209 (0.1172774E 00	, 0.7049751E-01)
210 (0.1250820E 00	, 0.3844125E 00)

THIS PAGE IS BEST QUALITY PRACTICABLE
FROM COPY FURNISHED TO DDC

PRINTOUT OF EXCITATION MATRIX...

1	(-0.1005299E 01 , 0.3436115E-02)
2	(-0.1005304E 01 , 0.1760722E-02)
3	(-0.1005307E 01 , 0.6135921E-03)
4	(-0.1005307E 01 , -0.1653822E-03)
5	(-0.1005307E 01 , -0.6135921E-03)
6	(-0.1005307E 01 , -0.6135921E-03)
7	(-0.1005307E 01 , -0.1653822E-03)
8	(-0.1005307E 01 , 0.6135921E-03)
9	(-0.1005304E 01 , 0.1760722E-02)
10	(-0.1005299E 01 , 0.3436115F-02)
11	(0.0000000E 00 , 0.0000000E 00)
12	(0.0000000E 00 , 0.0000000F 00)
13	(0.0000000E 00 , 0.0000000F 00)
14	(0.0000000E 00 , 0.0000000F 00)
15	(0.0000000E 00 , 0.0000000F 00)
16	(0.0000000E 00 , 0.0000000E 00)
17	(0.0000000E 00 , 0.0000000F 00)
18	(0.0000000E 00 , 0.0000000E 00)
19	(0.0000000E 00 , 0.0000000E 00)
20	(0.0000000E 00 , 0.0000000E 00)

MAGNETIC CURRENTS FOR XS = -100.000 AND YS = 0.400

1	-0.1041356F 01	0.3800805E 00	0.1108550E 01	0.1599485E 03
2	-0.8690500E 00	-0.5143996E-02	0.8690652E 00	-0.1796608F 03
3	-0.9510195F 00	-0.6967962E-01	0.9635422F 00	-0.1758529F 03
4	-0.1020225F 01	-0.1214982E 00	0.1027433E 01	-0.1732086F 03
5	-0.1057353E 01	-0.1415945F 00	0.1066792E 01	-0.1723726F 03
6	-0.1057343F 01	-0.1415946E 00	0.1066781E 01	-0.1723725E 03
7	-0.1020234E 01	-0.1214956E 00	0.1027442E 01	-0.1732088E 03
8	-0.9610143F 00	-0.6967777E-01	0.9635370F 00	-0.1758530F 03
9	-0.8690544F 00	-0.5143974E-02	0.8690696E 00	-0.1796608E 03
10	-0.1041354E 01	0.3800802F 00	0.1108548E 01	0.1599485E 03
11	-0.4538797F 00	-0.1127379E 01	0.1215315E 01	-0.1119295E 03
12	-0.1003134E 00	-0.9136119E 00	0.9191025F 00	-0.9626579E 02
13	-0.5931120F-01	-0.9311429E 00	0.9330299F 00	-0.9364456E 02
14	-0.2156582F-01	-0.9213710E 00	0.9216233E 00	-0.9134077E 02
15	-0.7313278E-02	-0.9183767E 00	0.9184054F 00	-0.9045618E 02
16	-0.7312000F-02	-0.9183670F 00	0.9183961F 00	-0.9045610F 02
17	-0.2156668E-01	-0.9213762E 00	0.9216285F 00	-0.9134077F 02
18	-0.5931240E-01	-0.9311371E 00	0.9330243F 00	-0.9364471F 02
19	-0.1003069E 00	-0.9136149E 00	0.9191048E 00	-0.9626541F 02
20	-0.4538861E 00	-0.1127376E 01	0.1215314F 01	-0.1119299E 03

XS
-0.1000000E 03
YS TRANSMISSION COEFF.
0.4000000E 00 0.9396020E 00

THIS PAGE IS BEST QUALITY PRACTICABLE
FROM COPY FURNISHED TO DDC

POWER GAIN PATTERN IN REGION C AND ANGLE IN DEGREES

-90.0	0.1042085E 00	0.5100097E-01
-80.0	0.1200446E 00	0.5473917E-01
-70.0	0.1762717E 00	0.6633121E-01
-60.0	0.2986771E 00	0.8634311E-01
-50.0	0.5253934E 00	0.1145157E 00
-40.0	0.8892853E 00	0.1489866E 00
-30.0	0.1383474E 01	0.1858285E 00
-20.0	0.1925999E 01	0.2192577E 00
-10.0	0.2362068E 01	0.2428136E 00
0.0	0.4006325E 02	0.1000000E 01
10.0	0.2362071E 01	0.2428138E 00
20.0	0.1925999E 01	0.2192577E 00
30.0	0.1383476E 01	0.1858286E 00
40.0	0.8892870E 00	0.1489868E 00
50.0	0.5253938E 00	0.1145158E 00
60.0	0.2986779E 00	0.8634323E-01
70.0	0.1762720E 00	0.6633127E-01
80.0	0.1200448E 00	0.5473922E-01
90.0	0.1042085E 00	0.5100096E-01

CODE USAGE OBJECT CODE= 49704 BYTES, ARRAY AREA= 45516
COMPILE TIME= 3.56 SEC, EXECUTION TIME= 4.88 SEC, WATFIV

THIS PAGE IS BEST QUALITY PRACTICABLE
FROM COPY FURNISHED TO DDC

B-3. Descriptions and Listings of Subroutines

```
SUBROUTINE PTB(W,D,WAVNB)
COMMON WAVNO,PI,U
COMPLEX U,WAVNB
WLB=2.*PI/(REAL(WAVNB)*WAVNO)
DD=.001*WLB
I=0
IF(D.EQ.0.) GO TO 10
IF(AIMAG(WAVNB).NE.0.) RETURN
DO 1 I=1,20
IF(ABS(WLB*I/2.-D).LE.1.E-04) GO TO 10
1 CONTINUE
GO TO 11
10 D=C+DD
100 FORMAT(' - ', 'D= ', 15.3X, 'TIMES HALF WAVELENGTH IN REGION B. CHANGED
* TC', E14.7)
WRITE(3,100) I,D
11 IF(AIMAG(WAVNB).NE.0.) RETURN
DO 2 I=1,20
IF(ABS(WLB*I/2.).LE.1.E-04) GO TO 15
2 CONTINUE
GO TO 16
15 W=W+DD
150 FORMAT(' - ', 'W= ', 15.3X, 'TIMES HALF WAVELENGTH IN REGION B. CHANGED
* TO', E14.7)
WRITE(3,150) I,W
16 RETURN
END
```

This subroutine checks to see whether w or d are integral multiples (up to 20) of a half wavelength in region b. If either d or w satisfy this condition they are changed by

$$d = d + .001 \lambda_b$$
$$w = w + .001 \lambda_b$$

If region b is lossy, the parameters d and w are unchanged unless d = 0 in which case only d is changed.

THIS PAGE IS BEST QUALITY PRACTICABLE
FROM COPY FURNISHED TO DDC

C LISTING OF SUBROUTINE YB
C

```
SUBROUTINE YB(Y,M2,WAVNB,ETANB,W,CY,NT,D,N)
COMMON WAVNO,PI,U
COMPLEX Y(M2),YB11,YB12,YSUM11,YSUM12,KBD,U,CONST,WAVNB,ETANB
COMPLEX ST1(150),ST2(150),CXP(150),CSQRT,CSIN,CCOS
DIMENSION SINC2(150)
N2=N*2
M=N*(N+1)/2
CONST=-U*DY*DY/W/ETANB
KBD=WAVNB*D
IF(ABS(AIMAG(KBD)).GE.50.) GO TO 1
YB12=CNST/CSIN(KBD)
YB11=YB12*CCOS(KBD)
GO TO 2
1 MF=-1
IF(AIMAG(KBD).GT.0.) MF=1
YB11=MF*CCNST*U
YB12=0.
2 CONTINUE
DO 3 I=1,NT
CXP(I)=CSQRT(1.-(I*PI/W/WAVNB)**2)
SINC2(I)=(SIN(I*PI/N2)/(I*PI/N2))**2
KBD=CXP(I)*WAVNB*D
IF(ABS(AIMAG(KBD)).GE.50.) GO TO 4
ST1(I)=CCOS(KBD)*SINC2(I)/CSIN(KBD)/CXP(I)
GO TO 6
4 MF=-1
IF(AIMAG(KBD).GT.0.) MF=1
ST1(I)=SINC2(I)/CXP(I)*MF*U
6 CONTINUE
3 CONTINUE
DO 7 I=1,NT
KBD=WAVNB*CXP(I)*D
IF(ABS(AIMAG(KBD)).GE.50.) GO TO 8
ST2(I)=ST1(I)/CCOS(KBD)
GO TO 9
8 ST2(I)=0.
9 CONTINUE
7 CONTINUE
K=1
DO 10 I=1,N
DO 10 J=1,I
YSUM11=0.
YSUM12=0.
DO 11 IP=1,NT
CS=COS(IP*PI*(I-.5)/N)*COS(IP*PI*(J-.5)/N)
YSUM11=YSUM11+ST1(IP)*CS
YSUM12=YSUM12+ST2(IP)*CS
11 CONTINUE
Y(K)=YB11+YSUM11*CONST*2.
Y(M+(I-1)*N+K)=YB12+YSUM12*CONST*2.
K=K+1
10 CONTINUE
```

```

K=N-1
N1=K
DO 14 I=1,N1
DO 15 J=1,K
Y(M+(I-1)*N+J+I*(I+1)/2)=Y(M+(J+I-1)*N+(J+I-1)*(J+I)/2+I)
15 CONTINUE
K=K-1
14 CONTINUE
K=1
DO 16 I=1,N
DO 16 J=1,I
Y(M+I*N+K)=Y(K)
K=K+1
16 CONTINUE
RETURN
END

```

This subroutine computes the upper right triangle of

$$\eta_o k_o \begin{bmatrix} [Y^{11}] & [Y^{12}] \\ [Y^{12}] & [Y^{11}] \end{bmatrix}$$

and returns the result in array Y. The major task is to compute approximations to the infinite sums in Eqs. (32) and (33). Rewriting Y_{mn}^{11} as it appears in Eq. (32), we have

$$\eta_o k_o Y_{mn}^{11} = -\frac{jk_o \eta_o (\Delta y)^2}{w} \frac{\cot k_b d}{\eta_b} - \frac{j2k_o \eta_o (\Delta y)^2 \infty}{w \eta_b} \sum_{p=1}^{\infty} \frac{\cot \sqrt{1 - \left(\frac{p\pi}{k_b w}\right)^2} k_b d}{\sqrt{1 - \left(\frac{p\pi}{k_b w}\right)^2}} \frac{\sin^2 \left(\frac{p\pi}{2N}\right)}{\left(\frac{p\pi}{2N}\right)^2} \cos \left[\frac{p\pi}{N} \left(m - \frac{1}{2} \right) \right] \cdot \cos \left[\frac{p\pi}{N} \left(n - \frac{1}{2} \right) \right] \quad (B-2)$$

where Eq. (A-2) has been used. A similar expression is obtained for

$\eta_o k_o Y_{mn}^{12}$. The complex constant CONST is set equal to $-j(\Delta y)^2 k_o \eta_o / w \eta_b$.

Since k_b is a complex number, we write $k_b = k'_b - jk''_b$ and if $k''_b d \geq 50$, then the limit of $\cot k_b d$ as $k''_b d \rightarrow \infty$ is used in computing the $p = 0$ term, YB11, for $\eta_o k_o Y_{mn}^{11}$. Next, DO loop 3 computes NT terms of the infinite summation for Y_{mn}^{11} where

$$CXP(p) = \sqrt{1 - \left(\frac{p\pi}{k_b w}\right)^2} \quad (B-3)$$

$$SINC2(p) = \frac{\sin^2\left(\frac{p\pi}{2N}\right)}{\left(\frac{p\pi}{2N}\right)^2} \quad (B-4)$$

and

$$ST1(p) = \frac{\cot \sqrt{1 - \left(\frac{p\pi}{k_b w}\right)^2} k_b d}{\sqrt{1 - \left(\frac{p\pi}{k_b w}\right)^2}} \frac{\sin^2\left(\frac{p\pi}{2N}\right)}{\left(\frac{p\pi}{2N}\right)^2} \quad (B-5)$$

Again if $\text{Im } \left(\sqrt{1 - \left(\frac{p\pi}{k_b w}\right)^2} k_b d\right) \geq 50$, the limit to $\cot x$ as $\text{Im } x \rightarrow -\infty$ is used. DO loop 7 computes the terms of summation for $\eta_o k_o Y_{mn}^{12}$ and stores them in array ST2 as $ST2(p) = ST1(p)/\cos(CXP(p)k_b d)$. DO loop 10 computes NT terms of Eq. (B-2) for $m,n = 1,2,\dots,N$ and stores the result in the first $N(N+1)/2$ locations of Y. Note the result is an upper right triangular matrix stored columnwise. The upper right triangle of the matrix $\eta_o k_o Y_{mn}^{12}$ is also computed here and stored in the appropriate locations in Y. Next, since $\eta_o k_o [Y^{12}]$ is symmetric, DO loops 14 and 15 fill in the rest of that portion of Y which $\eta_o k_o [Y^{12}]$ occupies. Finally, since $[Y^{11}] = [Y^{22}]$, DO loop 16 fills in the rest of Y which is then returned to the main program.

C
C

LISTING OF SUBROUTINE YHS

THIS PAGE IS BEST QUALITY PRACTICABLE
FROM COPY FURNISHED TO DDC

```
SUBROUTINE YHS(DY,N,YHSA,WAV,ETAN)
COMPLEX SUM,HANK02,YHSA(N),HANK12,U
COMMON WAVNO,PI,U
DIMENSION T(4),A(4)
DATA T/- .4305682,.4305682,-.1699905,.1699905/
DATA A/2*.3478548,2*.6521452/
DATA NL/3/
YHSA(1)=0.
DX=DY/NL
DO 1 I=1,2
DO 2 J=1,NL
X1=ARS((I-1)*DY-DX*(J-.5))
X2=X1*X1
H0=X1*(1.-X2/9.* (1.-X2/25.* (1.-X2/49.)))
H1=X2/3.* (1.-X2/15.* (1.-X2/35.* (1.-X2/63.)))
YHSA(1)=YHSA(1)+DX*(X1*((1.-H1)*HANK02(X1)+H0*HANK12(X1)))
CONTINUE
1 CONTINUE
YHSA(1)=YHSA(1)/(2.*ETAN*WAV)
C2=DY/?.
DO 3 K=2,N
C4=(K-.5)*DY
SUM=0.
DO 4 J=1,4
DO 5 I=1,4
SUM=SUM+A(J)*A(I)*HANK02(ABS(DY*(T(I)-T(J))+C2-C4))
CONTINUE
4 CONTINUE
YHSA(K)=SUM*C2**2/(2.*ETAN*WAV)
3 CONTINUE
RETURN
END
```

This subroutine computes Eq. (18) or (20) multiplied by the factor $(n_0 k_0)$. The parameters are:

DY = Δy_m times k_a or k_c where Δy_m is defined in Fig. B-1.

N = number of elements in one column of $[Y^{hsa}]$ or $[Y^{hsc}]$.

YHSA = array containing first column of $[Y^{hsa}]$ or $[Y^{hsc}]$.

WAV = k_a/k_0 or k_c/k_0

ETAN = n_a/n_0 or n_c/n_0

The exact elements stored in array YHSA are $n_0 k_0 Y_{m,1}^{hs}$, $m=1,2,\dots,N$.

When $m \neq 1$, a four-point Gaussian quadrature formula is used to evaluate the integral. Thus, for example, $n_0 k_0 Y_{m,1}^{hsa}$ becomes

$$\eta_o k_o Y_{m,1}^{\text{hsa}} \approx \frac{1}{2(\frac{k_a}{k_o})(\frac{n_a}{n_o})} \left(\frac{k_a \Delta y_1}{2} \right) \left(\frac{k_a \Delta y_m}{2} \right) \sum_{i=1}^4 \sum_{j=1}^4 A_i A_j H_o^{(2)}(|t_i - t_j|) \quad (\text{B-6})$$

where the A_i , t_i are weight coefficients and nodes respectively and are stored in arrays A and T. When $m=1$, the integrand is singular so the approximation

$$\eta_o k_o Y_{11}^{\text{hsa}} \approx \frac{1}{2(\frac{k_a}{k_o})(\frac{n_a}{n_o})} \sum_{i=1}^{NL} \int_{k_a \Delta y_1} H_o^{(2)} \left(|t - \frac{k_a \Delta y_1 (i - .5)}{NL}| \right) \frac{k_a \Delta y_1}{NL} dt \quad (\text{B-7})$$

is made. The integral inside the summation is then computed with the aid of the identity [10, 11.1.7]

$$\int_0^x H_o^{(2)}(t) dt = x H_o^{(2)}(x) + \frac{\pi x}{2} \{ H_o(x) H_1^{(2)}(x) - H_1(x) H_o^{(2)}(x) \} \quad (\text{B-8})$$

where $H_o(x)$ and $H_1(x)$ without superscripts are Struve functions of orders zero and one defined as

$$H_o(x) = \frac{2}{\pi} \left[x - \frac{x^3}{1^2 \cdot 3^2} + \frac{x^5}{1^2 \cdot 3^2 \cdot 5^2} - \dots \right] \quad (\text{B-9})$$

and

$$H_1(x) = \frac{2}{\pi} \left[\frac{x^2}{1 \cdot 3} - \frac{x^4}{1^2 \cdot 3^2 \cdot 5} + \frac{x^6}{1^2 \cdot 3^2 \cdot 5^2 \cdot 7} - \dots \right] \quad (\text{B-10})$$

C LISTING OF SUBROUTINE TEEXC
C

```
SUBROUTINE TEEXC(WAV,XS,YS,N,DY,VM,N2,ETAN,STK,W)
COMMON WAVNO,PI,U
COMPLEX VM(N2),STK,SUM,U,HANK02,HANK12
DIMENSION T(4),A(4)
DATA T/-4305682.,4305682,-1699905.,1699905/
DATA A/2*.3478548,2*.6521452/
RS0=SQRT(XS*XST+(YS-W/2.)*2)
STK=4.*U/HANK12(RS0)/WAV
```

THIS PAGE IS BEST QUALITY PRACTICABLE
FROM COPY FURNISHED TO DDC

```

DYZ=DY/2.
DO 2 J=1,N
SUM=0.
DO 1 I=1,4
SUM=SUM+A(I)*HANK02(SQRT(XS*XS+((J-.5)+T(I))*DY-YS)**2))
1 CONTINUE
VM(J)=-(SUM*STK*DYZ)/(ETAN**2.)
2 CONTINUE
N1=N+1
DO 3 I=N1,N2
VM(I)=0.
3 CONTINUE
RETURN
END

```

THIS PAGE IS BEST QUALITY PRACTICABLE
FROM COPY FURNISHED TO DDC

This subroutine computes the elements of Eq. (43) multiplied by $k_o n_o$. The input-output parameters are:

$$WAV = k_a / k_o$$

$$XS = k_a x_s$$

$$YS = k_a y_s$$

N = number of non-zero elements of excitation vector.

$$DY = k_a \Delta y_m$$

VM = output array containing excitation elements (right

hand side of Eqs. (11) multiplied by $n_o k_o$).

$$N2 = 2*N$$

$$ETAN = n_a / n_o$$

STK = Strength of line source which produces an incident electric field equal to unity at the origin.

$$W = k_a w$$

To produce a unit incident electric field at the origin, the strength of the magnetic line source K_u_z must be

$$STK = k_o K = \frac{4j \sqrt{x_s^2 + y_s^2}}{H_1^{(2)} (\sqrt{x_s^2 + y_s^2}) x_s k_a / k_o} \quad (B-11)$$

A four-point Gaussian quadrature rule is used to approximate the integral in Eq. (43) thus the elements computed are

$$\eta_o k_o I_m^1 = - \left(\frac{k_a \Delta y_m}{2} \right) \left(\frac{\eta_o}{2 \eta_a} \right) (k_o K) \sum_{i=1}^4 A_i H_o^{(2)} \left(\sqrt{(x_s k_a)^2 + (k_a y_s - t_i)^2} \right) \quad (B-12)$$

This is done in DO Loop 2.

C LISTING OF SUBROUTINE TRANS
C

```
SUBROUTINE TRANS(N,N2,YHSA,PT,T,VM,STK,W,XK,YK,ETANA,WAVNA,TN)
COMPLEX YHSA(N),YAUX(30),VM(N2),SUM,S,CONJG,STK,U
COMMON WAVNO,PI,U
DO 1 I=1,N
  YAUX(I)=CONJG(YHSA(I))
1 CONTINUE
N1=N-1
SUM=0.
DO 2 I=1,N1
  S=0.
  DO 3 J=1,I
    S=S+YAUX(I-J+1)*CONJG(VM(N+J))
3 CONTINUE
NI=N-I
DO 4 J=1,NI
  S=S+YAUX(J+1)*CONJG(VM(N+I+J))
4 CONTINUE
SUM=SUM+VM(N+I)*S
? CONTINUE
S=0.
DO 5 I=1,N
  S=S+YAUX(N-I+1)*CONJG(VM(N+I))
5 CONTINUE
SUM=SUM+VM(N2)*S
STKM=(CABS(STK))**2
A2=W*W
B2=XK*XK+(YK-W)**2
C2=XK*XK+YK*YK
THETA=ARCCOS((B2+C2-A2)/(2.*SQRT(B2*C2)))
THETAN=2.*ATAN(W/2./SQRT(XK*XK+YK*YK))
PT=REAL(SUM)
T=8.*PI*ETANA*PT/(THETA*WAVNA*STKM)
TN=8.*PI*ETANA*PT/(THETAN*WAVNA*STKM)
RETURN
END
```

This subroutine computes the slit transmission coefficient, T, according to Eq. (53). The input-output parameters are

N = number of elements in first column of $[Y^{hsc}]$

N2 = 2*N

YHSA = array containing first column of $[Y^{hsc}]$.

PT = $k_o n_o \operatorname{Re} \{\tilde{V}_2 [Y^{hsc}]^* \bar{V}_2^*\}$

T = transmission coefficient, Eq. (53).

VM = array containing the solution to Eqs. (11).

STK = $k_o K$

W = $k_o w$

XK = $k_o x_s$

YK = $k_o y_s$

ETANA = n_a / n_o

WAVNA = k_a / k_o

The auxiliary array YAUX contains the first column of $[Y^{hsc}]^*$. It has a minimum dimension of N. The computation of Eq. (50) is carried out in DO loops 2 through 5 and the power transmitted $k_o n_o P_{trans}$, is assigned to variable PT.

C LISTING OF SUBROUTINE GAIN
C

```
SUBROUTINE GAIN(PHIR,NI,N,N2,X,DY,W,GA,WAVNC,ETANC,PT,FP)
COMPLEX X(N2),U,S,ARG,CEXP
DIMENSION GA(91),FP(91),PHIR(91)
COMMON WAVNO,PI,U
DY2=DY/2.
DO 2 J=1,NI
SN=SIN(PHIR(J))
IF(SN.EQ.0.) GO TO 5
```

THIS PAGE IS BEST QUALITY PRACTICABLE
FROM COPY FURNISHED TO DDC

```

FT=SIN(DY2*WAVNC*SN)/WAVNC/SN
GO TO 6
5   FT=1./WAVNC
S=0.
DO 1 I=1,N
YM=WAVNC*((I-.5)*DY-W/2.)
ARG=U*YM*SN
S=S+X(I+N)*CEXP(ARG)*FT*2.
1   CONTINUE
F=CABS(S)
FP(J)=F
GA(J)=F*F*WAVNC/(2.*ETANC*PT)
2   CONTINUE
FM=FP(1)
DO 3 I=2,NI
IF(FM.LT.FP(I)) FM=FP(I)
3   CONTINUE
DO 4 I=1,NI
FP(I)=FP(I)/FM
4   CONTINUE
RETURN
END

```

THIS PAGE IS BEST QUALITY PRACTICABLE
FROM COPY FURNISHED TO DDC

This subroutine computes the power gain pattern according to Eq. (64). The input-output parameters are

PHIR = input array containing values of ϕ in radians at which each gain computation is made.

NI = number of elements in PHIR

N = number of elements in vector \bar{V}_2 in Eq. (64)

N2 = 2*N

X = array containing solution to Eqs. (11a,b) for a particular excitation.

DY = $k_o \Delta y$

W = $k_o w$

GA = output array containing G(ϕ)

WAVNC = k_c / k_o

ETANC = n_c / n_o

PT = $k_o n_o \text{ Real } \{\tilde{V}_2 [Y^{hsc}]^* \bar{V}_2^*\}$

FP = output array containing normalized H-field pattern.

The normalized field pattern is found using Eq. (63) and

$$FP(\phi) = \left| \frac{H_m(r_m, \phi)}{H_m(r_m, \phi)_{\max}} \right| \quad (B-13)$$

C LISTING OF SUBROUTINE GELS
C

```
SUBROUTINE GELS(R,A,M,N,M2)
COMPLEX A(M2)
COMPLEX R(1820),AUX(2000)
COMPLEX PIVI,TB
100 FORMAT('1', 'WARNING---ERROR CODE IER = ',15)
EPS=1.E-07
IF(M)24,24,1
1 IER=0
PIV=0.
L=0
DO 3 K=1,M
L=L+K
TBA=CABS(A(L))
IF(TBA-PIV) 3,3,2
? PIV=TBA
I=L
J=K
3 CONTINUE
TOL=EPS*PIV
LST=0
NM=N*M
LFND=M-1
DO 18 K=1,M
IF(PIV)24,24,4
4 IF(IEP)7,5,7
5 IF(PIV-TOL)6,6,7
6 IER=K-1
7 LT=J-K
LST=LST+K
PIVI=1./A(I)
DO 8 L=K,NM,M
LL=L+LT
TR=PIVI*R(LL)
R(LL)=R(L)
R(L)=TB
8 IF(K-M)9,19,19
9 LR=LST+(LT*(K+J-1))/2
LL=LR
L=LST
```

THIS PAGE IS BEST QUALITY PRACTICABLE
FROM COPY FURNISHED TO DDC

```

DO 14 II=K,LEND
L=L+II
LL=LL+1
IF(L-LR)12,10,11
10 A(LL)=A(LST)
TB=A(L)
GO TO 13
11 LL=L+LT
12 TB=A(LL)
A(LL)=A(L)
13 AUX(II)=TB
14 A(L)=PIVI*TB
A(LST)=LT
PIV=0.
LLST=LST
LT=0
DO 18 II=K,LEND
PIVI=-AUX(II)
LL=LLST
LT=LT+1
DO 15 LLD=II,LEND
LL=LL+LLD
L=LL+LT
15 A(L)=A(L)+PIVI*A(LL)
LLST=LLST+II
LR=LLST+LT
TBA=CABS(A(LR))
IF(TBA-PIV) 17,17,16
16 PIV=TBA
I=LR
J=II+1
17 DO 18 LR=K,NM,M
LL=LR+LT
18 P(LL)=R(LL)+PIVI*R(LR)
19 IF(LEND)24,23,20
20 II=M
DO 22 I=2,M
LST=LST-II
II=II-1
L=A(LST)+.5
DO 22 J=II,NM,M
TB=R(J)
LL=J
K=LST
DO 21 LT=II,LEND
LL=LL+1
K=K+LT
21 TB=TB-A(K)*R(LL)
K=J+L
P(J)=R(K)
22 F(K)=TB
23 FRETURN
24 IER=-1
WRITE(3,100) IER
RETURN
END

```

THIS PAGE IS BEST QUALITY PRACTICABLE
FROM COPY FURNISHED TO DDC

This subroutine solves the set of equations

$$[A]\bar{x} = [R]$$

where $[A]$ is a symmetric matrix. Input-output parameters are

R = excitation array of dimension $M \times N$.

A = symmetric matrix of coefficients, the upper right triangular portions of which is stored by columns.

M = number of equations in the system to be solved.

N = number of right hand sides or columns of R .

$M2$ = number of elements in upper right triangle of $[A]$.

The algorithm utilizes Gaussian elimination with pivoting on the main diagonal. For further details, see [11].

C LISTING OF FUNCTION SUBPROGRAM HANK12
C

```
COMPLEX FUNCTION HANK12(X)
COMPLEX U/(0.01.)
100 FORMAT(' ','WARNING--ARGUMENT OF ',E15.4, 'X, 'HAS BEEN ENCOUNTERED
1IN COMPUTING HANK12')
IF(X.LE.0.) WRITE(3,100) X
BSJ1=0.0
IF(X.EQ.0.) GO TO 2
Z=ABS(X)
IF(Z.GT.3.0) GO TO 1
Y=Z*Z/9.0
BSJ1=X*(0.5+Y*(-0.56249985+Y*(0.21093573+Y*(-0.03954289+Y*(0.00443
1319+Y*(-0.00031761+Y*0.00001109))))) )
GO TO 2
1 W=3./Z
F1=.79788456+W*(.00000155+W*(.01659667+W*(.00017105+W*(-.0024
19511+W*(.00113653-W*.00020033)))) )
P1=.78539816+W*(-.12499612+W*(-.00005650+W*(.00637879+W*(-.00
1074348+W*(-.00079824+W*.00029166)))) )
BSJ1=F1*SIN(Z-P1)/SQRT(Z)
IF(X.LT.0.0)BSJ1=-BSJ1
2 CONTINUE
BSY1=-1.0E75
IF(X.EQ.0.) GO TO 3
IF(Z.GT.3.) GO TO 4
```

THIS PAGE IS BEST QUALITY PRACTICABLE
FROM COPY FURNISHED TO DDC

THIS PAGE IS BEST QUALITY PRACTICABLE
FROM COPY FURNISHED TO DDC

```

BSY1=(-0.63661977+Y*(0.2212091+Y*(2.1682709+Y*(-1.3164827+Y*(0.312
13951+Y*(-0.0400975+Y*0.0027873)))))/Z+0.63661977*ALOG(0.5*Z)*BSJ1
GO TO 3
4 PSY1=-F1*COS(Z-P1)/SQRT(Z)
CONTINUE
HANK12=BSJ1-U*BSY1
RETURN
END

C LISTING OF FUNCTION SUBPROGRAM HANK02
C

COMPLEX FUNCTION HANK02(X)
COMPLEX U/(0.,1.)
10 FORMAT(1H , 'WARNING - ARGUMENT OF', F15.4, 'X, HAS BEEN ENCOUNTERED
IN CALCULATING HANK02(X)')
IF(X.LE.0.0)WRITE(3,10)X
PSJ0=1.0
IF(X.EQ.0.) GO TO 2
Z=ABS(X)
IF(Z.GT.3.0)GO TO 1
Y=Z*Z/9.0
RSJ0=1.0+Y*(-2.2499997+Y*(1.2556208+Y*(-0.3163866+Y*(0.0444479+Y*(
1-0.0039444+Y*0.00021))))))
GO TO 2
1 W=3./Z
FO=.79788456+W*(-.00000077+W*(-.0055274+W*(-.00009512+W*(.001
137237+W*(-.00072805+W*.00014476))))) )
FO=.78539816+W*(.04166397+W*(.00003954+W*(-.00262573+W*(.0005
14125+W*(.00029333-W*.00013558))))) )
PSJ0=F0*COS(Z-P0)/SQRT(Z)
? CONTINUE
RSY0=-1.0E75
IF(X.EQ.0.) GO TO 3
IF(Z.GT.3.) GO TO 4
PSY0=0.63661977*ALOG(0.5*Z)*BSJ0 +0.36746691+Y*(0.60559366+Y*(-0
1.74350384+Y*(0.25300117+Y*(-0.04261214+Y*(0.00427916-Y*0.00024846
2)))) )
GO TO 3
4 CONTINUE
PSY0=F0*SIN(Z-P0)/SQRT(Z)
CONTINUE
HANK02=BSJ0-U*BSY0
RETURN
END

```

These function subprograms compute the necessary Hankel functions

$$H_1^{(2)}(x) = J_1(x) - j Y_1(x)$$

and

$$H_0^{(2)}(x) = J_0(x) - j Y_0(x)$$

by using polynomial approximations as given in [10, Sec. 9.4].

B-4. Description and Listings of Plot Subroutines

Following is a list of subroutines used to plot Figures 6 through 21 in this report. The driver program is included here as an example of how the subroutines are called. Punched output was generated by the main program described in Appendix B-2 for use by the driver program. In each of the subroutines the initialization statement

```
CALL PLOTS( 0, 0, 0, 20., 11.)
```

is made. This is standard procedure at Syracuse University and simply tells the operator that a 20" by 11" space is to be reserved on the plotting roll.

LISTING OF DRIVER PROGRAM

```
$JOB      AUCK,TIME=2,PAGES=40
C-----PROGRAM TO PLOT FIGURES 6 THROUGH 21...
      DIMENSION CUR(300),PHASE(300),FP(300),ANG(300),ANG2(300)
      DIMENSION GA(300),SF(3)
      DATA SF/1..1..,5/
100   FORMAT(15)
101   FORMAT(39X,2E17.7)
102   FORMAT(5X,F10.2)
103   FORMAT(F20.1,2E20.7)
104   FORMAT(2E11.4,11X,E11.4)
C-----PLOT FIG. 6
      READ(1,100) N
      N2=2*N
      DO 1 I=1,3
      DO 1 J=1,N2
      READ(1,101) CUR(J+(I-1)*N2),PHASE(J+(I-1)*N2)
1     CONTINUE
      CALL PCUR(CUR,N,N2,1.5,3)
      CALL PPHAS(PHASE,N,N2,3)
C-----PLOT FIG. 7
      DO 2 I=1,3
      DO 2 J=1,N2
      READ(1,101) CUR(J+(I-1)*N2),PHASE(J+(I-1)*N2)
2     CONTINUE
      CALL PCUR(CUR,N,N2,1.5,3)
      CALL PPHAS(PHASE,N,N2,3)
C-----PLDT FIG. 8
      READ(1,100) NFP
```

THIS PAGE IS BEST QUALITY PRACTICABLE
FROM COPY FURNISHED TO DDC

THIS PAGE IS BEST QUALITY PRACTICABLE
FROM COPY FURNISHED TO DDC

```
NFP3=3*NFP
DO 3 I=1,NFP3
READ(1,103) ANG(I),GA(I),FP(I)
ANG2(I)=ANG(I)
3 CONTINUE
CALL PFP(ANG,FP,NFP,3)
CALL PGA(ANG2,GA,NFP,1.,3)
C-----PLOT FIG. 9
READ(1,100) NFP
NFP3=3*NFP
DO 4 I=1,NFP3
READ(1,103) ANG(I),GA(I),FP(I)
ANG2(I)=ANG(I)
4 CONTINUE
CALL PFP(ANG,FP,NFP,3)
CALL PGA(ANG2,GA,NFP,1.,3)
C-----PLOT FIG. 10
READ(1,100) N
N2=2*N
NP1=N+1
DO 5 J=1,N
READ(1,101) CUR(J)
5 CONTINUE
DO 6 J=NP1,N2
READ(1,102) CUR(J)
6 CONTINUE
CALL PCUR(CUR,N,N2,1..1)
C-----PLOT FIG. 11
READ(1,100) N
N2=2*N
NP1=N+1
DO 7 J=1,N
READ(1,101) CUR(J)
7 CONTINUE
DO 8 J=NP1,N2
READ(1,102) CUR(J)
8 CONTINUE
CALL PCUR(CUR,N,N2,1..1)
C-----PLOT FIGS. 12,13, AND 14
READ(1,100) N
N2=2*N
DO 9 I=1,3
DO 10 J=1,N2
READ(1,101) CUR(J),PHASE(J)
10 CONTINUE
CALL PPHAS(PHASE,N,N2,1)
CALL PCUR(CUR,N,N2,SF(I),1)
9 CONTINUE
C-----PLOT FIG. 15
READ,N,NFP,PHI0,DPHI
NFP3=NFP*3
```

THIS PAGE IS BEST QUALITY PRACTICABLE
FROM COPY FURNISHED TO DDC

```
DO 11 I=1,NFP3
READ(1,103) ANG(I),GA(I),FP(I)
ANG2(I)=ANG(I)
11 CONTINUE
CALL PFP(ANG,FP,NFP,3)
CALL PGA(ANG2,GA,NFP,1..3)
C-----PLOT FIG. 16
READ,N,NFP,PHI0,DPHI
NFP3=NFP*3
DO 12 I=1,NFP3
READ(1,103) ANG(I),GA(I),FP(I)
ANG2(I)=ANG(I)
12 CONTINUE
CALL PFP(ANG,FP,NFP,3)
CALL PGA(ANG2,GA,NFP,2..3)
C-----PLOT FIGS. 17,18, AND 19
READ(1,100) N
N2=2*N
DO 13 I=1,3
DO 14 J=1,N2
READ(1,101) CUR(J),PHASE(J)
14 CONTINUE
CALL PPHAS(PHASE,N,N2,1)
CALL PCUR(CUR,N,N2,1..1)
13 CONTINUE
C-----PLOT FIG. 20
NTP=41
DO 15 I=1,3
DO 15 J=1,NTP
K=J+(I-1)*NTP
READ(1,104) ANG(K),ANG2(K),GA(K)
15 CONTINUE
CALL PTRANS(ANG,ANG2,GA,NTP,3,-1)
C-----PLOT FIG. 21
NP=2
DO 16 I=1,NP
DO 16 J=1,NTP
K=J+(I-1)*NTP
READ(1,104) ANG(K),ANG2(K),GA(K)
16 CONTINUE
CALL PTRANS(ANG,ANG2,GA,NTP,NP,1)
STOP
END
```

THIS PAGE IS BEST QUALITY PRACTICABLE
FROM COPY FURNISHED TO DDC

C LISTING OF SUBROUTINE PCUR
SUBROUTINE PCUR(Y,N,N2,SC,NP)
C-----PROGRAM TO PLOT CURRENTS
DIMENSION XX(5),YY(5),X(300)
DIMENSION Y1(150),Y2(150),Y(300)
DATA XX/2.,7.,7.,2.,2./,YY/1.,1.,5.,5.,1./
NSN=5
SN=SC*2.
XW=XX(2)-XX(1)
YW=YY(3)-YY(2)
SF=YW/SN
DX=XW/N
DX2=DX/2.
CALL PLOTS(0,0,0,20.,11.)
CALL LINE(XX(1),YY(1),5,1,0,0)
JT=1
NP1=N+1
DO 2 J=1,2
YS=YY(1)+(J-1)*YW
XS=XX(2)-(J-1)*XW
DO 1 I=1,NP1
XI=XX(1)+(J-1)*XW+(I-1)*DX*JT
CALL SYMBOL(XI,YS,.14,.13,0.,-1)
1 CONTINUE
DO 3 I=1,NSN
YI=YY(1)+(J-1)*YW+(I-1)*JT
CALL SYMBOL(XS,YI,.14,.13,.90.,-1)
3 CONTINUE
JT=-JT
2 CONTINUE
SN2=SN/4.
DO 4 I=1,NSN
YI=YY(4)-(I-1)-.07
CALL NUMBER(XX(1)-.64,YI,.14,SN,0.,2)
SN=SN-SN2
4 CONTINUE
CALL SYMBOL(XX(1)-.7,YY(1)+1.4,.14,9HMAGNITUDE,.90.,9)
CALL SYMBOL(XX(1)-.03,YY(1)-.27,.14,112,0.,-1)
CALL SYMBOL(XX(1)+XW/2.,YY(1),.2,.13,0.,-1)
CALL SYMBOL(XX(1)+XW/2.-.17,YY(1)-.27,.14,'W/2',0.,3)
CALL SYMBOL(XX(1)+2.00,YY(1)-.6,.14,8HPOSITION,0.,8)
CALL SYMBOL(XX(2)-.035,YY(1)-.27,.14,102,0.,-1)
DO 5 I=1,N
X(I)=XX(1)+(I-.5)*DX
5 CONTINUE
DO 10 K=1,NP
DO 6 I=1,N
Y1(I)=Y(I+(K-1)*N2)*SF+YY(I)
6 CONTINUE
DO 7 I=NP1,N2
Y2(I-N)=Y(I+(K-1)*N2)*SF+YY(I)
7 CONTINUE

THIS PAGE IS BEST QUALITY PRACTICABLE
FROM COPY FURNISHED TO DDC

```
DO 8 I=1,N
CALL SYMBOL(X(1),Y1(1),.07,0,0,-1)
CALL SYMBOL(X(1),Y2(1),.07,2,0,-1)
8 CONTINUE
CALL LINE(X(1),Y1(1),N,1,0,0)
CALL LINE(X(1),Y2(1),N,1,0,0)
10 CONTINUE
RETURN
END
```

This subroutine plots the magnitude of \bar{M}_1 and \bar{M}_2 versus their position on the face Γ_1 or Γ_2 and connects the points with straight lines. The argument parameters are:

Y = array containing $|\bar{M}_1|$ and $|\bar{M}_2|$ sequentially stored.

N = number of expansion functions on slit face Γ_1 and Γ_2 .

N2 = 2*N

SC = scale factor such that the maximum value of the plot ordinate equals SC*2.

NP = number of plots of $|\bar{M}_1|$ and $|\bar{M}_2|$ to be drawn for one picture.

The arrays having minimum dimensions are Y(N2*NP), X(N), Y1(N), and Y2(N). All of the statements up to DO loop 5 generate the picture frame with labels. Inside DO loop 10, the values of $|\bar{M}_1|$ and $|\bar{M}_2|$ are taken out of array Y, placed in the dummy array Y1 and Y2, and marked with squares and triangles respectively. This is done for NP arrays of $|\bar{M}_1|$ and $|\bar{M}_2|$.

THIS PAGE IS BEST QUALITY PRACTICABLE
FROM COPY FURNISHED TO DDC

C LISTING OF SUBROUTINE PPHAS
C
SUBROUTINE PPHAS(Y,N,N2,NP)
DIMENSION XX(5),YY(5),X(50),Y(300),XF(5)
DATA XF/.5,.35,.23,.5,.65/
DATA XX/2.,7.,7.,2.,2./,YY/1..1.,5.,5.,1./
XW=XX(2)-XX(1)
YW=YY(3)-YY(2)
NSN=5
DX=XW/N
CALL PLOTS(0,0,0,20.,11.)
CALL LINE(XX(1),YY(1),5,1,0,0)
JT=1
NP1=N+1
DO 2 J=1,2
YS=YY(1)+(J-1)*YW
XS=XX(2)-(J-1)*XW
DO 1 I=1,NP1
XI=XX(1)+(J-1)*XW+(I-1)*DX*JT
CALL SYMBOL(XI,YS,.14,13,0.,-1)
1 CONTINUE
DO 3 I=1,NSN
YI=YY(1)+(J-1)*YW+(I-1)*JT
CALL SYMBOL(XS,YI,.14,13,90.,-1)
3 CONTINUE
JT=-JT
2 CONTINUE
SN=180.
DO 4 I=1,NSN
YI=YY(4)-(I-1)
CALL NUMBER(XX(1)-XF(I),YI-.06,.14,SN,0.,-1)
SN=SN-90.
4 CONTINUE
CALL SYMBOL(XX(1)-.7,YY(1)+1.67,.14,5HPHASE,90.,5)
CALL SYMBOL(XX(1)-.03,YY(1)-.27,.14,112,0.,-1)
CALL SYMBOL(XX(1)+XW/2.,YY(1)..2,13,0.,-1)
CALL SYMBOL(XX(1)+XW/2.-.17,YY(1)-.27,.14,4W/2,0.,3)
CALL SYMBOL(XX(2)-.035,YY(1)-.27,.14,102,0.,-1)
CALL SYMBOL(XX(1)+2.,YY(1)-.6,.14,8HPOSITION,0.,8)
DO 10 K=1,NP
DO 5 I=1,N
X(I)=XX(1)+(I-.5)*DX
5 CONTINUE
DO 6 I=1,N
Y(I)=Y(I+(K-1)*N2)/90.+3.
6 CONTINUE
DO 7 I=NP1,N2
Y(I)=Y(I+(K-1)*N2)/90.+3.
7 CONTINUE
DO 8 J=1,N
CALL SYMBOL(X(J),Y(J),.07,0,0.,-1)
CALL SYMBOL(X(J),Y(J+N),.07,2,0.,-1)
8 CONTINUE

THIS PAGE IS BEST QUALITY PRACTICABLE
FROM COPY FURNISHED TO DDC

```
CALL LINE(X(1),Y(1),N,1,0,0)
CALL LINE(X(1),Y(NP1),N,1,0,0)
10 CONTINUE
RETURN
END
```

This subroutine plots the phase of \bar{M}_1 and \bar{M}_2 versus their position on slit face Γ_1 or Γ_2 and connects the points with straight lines. The argument parameters are:

Y = array containing the phase of \bar{M}_1 and \bar{M}_2 in degrees.

N = number of expansion functions on slit face Γ_1 and Γ_2 .

N2 = 2*N

NP = number of phase plots desired per picture.

The arrays having minimum dimensions are Y(N2*NP) and X(N). All of the statements up to DO loop 10 generate the picture frame with labels. DO loop 10 then takes the phases out of array Y and plots the phase of \bar{M}_1 with squares and the phase of \bar{M}_2 with triangles. This is done for NP arrays of \bar{M}_1 and \bar{M}_2 .

```
C      LISTING OF SUBROUTINE PFP
C
C      SUBROUTINE PFP(X,Y,NFP,NP)
C-----SUBROUTINE TO PLOT NORMALIZED FIELD PATTERN.
DIMENSION XX(5),YY(5),X(300),Y(300)
DATA XX/2.,8.,8.,2.,2./,YY/1.,1.,5.,5.,1./
CALL PLOTS(0,0,0,20,,11.)
CALL LINE(XX(1),YY(1),5,1,0,0)
XW=XX(2)-XX(1)
YW=YY(3)-YY(2)
DX=XW/6.
JT=1
NY=6
NX=7
DO 2 J=1,2
YS=YY(1)+(J-1)*YW
XS=XX(2)-(J-1)*XW
DO 1 I=1,NX
XI=XX(1)+(J-1)*XW+(I-1)*DX*JT
CALL SYMBOL(XI,YS,.14,.13,0.,-1)
1 CONTINUE
2
```

THIS PAGE IS BEST QUALITY PRACTICABLE
FROM COPY FURNISHED TO DDC

```
DO 3 I=1,NY
  YI=YY(1)+(J-1)*YW+(I-1)*.8*JT
  CALL SYMBOL(XS,YI,.14,.13,.90,-1)
3  CONTINUE
  JT=-JT
2  CONTINUE
  SN=1.
  DO 4 I=1,NY
    YI=YY(4)-(I-1)*.8-.07
    CALL NUMBER(XX(1)-.5,YI,.14,SN,0.,1)
    SN=SN-.2
4  CONTINUE
  CALL SYMBOL(XX(1)-.7,YY(1)+.32,.14,24NORMALIZED FIELD PATTERN,
* 90.,24)
  SN=-90.
  DO 5 I=1,3
    XI=XX(1)-.17+(I-1)
    CALL NUMBER(XI,YY(1)-.3,.14,SN,0.,-1)
    SN=SN+30.
5  CONTINUE
  CALL SYMBOL(XX(1)+XW/2-.04,YY(1)-.3,.14,112,0.,-1)
  SN=30.
  DO 6 I=5,7
    XI=XX(1)-.1+(I-1)
    CALL NUMBER(XI,YY(1)-.3,.14,SN,0.,-1)
    SN=SN+30.
6  CONTINUE
  CALL SYMBOL(XX(1)+2.7,YY(1)-.6,.14,SHANGLE,0.,5)
  DO 11 K=1,NP
  DO 10 I=1,NFP
    X(I)=XX(1)+(XW/180.)*(X(I+(K-1)*NFP)+90.)
    Y(I)=Y(I+(K-1)*NFP)*YN+YY(1)
10  CONTINUE
  CALL LINE(X(1),Y(1),NFP,1,0,0)
11  CONTINUE
  RETURN
END
```

This subroutine plots the normalized far field pattern measured in the half space region c as a function of the observation angle measured from the x axis. The argument parameters are:

X = array containing values of the angle at which the far field measurements are made.

Y = array containing far field measurements normalized so that the largest measurement equals unity.

THIS PAGE IS BEST QUALITY PRACTICABLE
FROM COPY FURNISHED TO DDC

NFP = number of far field measurements made

NP = number of plots desired per picture.

The arrays with minimum dimensions are X(NFP*NP), Y(NFP*NP). All of the statements up to DO loop 11 generate the picture frame with labels. Each value of X and Y is scaled accordingly and connected by a straight line.

```
C      LISTING OF SUBROUTINE PGA
C
C      SUBROUTINE PGA(X,Y,NFP,SC,NP)
C-----SUBROUTINE TO PLOT GAIN PATTERN.
      DIMENSION X(300),Y(300),XX(4),YY(4)
      DATA XX/2.,7.,3.,3./,YY/4.,4.,2.,6./
      DATA NX/4/,NY/5/,PI/3.141593/
      CALL PLOTS(0,0,0,20.,11.)
      CALL LINE(XX(1),YY(1),2,1,0,0)
      SN=4.*SC
      DO 1 I=1,NX
      XI=XX(2)-(I-1)
      CALL SYMBOL(XI,YY(1),.14,.13,0.,-1)
      CALL NUMBER(XI-.03,YY(1)-.22,.14,SN,0.,-1)
      SN=SN-SC
1     CONTINUE
      CALL LINE(XX(3),YY(3),2,1,0,0)
      DO 2 I=1,NY
      YI=YY(4)-(I-1)
      CALL SYMBOL(XX(1)+1.,YI,.14,.13,90.,-1)
2     CONTINUE
      XN=XX(1)+.86
      CALL NUMBER(XN,YY(4)-.07,.14,2.*SC,0.,-1)
      CALL NUMBER(XN,YY(4)-1.07,.14,SC,0.,-1)
      CALL NUMBER(XN,YY(3)-.07,.14,2.*SC,0.,-1)
      CALL NUMBER(XN,YY(3)+.93,.14,SC,0.,-1)
      DO 4 K=1,NP
      DO 3 I=1,NFP
      YT=Y(I+(K-1)*NFP)
      Y(I)=YY(1)+Y(I+(K-1)*NFP)*SIN(PI*X(I+(K-1)*NFP)/180.)/SC
      X(I)=XX(1)+YT*COS(PI*X(I+(K-1)*NFP)/180.)/SC+1.
3     CONTINUE
      CALL LINE(X(1),Y(1),NFP,1,0,0)
4     CONTINUE
      CALL SYMBOL(XX(3)+.5,YY(3)-.5,.14,*GAIN PATTERN*,0.,12)
      RETURN
      END
```

This subroutine plots a polar pattern of the gain computed in the main program for the half space region c. The argument parameters are:

X = array containing the gain measurement angle measured from the x axis.

Y = array containing the gain measurement.

NFP = number of gain measurements made per pattern.

SC = scale factor such that $4 \leq SC * \text{maximum gain value}$.

NP = number of patterns desired per picture.

The arrays with minimum dimensions are X(NFP*NP) and Y(NFP*NP).

All of the statements up to DO loop 4 generate the axes with labels.

The data is then scaled and plotted using polar coordinates.

C LISTING OF SUBROUTINE PTRANS
C

```
SUBROUTINE PTRANS(X,Y,T,NTP,NP, ID)
DIMENSION X(300),Y(300),T(300)
DIMENSION XX(5),YY(5)
DIMENSION DUMX(86),DUMY(86)
DIMENSION TMF(8),PHI(8),TMF1(8),TMD(8),PHD(8),TMD1(8)
DATA PHI/0.,.10.,.20.,.30.,.40.,.50.,.60.,.70./
DATA TMF/1.,.975,.925,.86,.75,.65,.56,.485/
DATA TMF1/.98,.95,.92,.85,.79,.725,.66,.62/
DATA XX/2.,.6.,.6.,.2.,.2./,YY/1.,.1.,.4.,.4.,.1./
DATA PI/3.141593/
XW=XX(2)-XX(1)
YW=YY(3)-YY(2)
DX=XW/9.
DY=YW/10.
CALL PLOTS(0,0,0,20.,11.)
CALL LINE(XX(1),YY(1),5,1,0,0)
JT=1
DO 2 J=1,2
YS=YY(1)+(J-1)*YW
XS=XX(2)-(J-1)*XW
DO 1 I=1,10
XI=XX(1)+(J-1)*XW+(I-1)*DX*JT
CALL SYMBOL(XI,YS,.14,.13,0.,-1)
1      CONTINUE
```

THIS PAGE IS BEST QUALITY PRACTICABLE
FROM COPY FURNISHED TO DDC

```
DO 3 I=1,11
YI=YY(1)+(J-1)*YW+(I-1)*JT*DY
CALL SYMBOL(XS,YI,.14,.13,.90.,-1)
3 CONTINUE
JT=-JT
2 CONTINUE
SN=1.
DO 4 I=1,3
YI=YY(4)-(I-1)*1.5-.07
CALL NUMBER(XX(1)-.50,YI,.14,SN,0.,1)
SN=SN-.5
4 CONTINUE
CALL SYMBOL(XX(1)-.6,YY(1)+1.13,.14,'T',.90.,1)
CALL SYMBOL(XX(1)-.6,YY(1)+1.33,.14,'COS',.90.,3)
CALL SYMBOL(XX(1)-.6,YY(1)+1.77,.14,.36,.90.,-1)
CALL NUMBER(XX(1)-.035,YY(1)-.25,.14,0.,0.,-1)
CALL NUMBER(XX(2)-.115,YY(1)-.25,.14,.90.,0.,-1)
CALL SYMBOL(XX(1)+.75,YY(1)-.4,.14,'ANGLE OF INCIDENCE',.0.,18)
DO 6 J=1,NP
DO 5 I=1,NTP
K=I+(J-1)*NTP
DUMX(I)=XX(2)-(2.*XW/PI)*(ABS(ATAN2(Y(K),X(K)))-PI/2.)
DUMY(I)=T(K)*YW+YY(2)
5 CONTINUE
CALL LINE(DUMX(I),DUMY(I),NTP,1,0,0)
6 CONTINUE
IF(ID.EQ.-1) GO TO 10
DO 8 I=1,8
PHD(I)=XX(1)+XW*PHI(I)/90.
TMD(I)=YY(1)+TMF(I)*YW
TMD1(I)=YY(1)+TMF1(I)*YW
CALL SYMBOL(PHD(I),TMD1(I),.07,.2,0.,-1)
CALL SYMBOL(PHD(I),TMD(I),.07,0,0.,-1)
8 CONTINUE
10 CONTINUE
RETURN
END
```

This subroutine plots $T\cos\phi$ versus ϕ where T is the transmission coefficient computed in the main program and ϕ is the angle of incidence measured from the negative x axis. The argument parameters are:

X = array containing x coordinate of line source.

Y = array containing y coordinate of line source.

T = array containing values of $T\cos\phi$ where $\phi = \tan^{-1}|\frac{y}{x}|$.

NTP = number of values of T computed.

NP = number of plots of $T\cos\phi$ versus ϕ desired per picture.

ID = integer option variable. If ID = 1, the sample data placed in arrays TMF, TMFL, and PHI will be plotted with symbols, i.e., for comparison purposes. If ID = -1, this data is ignored.

The arrays with minimum dimensions are X(NTP*NP), Y(NTP*NP), T(NTP*NP), DUMX(NTP), and DUMY(NTP). All of the statements up to DO loop 6 generate the picture frame with labels. Each angle ϕ is computed in DO loop 5 and stored in the dummy array DUMX. Array T is scaled and stored in array DUMY. Straight lines are then drawn between consecutive points.

REFERENCES

- [1] G. W. Lehman, "Diffraction of Electromagnetic Waves by Planar Dielectric Structures. I. Transverse Electric Excitation," Journal of Math. Physics, vol. 11, May 1970, pp. 1522-1535.
- [2] S. C. Kashyap, M.A.K. Hamid, "Diffraction Characteristics of a Slit in a Thick Conducting Screen," IEEE Trans. on Ant. and Prop., vol. AP-19, July 1971, pp. 499-507.
- [3] Kohei Hongo, "Diffraction of Electromagnetic Plane Waves by Infinite Slit Perforated in a Conducting Screen with Finite Thickness," Elec. and Comm. in Japan, Vol. 54-B, No. 8, 1971, pp. 90-96.
- [4] F. L. Neerhoff, G. Mur, "Diffraction of a Plane Electromagnetic Wave by a Slit in a Thick Screen Placed Between Two Different Media," Appl. Sci. Res., Vol. 28, July 1973, pp. 73-88.
- [5] R. F. Harrington, J. R. Mautz, "A Generalized Network Formulation for Aperture Problems," Syracuse University Technical Report TR-75-13, November 1975.
- [6] R. F. Harrington, J. R. Mautz, "A Generalized Network Formulation for Aperture Problems," IEEE Trans. on Ant. and Prop., Vol. AP-24, November 1976, pp. 870-873.
- [7] R. F. Harrington, "Time-Harmonic Electromagnetic Fields," McGraw-Hill Book Company, New York, 1961.
- [8] C. M. Butler, K. R. Umashankar, "Electromagnetic Penetration through an Aperture in an Infinite, Planar Screen Separating Two Half Spaces of Different Electromagnetic Properties," Radio Science, Vol. 11, July 1976, pp. 611-619.
- [9] S. C. Kashyap, et al., "Diffraction Pattern of a Slit in a Thick Conducting Screen," Journal of Applied Physics, Vol. 42, February 1971, pp. 894-895.
- [10] M. Abramowitz, I. Stegun, "Handbook of Mathematical Functions," Dover Publications, Inc., New York, 1965.
- [11] IBM, System/360 Scientific Subroutine Package, Version III, p. 133.
- [12] J. Chou, A. T. Adams, "Method of Moments Applications aperture Coupling Through Long Slots," Rome Air Development Center Technical Report, RADC-TR-73-217, December 1975, A019771, Vol VII.
- [13] P. M. Morse, P. J. Rubenstein, "The Diffraction of Waves by Ribbons and by Slits," Physical Review, vol. 54, December 1938, pp. 895-898.